Preliminary Report
of
The Hakuhō Maru Cruise KH-88-2

(OMLET Cruise)

April 15-May 11, 1988

The Western North Pacific
South of Japan

Ocean Research Institute
University of Tokyo
1988

Preliminary Report
of
The Hakuhō Maru Cruise KH-88-2

(OMLET Cruise)

April 15-May 11, 1988

The Western North Pacific
South of Japan

By

The Scientific Members of the Expedition

Edited by

Tomio Asai

1988

Contents

1. Introduction

T. Asai
Chief Scientist
(Ocean Research Institute, University of Tokyo)

The objective of the KH-88-2 Cruise of the Hakuho Maru is to perform observations concerning structures of atmospheric and oceanic mixed layers and their temporal variations, air-sea exchanges of energy, momentum and materials in the western North Pacific around the former OWS-T (29°N,135°E) south of Japan and thereby to improve our understanding of the physical processes of an atmosphere-ocean coupled boundary layer. The cruise is a part of observational studies of (1) the Ocean Mixed Layer Experiment (OMLET) and (2) evolution of extended marine clouds, both of which are components of the first phase of the WCRP in Japan.

The KT-88-6 Cruise of the Tansei Maru is to be in cooperation jointly with present cruise for its last half period to intensify observation of the ocean mixed layer including the Subtropical Mode Water.

During the cruise thirty six scientists from nine universities and one governmental organization are engaged in many different types of observations: (1) aerological observation using the Omega wind-finding system, (2) sounding of atmospheric boundary layer using a tethered balloon, (3) direct measurement of turbulent fluxes of momentum and energy in the surface boundary layer by sonic anemometer-thermometers, (4) radiation measurement, (5) surface wave observation, (6) oceanographic observations by using CTD and XBT, (7) surface-buoy mooring observations of temperature and current profiles, (8) Acoustic Doppler Current Profiler (ADCP) measurement, (9) current measurement by using SOFAR as well as (10) routine marine meteorological observations. Some groups take this opportunity to observe concentrations of CO_2, O_3, CFC, aerosols and some other minor constituents in the marine atmosphere.

As is shown in Fig. 1.1, the cruise during the period of twenty seven days from April 15 to May 11, 1988, consists of two legs: Leg 1 from Tokyo to Kochi via the OWS-T and Leg 2 from Kochi to Tokyo via the OWS-T.

This cruise is also performed as a part of the WESTPAC/IOC.

On behalf of all scientists aboard I would like to extend our thanks to Captain Shimamune and all the crew of the R.V. Hakuho Maru.

List of the scientists aboard

Asai, Tomio: Chief scientist, Ocean Research Institute, University of Tokyo
Taira, Keisuke: Ocean Research Institute, University of Tokyo
Nakamura, Kozo: Ocean Research Institute, University of Tokyo
Fukasawa, Masao: Ocean Research Institute, University of Tokyo
Kawabe, Masaki: Ocean Research Institute, University of Tokyo
Ishikawa, Koji: Ocean Research Institute, University of Tokyo
Misawa, Nobuhiko: Ocean Research Institute, University of Tokyo
Otobe, Hirotaka: Ocean Research Institute, University of Tokyo
Kitagawa, Shoji: Ocean Research Institute, University of Tokyo
Kastro: Center for Oceanological Research and Development-L1P1
Suzuki, Yasushi: Ocean Research Institute, University of Tokyo
Urano, Akira: Ocean Research Institute, University of Tokyo
Yang, Sung-Kee: Ocean Research Institute, University of Tokyo
Uehara, Katsuto: Ocean Research Institute,University of Tokyo
Hamatani, Masanobu: Ocean Research Institute, University of Tokyo
Watanabe, Shuichi: Faculty of Fisheries, Hokkaido University
Saito, Shimei: Faculty of Fisheries, Hokkaido University
Todoroki, Tomohiro: Faculty of Fisheries, Hokkaido University
Toba, Yoshiaki: Geophysical Institute, Tohoku University
Suga, Toshio: Geophysical Institute, Tohoku University
Kidsu, Shoichi: Geophysical Institute, Tohoku University
Tanaka, Masafumi: Water Research Institute, Nagoya University
Ohtaki, Eiji: School of General Education, Okayama University
Tsukamoto, Osamu: School of General Education, Okayama University
Ishida, Hiroshi: Kobe University of Mercantile Marine
Horiguchi, Mituaki: Disaster Prevention Research Institute, Kyoto University
Mizuno, Shinjiro: Research Institute for Applied Mechanics, Kyushu University
Kaneko, Arata: Research Institute for Applied Mechanics, Kyushu University
Ishibashi, Michiyoshi Research Institute for Applied Mechanics, Kyushu University
Masumoto, Yukio: Research Institute for Applied Mechanics, Kyushu University
Nishikido, Takeshi: Faculty of Technology, Kagoshima University
Fujichika, Yuuichi: Faculty of Technology, Kagoshima University
Nakayama, Fumito: Faculty of Technology, Kagoshima University
Nishihara, Naoki: Faculty of Technology, Kagoshima University

Takashima, Tsutomu: Meteorological Research Institute
Takayama, Yozo: Meteorological Research Institute

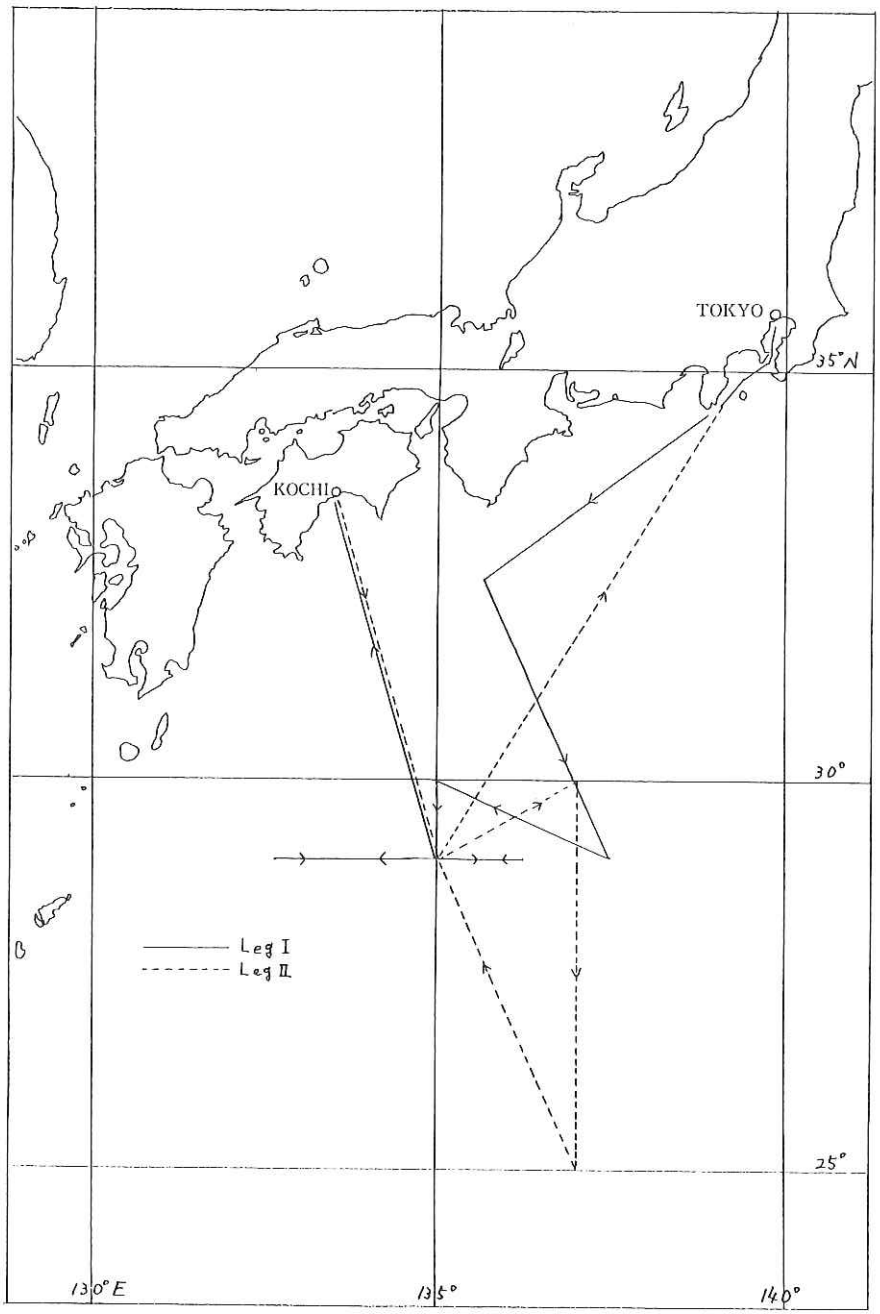

Fig. 1.1 Track chart of the KH-88-2 Cruise of the Hakuho Maru.

2. Aerological observations with Omega-sonde sounding system

T. Asai, K. Nakamura, K. Ishikawa, N. Misawa, Y. Suzuki and A. Urano
(Ocean Research Institute, University of Tokyo)

2.1 Introduction

Cloud topped boundary layers (CTBL) play an important role in the global radiation budget of the atmosphere and in the linkage between the troposphere and the earth's surface. The CTBL reduces the surface radiative heating due to the significant decrease in solar energy at the surface, while it reduces the surface radiative cooling due to the longwave radiation from the surface. For further progress in climate research, we must advance our knowledge of how clouds from and maintain in the boundary layer.

Although there is a large variety of CTBL regimes, they can be divided into two types. One is the CTBL which develops over cold ocean currents to the west of continents and is largely driven by cooling from above. The Californian coastal stratocumulus, which the First ISCCP Regional Experiment, FIRE, is studying, is one of the typical examples of this type of CTBL. The other is the CTBL which forms when cold air moves over relatively warmer water, especially to the east of continents over warm ocean currents, and it is largely driven by heating from below. This is the boundary layer to be investigated in the Western North-Pacific Cloud-Radiation Experiment. The structure of the CTBL depends strongly on the dominant processes responsible for generating turbulence. Therefore, it is important to investigate the structure and maintaining mechanism of this CTBL regime, in comparison with the results found in FIRE.

2.2 Temporal variation of the weather situation

The upper-air observations by Omega-sonde system were made every 6 hours from 09 JST 21 April to 21 JST 24 April and from 09 JST 1 May to 15 JST 8 May. Two additional soundings were performed at 18 JST and 24 JST 7 May during the passage of a cold front. All data at standard levels are tabulated in Appendix II.

Fig. 2.1 shows the temporal variation of meteorological conditions by the synoptic high and low pressures and warm and cold fronts along the 135°E in the weather map. Although the ship passed from 35°N to 25°N, most of the observations were performed around 29°N at the OWS-T. After the passage of the

cold fronts, such as 22 April, 5 and 8 May, cold outbreaks occurred and the mixed layer was created by a large amount of heat supply from the sea surface.

Fig. 2.2 shows an example of vertical-time sections obtained by the upper air observation. Potential temperature and specific humidity are indicated by a solid line and a dashed line, respectively. The cold outbreaks are indicated by the upward propagation of cooling in the lower atmosphere, and the development of the mixed layer in the cold airmass are indicated by the constant potential temperature in the lowest layer of the atmosphere.

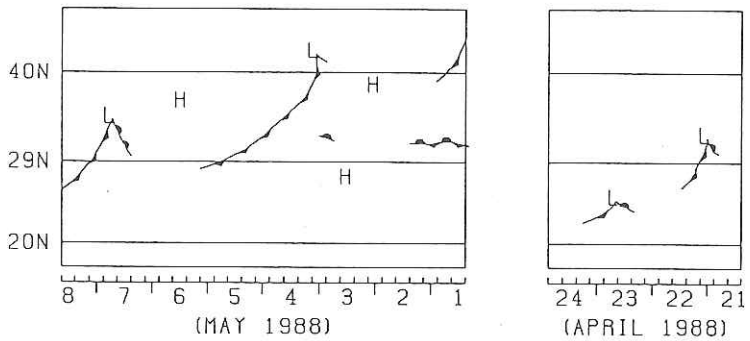

Fig. 2.1 Temporal variation of meteorological condition along 135°E. H and L indicate synoptic high and low pressures, respectively.

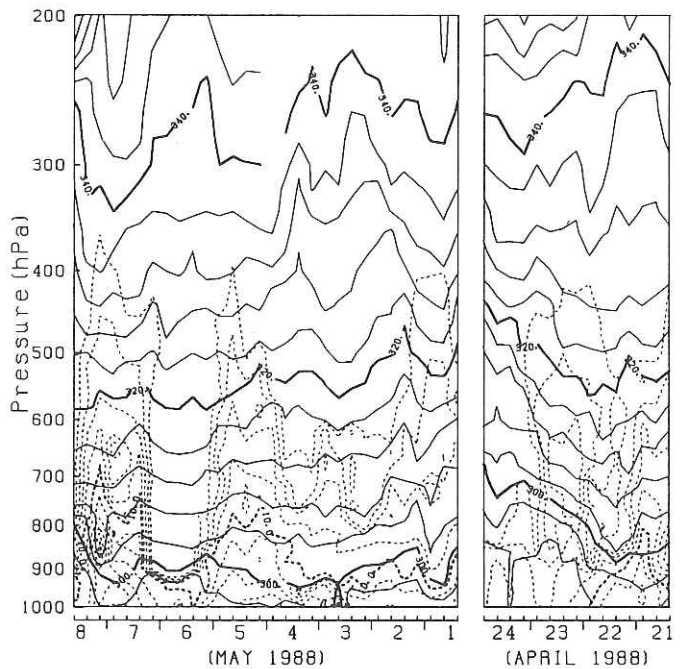

Fig. 2.2 Vertical-time section of potential temperature (solid line) and specific humidity (dashed line).

2.3 Boundary layer structure

Fig. 2.3 shows typical examples of the vertical profiles of temperature and dew point temperature in the boundary layer. The profiles in (a) are the example of post frontal case at 03 JST 24 April, when cumulus clouds are observed, and the profiles in (b) are the example of pre frontal case at 21 JST 07 May, when stratifrom clouds are observed.

The boundary layer in (a) is composed of three layers: subcloud layer below 880 hPa with the constant potential temperature and almost constant mixing ratio, cloud layer between 720 hPa and 880 hPa with conditionally unstable stratification, and inversion layer between 680 hPa and 720 hPa with increasing temperature with respect to height.

The structure indicates the same characteristics as the trade cumulus equilibrium structure as follows (Betts, 1982) : 1) The instability criterion for the breakup of a stratocumuls layer is well satisfied: equivalent potential temperature of the subsiding dry air at inversion top is well to the left of the moist adiabat through cloud-base. 2) The cumulus layer lapse-rate is also well to the left of the moist adiabat. 3) The lapse-rate in the conditionally unstable cumulus layer between cloud-base and inversion base, parallels closely to the mixing curve, which does not favor downdrafts in this layer. 4) Within the cumulus layer and the inversion layer, saturation points of the environment lie to the left of the mixing line.

The profiles in (b) indicates that the instability criterion for the breakup of a stratocumulus layer is not satisfied. The lapse rate in the cloud layer is almost the same as the moist adiabatic one.

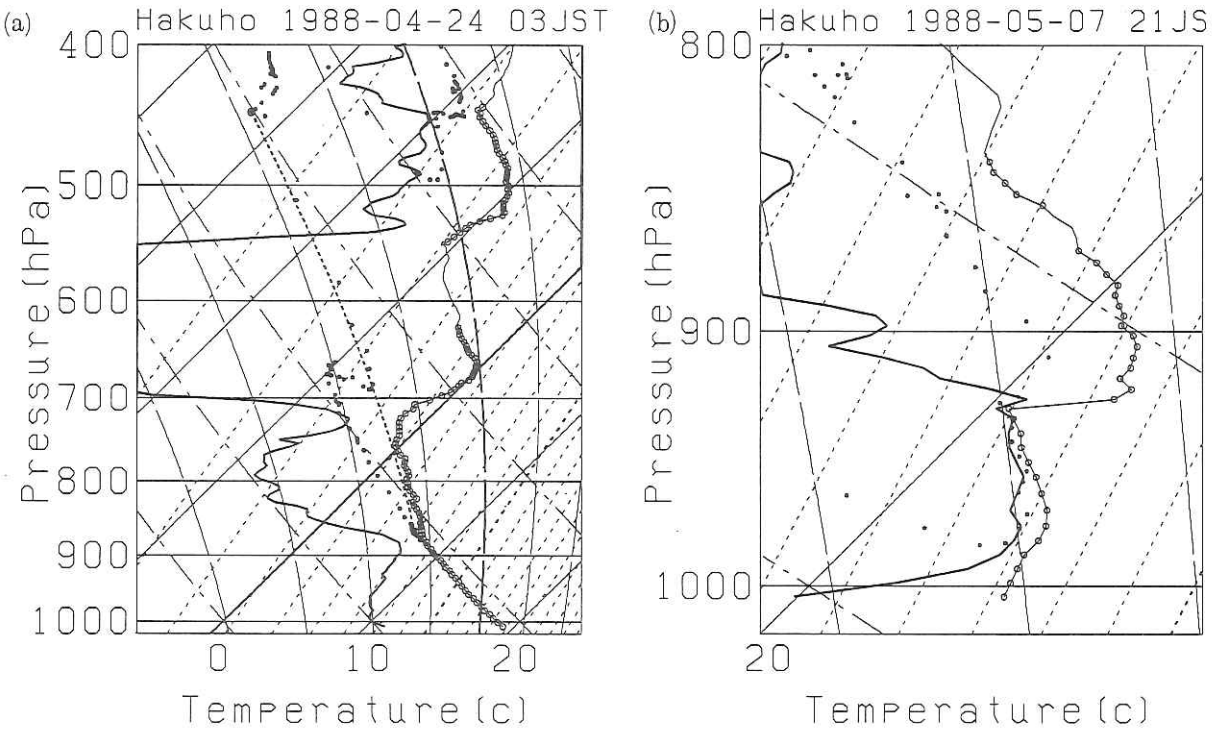

Fig. 2.3 Two examples of the soundings in skew-T diagram. The profiles in (a) are sounding at 03 JST on 24 April when cumulus clouds were observed, and the profiles in (b) are sounding at 21 JST on 07 May when stratiform clouds were observed. Solid lines, dash-dotted lines and dashed lines are isopleths of temperature, potential temperature, and saturation equivalent potential temperature at every 10 degrees. Dotted lines are isopleths of saturation mixing ratio at every 1 $gkg.^{-1}$ The thin solid line with open circles indicates the temperature soundinds and the thick solid line indicates the dew point temperature soundings. Solid circles indicate saturation points of each open circle assuming no liquid water contained. Thick dash-dotted line in (a) is the mixing line between the saturation points of subcloud layer air and inversion top air.

3. Atmospheric boundary layer observations by tethered balloon

T. Asai, K. Nakamura, K. Ishikawa, N. Misawa, Y. Suzuki and A. Urano
(Ocean Research Institute, University of Tokyo)

The purpose of this observation is to investigate the structure of the cloud topped boundary layer and its relation to the surface layer quantities over the ocean. The sonde mounted on the tethered balloon measures the vertical profiles of dry- and wet- bulb temperature, pressure, and horizontal wind speed and direction. The output signals of these sensors are converted into frequency modulated signals and sent to the ship by time shearing method. The data sampling time is about 13-14 sec, which corresponds to the data resolution about 10 m.

The observations during the cruise are listed in Table 3.1. The observation is performed only under the weak wind condition; when the wind speed is larger than 6 ms^{-1}, the observation cannot be performed. Furthermore, the height the balloon could reach was lower when the wind speed was large.

Fig. 3.1 shows an example of the observation at 15:00 JST on 23rd April. The high resolution data may be useful to analyze the boundary layer structure, though the difference between the data during ascending and during descending must be managed. The data analysis is in progress.

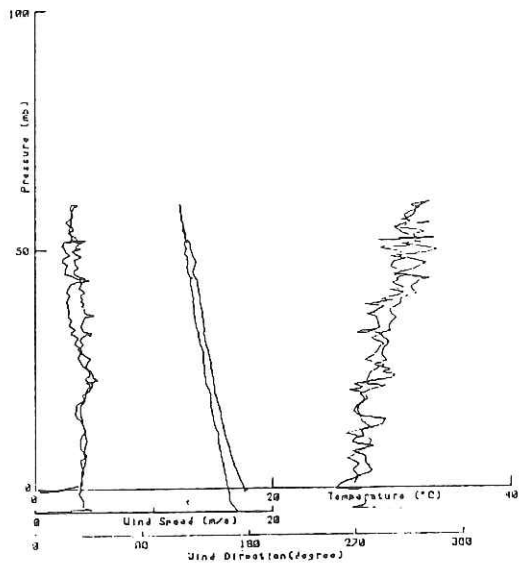

Fig. 3.1 An example of the tethered balloon sounding at 15 JST on 23 April.

Table 3.1 Tethered balloon observations.

Run	Date	Time	Location (N)	(E)	Surface data (observation start time) pressure (hPa)	dry temp. (°C)	wet temp. (°C)	relative humidity (%)	wind direction (°)	wind speed (m/s)
1	April 23	14:30-15:25	29.13°	134.97	1008.2	18.5	12.8	52	280.	6.0
2	April 23	20:55-21:32	29.32°	135.33°	1009.2	18.4	14.5	65	250.	7.0
3	April 24	02:51-	28.97°	135.02°	1008.3	19.2	14.7	60	280.	10.0
4	May 3	08:45-09:30	26.35°	137.17°	1016.6	24.0	20.4	72	45.	6.8
5	May 3	14:12-15:09	25.68°	137.00°	1018.8	30.4	22.7	51	91.	4.3
6	May 3	20:16-20:43	25.11°	137.00°	1014.0	23.8	22.4	87	140.	6.0
7	May 4	02:15-02:55	25.65°	136.71°	1011.7	24.0	23.3	94	182.	5.3
8	May 4	08:01-08:50	26.55°	136.30°	1012.3	23.2	22.3	92	190.	5.0

4. Radiometric investigations of sea surface fluxes for satellite data analysis

T. Takasima and Y. Takayama
(Meteorological Research Institute)

4.1 Introduction

To estimate radiative flux at sea surface from satellite observation, it is necessary to have knowledge of characteristics of interaction of radiation with atmospheric gases and particulate. To investigate scattering and absorbing characteristics of atmosphere, intensity and state of polarization of downward radiation in visible and near infrared spectral region were measured in maritime atmospheric condition from the research vessel. The radiation measurement over ocean surface with low reflecting and optically uniform properties provide useful information on atmospheric element affecting to the radiation, because of weak interaction in radiation between atmosphere and sea surface.

In longwave spectral region, sea surface skin temperature, sea surface temperature, sea surface air temperature and humidity, were measured.

4.2 Observational Instruments

Intensity of downward radiation were measured by spectro-radiometer. The radiometer has variable bandpass filter for measuring spectral intensity and Si photodiode as detector. The spectral resolution of the radiometer was about 30nm. Polarization components of radiation, which electric field vectors are parallel and perpendicular to the scattering plane, were measured by attached polarizer in front of optical head. Angular distribution of radiation was obtained by changing elevation angle of the radiometer. Observation azimuthal angle refering to position of the sun, was selected to 0 or 180 degree (principal plane).

Sea surface brightness temperature was measured through the cruise by infrared radiometric thermometer, setting observation angle of about 40 degree. The calibration of the infrared thermometer was done by inserting black painted alminium plate which temperature was monitored by Pt register thermometer, into sight of view of the thermometer.

4.3 Result

Fig. 4.1 shows the intensity (symbol +; unit $\mu m/cm^2/nm/sr$), and degree of

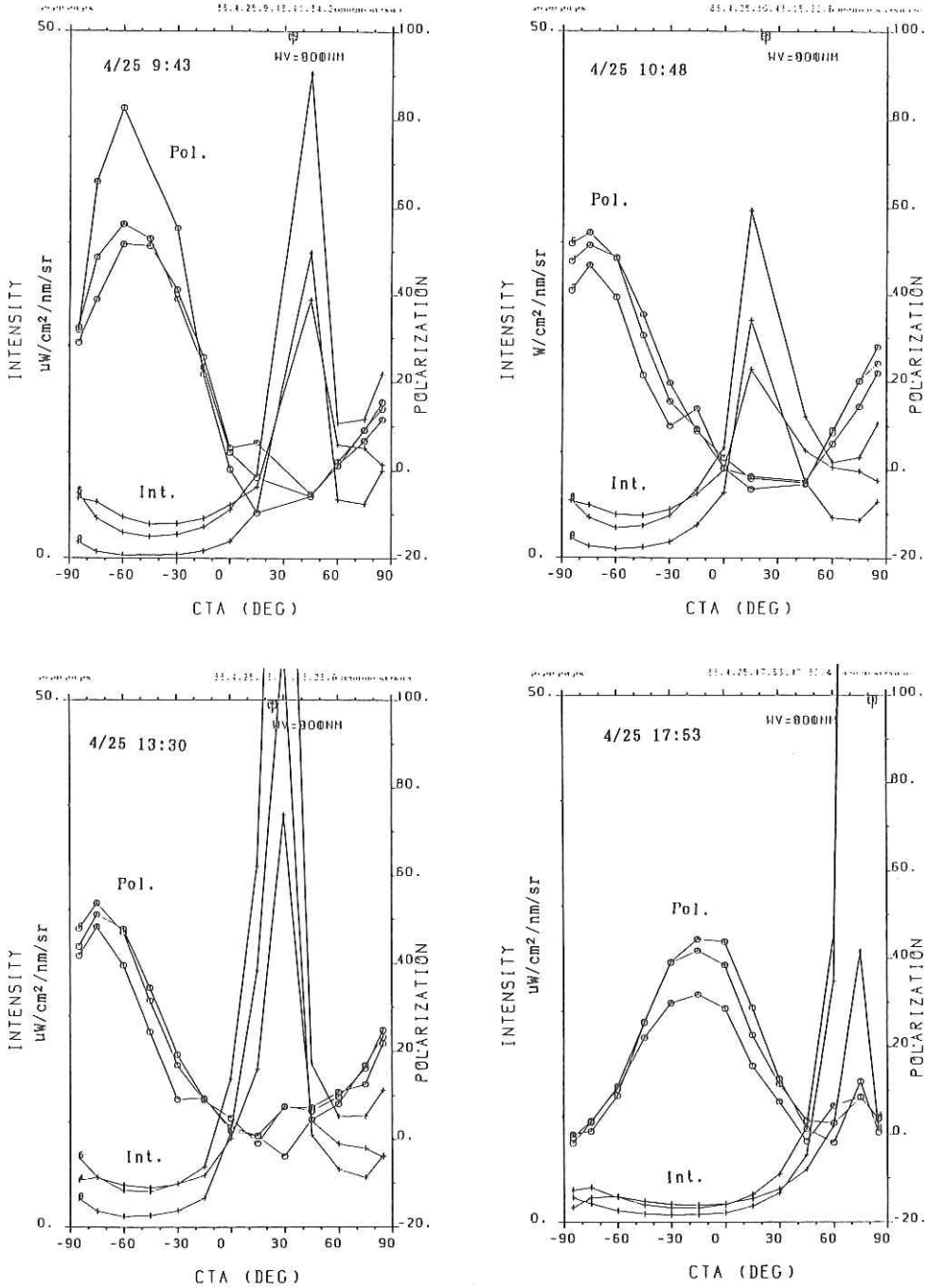

Fig. 4.1 Measured intensity and degree of polarization of downward radiations at wavelength of 400nm, 600nm and 900nm at the sea surface in clear sky condition. The position of the sun (symbol Ψ) was changed with observation time.

polarization (0) of downward radiation in wavelength of 400nm, 600nm, and 900nm obtaining clear sky condition at various elevation of the sun on April 25, 1988. Negative zenith angle of observation means unti sun plane (ϕ-ϕ_0 = 180°). Symbol * represent position of the sun. The position of the sun was given by location of observer and time, as follows,

$$\cos a_Z = \sin d \sin p + \cos d \cos p \cos w$$

where a_Z is the zenith angle, w is the hour angle, p is geographic latitude, and d is the declination of the sun, which is given by day of year D as,

$$d = 0.00698 - 0.399912 \cos D + 0.070257 \sin D - 0.006758 \cos 2D + 0.000907 \sin 2D - 0.002697 \cos 3D + 0.00148 \sin 3D$$

The maximum polarization appeared at the point about 90° degree away from the position of the sun in all spectral region. The dependence of intensity variation on zenith angle of observation is small for 400nm, because of large scattering cross section of atmospheric molecules and particles for this wavelength.

Fig. 4.2 shows intensity and degree of polarization of downward radiation from overcast sky without precipitation. The intensity become large caused by large scattering of radiation from cloud particle. The cloud layer lessened the degree of polarization of solar radiation through randomization of polarization by multiple scattering.

Fig. 4.3 shows the sea surface temperature(o), sea surface brightness temperature(+), sea surface air temperature ($\hat{V}$), and relative humidity(x) observed during this cruise. Fig. 4.4 is comparison of sea surface temperature vs sea surface brightness temperature measured by infrared thermometer during day(a) and night(b). Fig. 4.5 shows correlation between the difference in brightness and sea surface temperature, and the difference in surface air temperature and sea surface temperature. Sea surface brightness temperature matched with sea surface temperature having rms temperature difference of 0.55 and 0.66°C, bias; – 0.38 and – 0.50°C, correlation coefficient of 0.96 and 0.96 for day and night, respectively. Correlation coefficients between the difference in brightness temperature and surface temperature, and the difference in temperature of air and surface are 0.54 and 0.69 for day and night respectively.

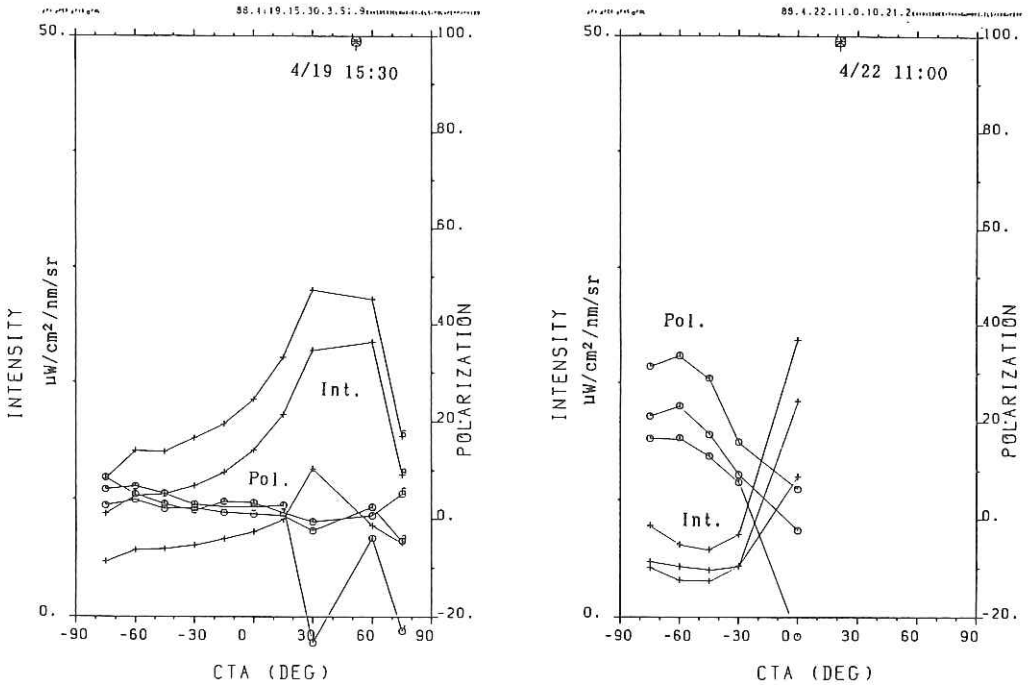

Fig. 4.2 The same as Fig. 4.1 but for observation time and cloudy condition.

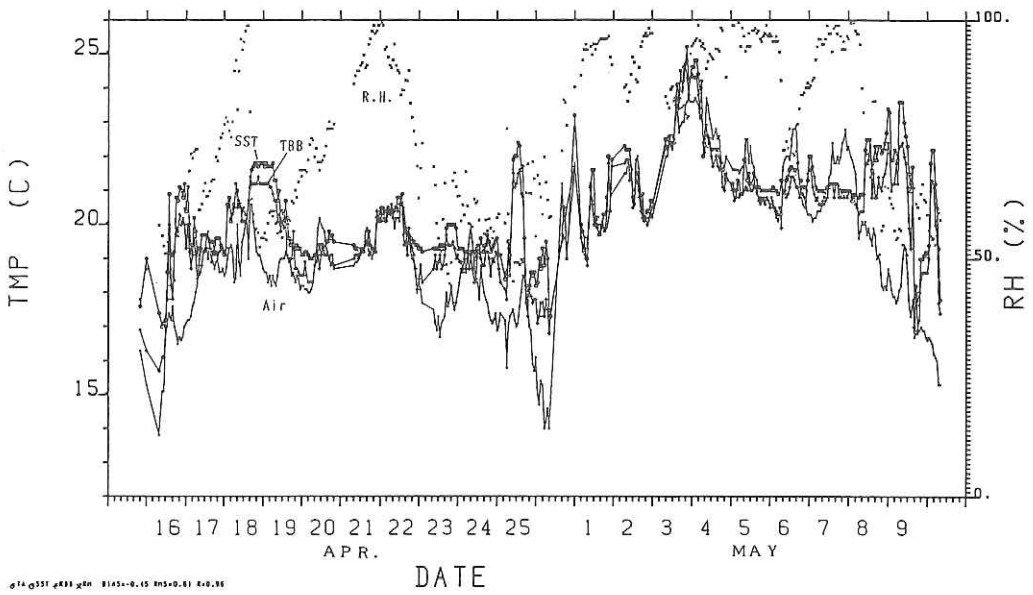

Fig. 4.3 Sea surface temperature, sea surface brightness temperature, surface air temperature and relative humidity observed during the cruise.

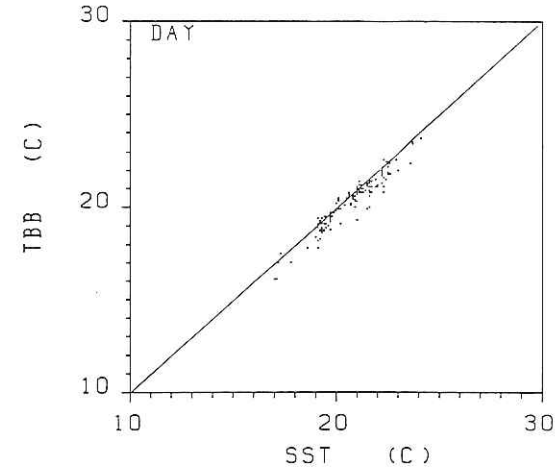

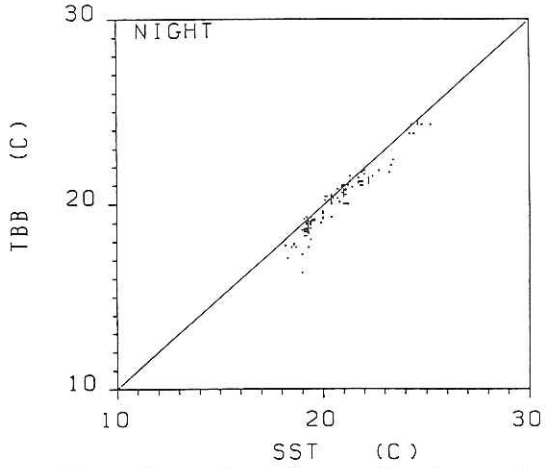

Fig. 4.4 Comparison of sea surface temperature with sea skin temperature in day time and night.

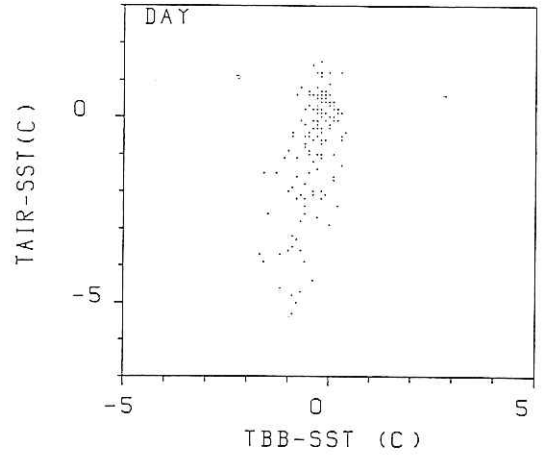

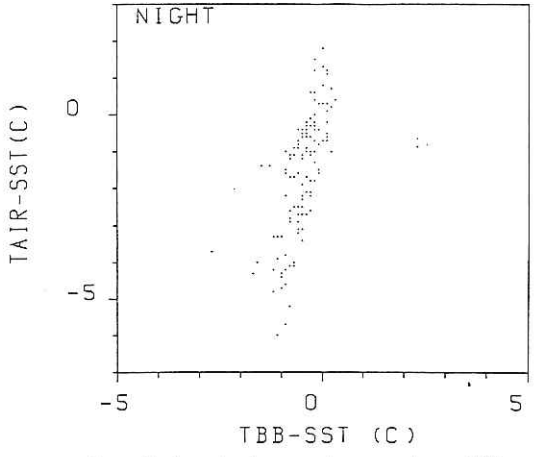

Fig. 4.5 Correlation between temperature difference of skin and sea surface temperature, and difference of temperature of air and sea surface in day and night.

5. SST measurement from IRT attached to a tethered balloon

H. Otobe, K. Nakamura, K. Ishikawa, N. Misawa, Y. Suzuki
A. Urano and T. Asai
(Ocean Research Institute, University of Tokyo)

In order to investigate the influence of the atmosphere on sea surface temperature (SST) observation by remote sensing using an infrared radiometer, SST measurement from IRT (Infrared radiation thermometer) was made on board on 4 May 1988 at 27° N, 136° E. An IRT (Model ER2007, Matsushita Communication Industrial Co., Ltd., Yokohama) with digital data recorder (Model DATAMARK LT2001 Hakusan Industrial Co., Ltd., Tokyo) and Omega radiosonde sensors of air temperature, dew-point temperature and atmospheric pressure (see section 2) attached to a tethered balloon (see section 3).

Results are shown in Figure 5.1.

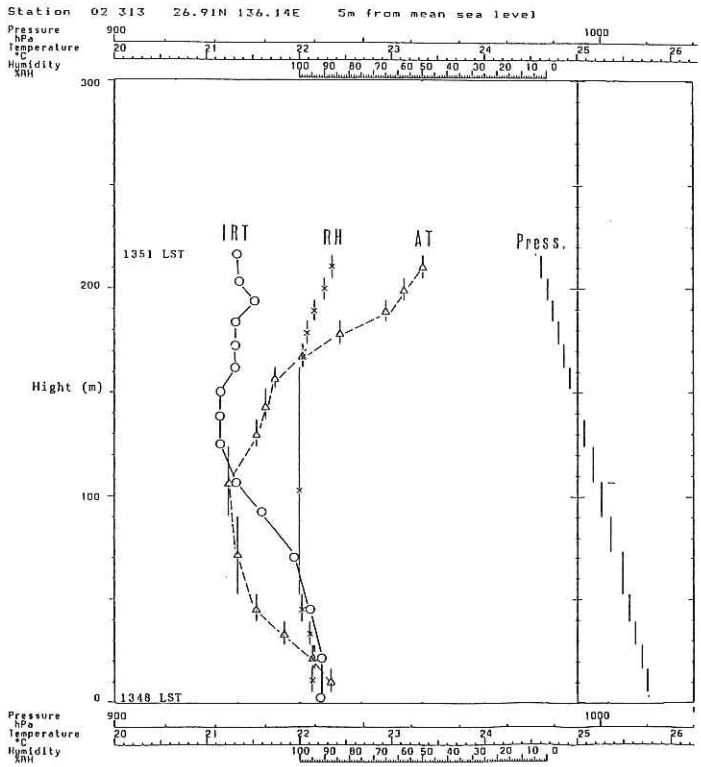

Fig. 5.1 Vertical profiles of apparent SST from IRT, air temperature (AT), relative humidity (RH) and atmospheric pressure (Press.) during from 1348 LST to 1351 LTS on May 4 1988.

6. Radiation measurement and heat budget at the sea surface

H. Otobe
(Ocean Research Institute, University of Tokyo)

Downward fluxes of short- and long-wave radiation were measured directly on board and estimation of the heat budget at the sea surface was made in the western North Pacific. A shortwave sensor (Neo Pyranometer Model MS-41, Eiko Seiki Sangyo Co., Tokyo) and a long-wave sensor (Ishikawa Radiometer Model RL-5, Ishikawa Sangyo Co., Tokyo) mounted on the gimbals were installed on the handrail of the upperbridge of the vessel.

Heat budget at the sea surface (Q) is given by

$$Q = Rn - (\ell E + H) \tag{6.1}$$

and

$$Rn = (1 - r)S\downarrow - \epsilon(\sigma T^4 - L\downarrow) \tag{6.2},$$

where Rn is the net radiation flux, ℓE latent heat flux, H sensible heat flux, r albedo, $S\downarrow$ downward short-wave radiation, T sea surface temperature, ϵ emissivity of sea water, and σ Stefan-Boltzman constant, $L\downarrow$ downward long-wave radiation. ℓE and H were estimated by an aerodynamic bulk method (Kondo, 1975) using the routine meteorological data obtained three hour intervals. Payne's table (Payne, 1972) was used for the values of r. The results were shown in Figs. 6.1 – 6.4.

References

Kondo J. (1975) Air-Sea bulk transfer coefficients in diabatic condition. Boundary-Layer Meteorology, 9, 91-112.

Payne R.E. (1972) Albedo of the sea surface. Journal of the Atmospheric Sciences, 29, 959-970.

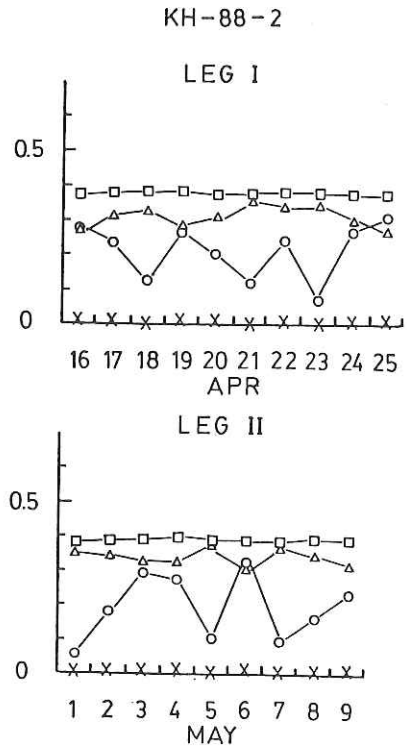

Fig. 6.1 Day to day variation of the radiation fluxes during Leg 1 and Leg 2.
○ : downward short-wave (S↓), □ : upward long-wave (σT^4)
X : upward short-wave (rS↓), (unit: KWm^{-2})
△ : downward long-wave (L↓),

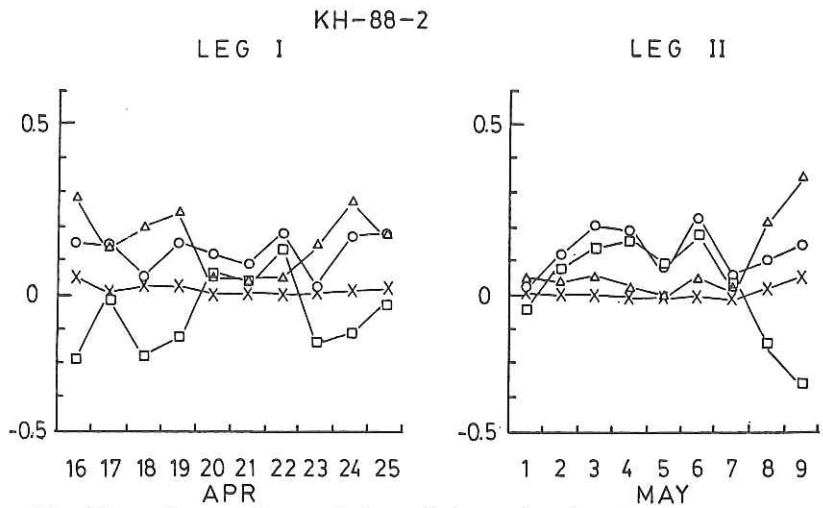

Fig. 6.2 Day to day variation of the surface heat budget and it's components during Leg 1 and Leg 2.
○ : net radiation (Qn), □ : heat budget (Q)
X : sensible heat (H), (unit: KWm^{-2})
△ : latent heat (ℓE),

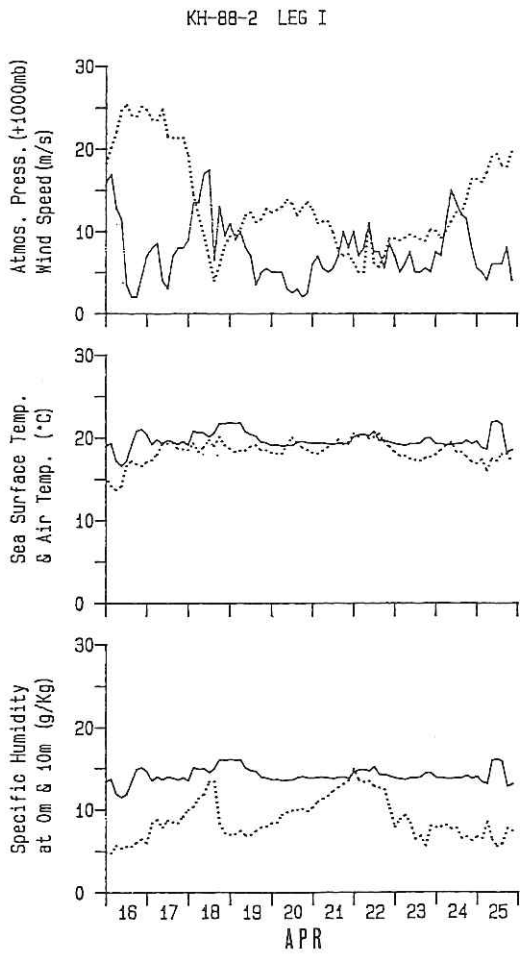

Fig. 6.3 Variation of surface meteorological elements at 3 hours interval during Leg 1.

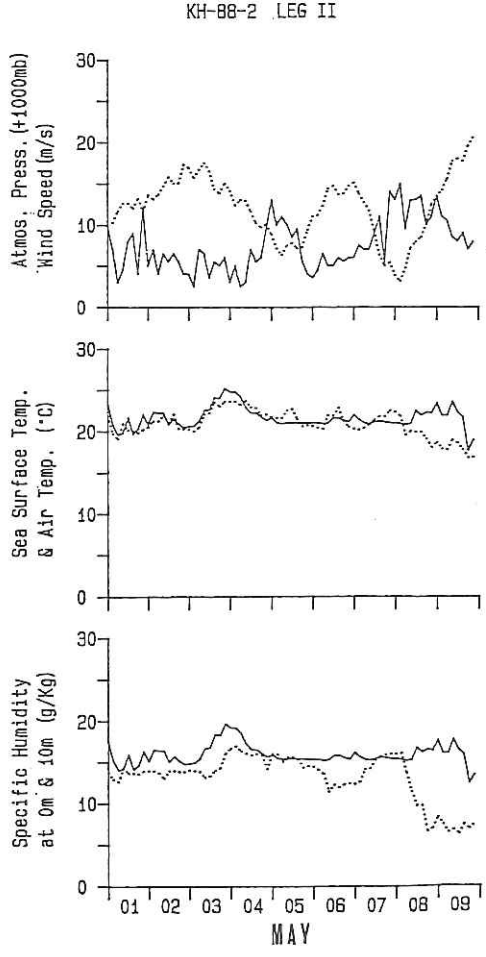

Fig. 6.4 Same as Fig. 6.3 but Leg 2.

7. Measurements of Turbulent Fluxes at the Sea Surface

7.1 Direct Measurements of Momentum, Sensible Heat and Water Vapor Fluxes

O. Tsukamoto, E. Ohtaki
(College of Liberal Arts and Sciences, Okayama University)
H. Ishida
(Kobe University of Merchantile Marine)
and
M. Horiguchi
(Disaster Prevention Research Institute, Kyoto University)

7.1.1 Measurements

Turbulent fluxes of momentum, sensible heat and water vapor were measured with eddy correlation technique during the cruise. A combination of three dimensional sonic anemometer thermometer (Kaijo Denki, DAT-300) and a fine wire copper-constantan thermocouple psychrometer (Kaijo Denki, PY-100) was used to measure fluctuations of wind velocity components, air temperature and wet- and dry-bulb temepratures. Specific humidity was evaluated from the data of wet- and dry-bulb temperatures. These sensors were mounted at the top of the foremast (23m above the sea level). Usually the ship heading was against the wind direction during the turbulence observation in order to reduce the blockage effect of the ship body.

In order to make correction of ship motion for the wind velocity components, a combination of vertical gyro (Tokyo Aircraft Instruments Co., Model 230) and an accelerometer (Tokyo Keiki, TA-25) was installed at the floor of No.1 Research Room. Pitching and rolling angles and acceleration of vertical component were measured with this system. The signals of ship speed and bow azimuth were given from the navigation system of the ship. All these signals were recorded on magnetic tape in FM analog form (TEAC R-280). A block diagram of the observation system is shown in Fig. 7.1.1.

The original analog data were converted to digital form at 10Hz and were averaged for 0.4 sec. The correction of wind velocity and statistical processing were made with this averaged data. The list of runs obtained during the cruise is tabulated in Table 7.1.1.

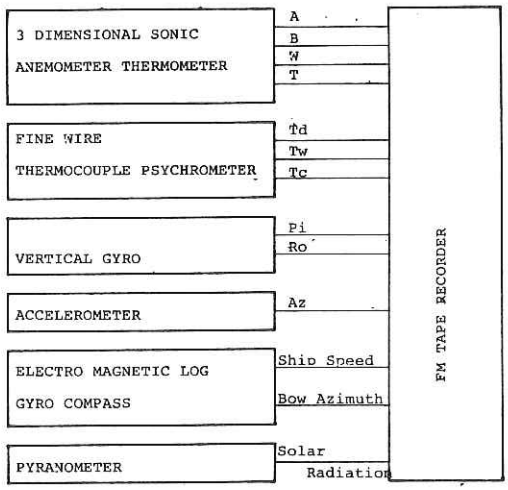

Fig. 7.1.1 Blockdiagram of turbulence measurement

Table 7.1.1 List of runs obtained during the cruise

Run	Date	Time	Lat. (° ′)	Long. (° ′)	WD (deg)	WS (m/s)
1	16 Apr	17:48 - 18:50	32 11	136 01	S	6
2	18	08:02 - 09:43	28 57	133 35	SE	18
3	18	11:20 - 12:17	28 55	133 42	S	15
4	18	15:15 - 16:15	29 02	133 35	NW	10
5	18	18:42 - 19:42	29 02	133 27	NW	12
6	22	02:30 - 03:30	28 59	134 33	SW	6
7	22	20:32 - 21:30	28 59	135 18	NW	10
8	23	02:30 - 03:30	29 07	135 00	NW	6
9	23	14:32 - 15:28	29 07	134 57	W	4
10	23	20:35 - 21:32	29 18	135 19	W	4
11	24	02:32 - 03:30	28 58	135 01	W	5
12	24	08:33 - 09:29	28 59	134 59	W	15
13	24	14:45 - 16:30	29 01	135 12	NW	10
14	24	20:34 - 21:28	29 34	134 49	NW	7
15	25	09:25 - 11:33	32 07	134 02	N	5
16	25	11:38 - 13:27	32 21	134 00	N	5
17	1 May	08:15 - 09:30	30 39	134 31	S	5
18	1	12:30 - 13:58	29 53	134 46	S	10
19	2	08:04 - 08:58	29 59	136 59	SW	7
20	2	14:02 - 14:58	29 01	136 59	W	7
21	2	20:03 - 20 59	28 13	136 59	SW	4
22	3	08:00 - 09:04	26 20	137 00	NE	7
23	3	14:03 - 14:58	25 40	137 00	E	5
24	3	20:10 - 21:10	25 06	137 00	SE	7
25	4	02:05 - 03:01	25 39	136 43	S	5
26	4	08:04 - 09:00	26 32	136 18	S	4
27		None				
28	4	20:05 - 20:58	27 31	135 51	S	10
29	5	02:02 - 02:58	28 25	135 26	S	10
30	5	05:03 - 06:00	28 39	135 19	SW	12
31	5	08:03 - 09:01	28 39	135 20	SW	10
32	5	11:00 - 11:58	28 39	135 20	SW	9
33	5	14:01 - 14:55	28 40	135 19	SW	9
34	5	17:01 - 17:58	28 38	135 20	W	7
35	5	20:00 - 20:58	28 39	135 20	SW	4
36	5	23:03 - 23:59	28 40	135 21	NW	6
37	6	02:01 - 02:58	28 39	135 19	NW	3
38	6	08:00 - 09:00	28 40	135 19	N	5
39	6	14:02 - 14:58	28 44	135 08	E	5
40	6	19:58 - 20:56	28 59	134 48	SE	4
41	7	14:02 - 14:59	29 10	134 57	SW	12
42	7	19:57 - 20:57	29 04	134 50	SW	14

7.1.2 Procedure for correction of ship motion

The wind sensor is fixed to the top of the foremast and sways with ship body. Therefore the observed wind velosity components relative to the frame fixed to the ship should be corrected for ship motion to obtain true velocity components relative to earth coordinate. This technique was developped by Mitsuta and Fujitani (1974), Fujitani (1981) and Fujitani (1985). It is explained briefly here.

The correction equation is expressed in vector notation as follows.

$$\underset{(A)}{\mathbf{V} = \mathrm{T}\,\mathbf{V}_{\mathrm{O}}} + \underset{(B)}{\Omega \times \mathrm{T}\,\mathbf{R}} + \underset{(C)}{\mathbf{V}_{\mathrm{S}}} \qquad (7.1.1)$$

where $\mathbf{V}$ is the wind velosity components relative to earth coordinate, $\mathbf{V}_{\mathrm{O}}$ is the observed wind velocity relative to ship coordinate, T is the coordinate transformation matrix, Ω is the angular velocity vector of the ship coordinate around the earth coordinate. $\mathbf{R}$ is the position vector of the wind sensor with respect to ship coordinate. The motion sensor is not located at the center of gravity of the ship body, and the last term (C) is rewritten as follows.

$$\mathbf{V}_{\mathrm{S}} = \mathbf{V}_{\mathrm{SO}} - \Omega \mathrm{x}\,\mathrm{T}\,\mathbf{L} \qquad (7.1.2)$$

where $\mathbf{V}_{\mathrm{SO}}$ = (Ship speed, O, Az dt) is the observed velosity vector of the ship translation and $\mathbf{L}$ is the position vector of the motion sensor (accelerometer). Here the vertical acceleration Az is transformed from observed value, Az_{O} with pitching angle, θ and rolling angle, ϕ (correction for ship careen).

$$\mathrm{Az} = \mathrm{Az}_{\mathrm{O}}/(\cos\theta \cos\phi) \qquad (7.1.3)$$

Fig. 7.1.2 shows an example of the correction for vertical wind velocity component. The time series shows observed (top) and three terms ((A), (B), (C)) in Eq. (7.1.1) and corrected (bottom) data.

Fig. 7.1.3 shows the comparison of power spectra of w component before and after correction. The dominant peak, which corresponds to peak of pitching and rolling motion, is almost reduced due to the correction procedure. The cospectra of u(longitudinal) and w(vertical), which contribute to momentum flux, shows remarkable improvement after the correction.

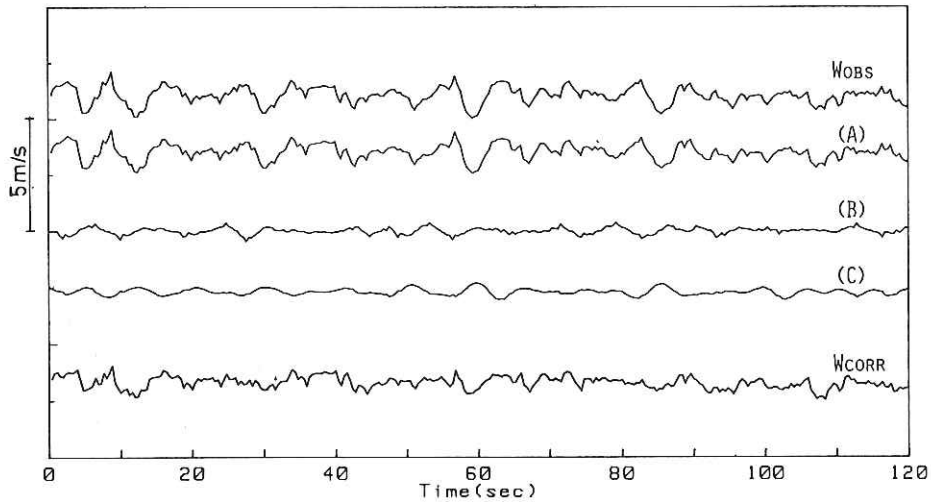

Fig. 7.1.2 An example of time series through correction process for vertical velocity. The top time series is the raw data observed on the swaying mast. Middle three lines are correction terms (A), (B) and (C) in Eq. (7.1.1). The bottom is the corrected vertical velocity (=(A)+(B)+(C)).

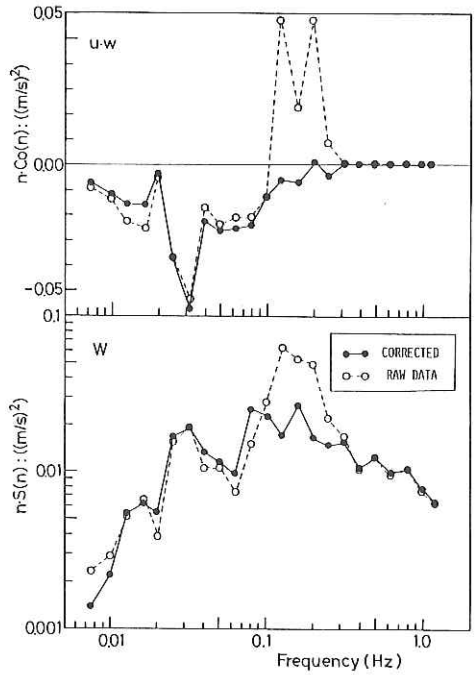

Fig. 7.1.3 Examples of power spectra of vertical velocity and cospectra between longitudinal and vertical components of wind velocity before and after the correction.

7.1.3 Preliminary results

Turbulent fluxes of momentum, sensible heat and latent heat (water vapor flux) were calculated for a part of the data and tabulated in Table 7.1.2. Large amount of momentum flux was transferred to the sea surface during high wind condition but heat fluxes were not obtained due to rain fall. Turbulent fluxes of sensible heat and latent heat were small except for runs over Kuroshio (Run 15, 16). Stability parameter, z/L ranged from -1.0 to 0.2 for the most part and Bowen ratio is roughly estimated as 0.2 – 0.3 for the cases of upward heat fluxes. Haet fluxes over Kuroshio is about two or three times larger than those at point 'Tango'.

In order to evaluate bulk transfer coefficients, C_D, C_H and C_E turbulent fluxes are plotted against U^2, $U\Delta T(\Delta T=T_s-T_{air})$ and $U\Delta q(\Delta q=q_s-q_{air})$ in Fig.7.1.4. According to this preliminary results, transfer coefficients are roughly evaluated as $C_D=1.0\times10^{-3}$, $C_H=1.5\times10^{-3}$ and $C_E=0.8\times10^{-3}$.

Further efforts will be continued to calculate turbulent fluxes for other runs.

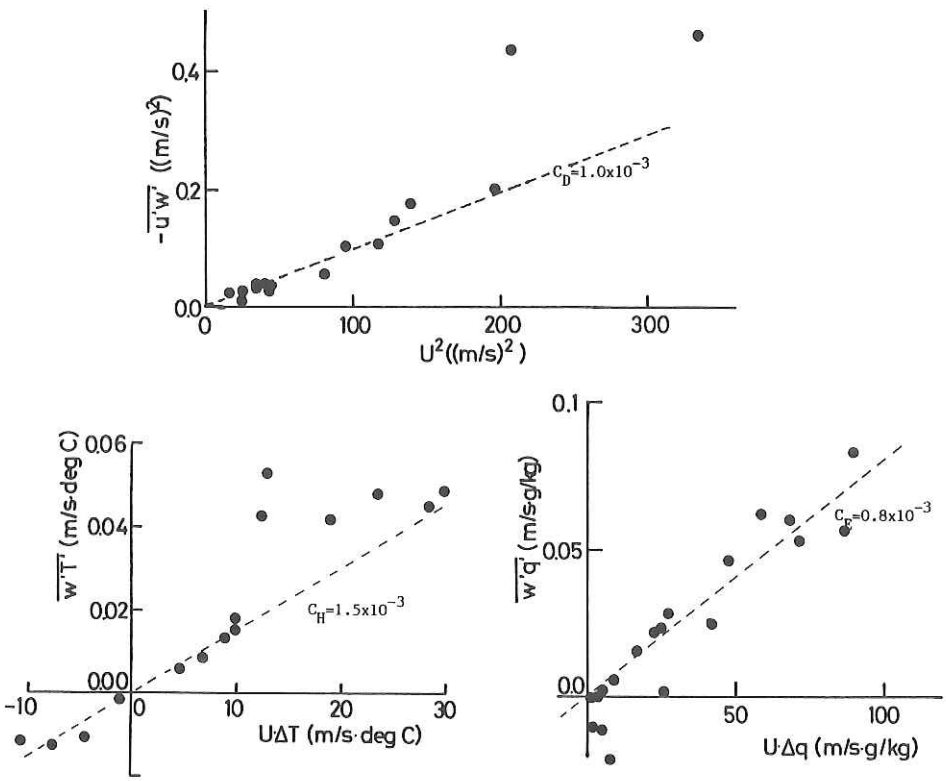

Fig. 7.1.4 Turbulent fluxes versus bulk parameter, U^2, $U\Delta T$ and $U\Delta q$. Dashed lines are roughly fitted by eyes.

Table 7.1.2 Preliminary results of turbulent fluxes

Run	Date	Time	U (m/s)	σu (m/s)	σw (m/s)	σT (°C)	σq (g/kg)	τ (N/m²)	H (W/m²)	E (W/m²)
1	16 Apr	18:00 - 18:30	2.3	0.51	0.38	0.11	-0.23	-	18	63
2	18	08:09 - 08:39	18.2	1.5	0.81	-	-	0.55	-	-
4	18	15:41 - 16:11	14.4	1.4	0.78	-	-	0.53	-	-
6	22	02:59 - 03:29	6.0	0.43	0.26	0.027	0.056	0.045	1.6	17
8	23	02:56 - 03:26	4.9	0.52	0.25	0.078	0.030	0.013	10	4.9
11	24	02:34 - 03:04	6.5	0.56	0.27	0.053	0.22	0.032	7.4	72
15-1	25	09:59 - 10:29	4.1	0.79	0.41	0.18	0.23	-	51	133
15-2	25	10:30 - 11:00	5.1	0.79	0.42	0.18	0.26	-	58	180
16-1	25	12:07 - 12:37	5.9	0.69	0.40	0.20	0.37	-	56	175
16-2	25	12:38 - 13:08	6.2	0.69	0.46	0.19	0.33	-	59	155
17-1	1 May	08:24 - 08:54	4.0	0.42	0.15	0.077	0.074	0.029	-2.2	-2.6
17-2	1	08:55 - 09:25	6.4	0.38	0.24	0.042	0.034	0.046	0.7	6.6
22-1	3	08:21 - 08:51	5.9	0.41	0.27	0.085	0.20	0.040	16	68
22-2	3	08:52 - 09:22	6.6	0.39	0.29	0.097	0.19	0.045	22	83
28	4	20:12 - 20:42	8.9	0.43	0.30	0.094	0.077	0.068	-13	-26
30	5	05:04 - 05:34	10.8	0.71	0.40	0.091	0.068	0.13	-15	-34
31	5	08:06 - 08:36	9.7	0.64	0.36	0.087	0.10	0.10	-14	-31
40	6	19:59 - 20:29	5.0	0.35	0.20	0.015	0.16	0.032	0.5	46
42	7	20:27 - 20:57	14.0	0.90	0.55	0.11	0.095	0.24	21	-61

References

Mitsuta, Y. and T. Fujitani, 1974: Direct measurement of turbulent fluxes on a cruising ship, Boundary Layer Meteorology, **6**, 203-207.

Fujitani, T. 1981: Direct measurement of turbulent fluxes over the sea during AMTEX, Papers in Meteorology and Geophysics, **32**, 119-134.

Fujitani, T. 1985: Method of turbulent flux measurement on a ship by using a stable platform system, Papers in Meteorology and Geophysics, **36**, 157-170.

7.2 Turbulent transport of carbon dioxide over the ocean

E. Ohtaki, O. Tsukamoto
(College of Liberal Arts and Sciences, Okayama University)
H. Ishida
(Kobe University of Merchantile Marine)
and
M. Horiguchi
(Disaster Prevention Research Institute, Kyoto University)

7.2.1 Objective and instrument

The accurate measurement of turbulent transport of carbon dioxide over the ocean has been expected to achieve deep understanding of carbon dioxide – climate problem. The objective of the present study is to examine the possibility of meteorological approaches for flux measurements of carbon dioxide over the ocean. The aerodynamic, eddy correlation and NIFTI (Near Isotropic Flux Turbulence Instrumentation) techniques were examined in this study.

Main instruments used in the present experiment were briefly described here. The carbon dioxide concentration was measured by the infrared gas analyser in differential type (Shimazu Co. URA-106). In the present experiment, a standard gas of fixed concentration of carbon dioxide (350 ppm) was continuously passed through the reference cell at the rate of 5 ml per min to maintain the constant sensitivity of the analyser. The calibration was carried out at the beginning and the end of the present KH-88-2 cruise using standard gases of carbon dioxide. The results showed that there was no appreciable change in the sensitivity. It was 80.8 mg m^{-3} per volt. Air samples were alternately drawn from 5 m and 23 m above the sea surface. Three-way solenoid valves activated this cyclic processes every 5 min. Sampled air was pre-dried by passing through a refrigerator maintained at 2°C before passing through the sampling cell. In order to reduce the effect of remaining water vapor on carbon dioxide measurements, the interference narrow band-pass filter was inserted in front of an infrared detector. This filter isolates the infrared beam of 4.3 μm which corresponds to the absorption band of carbon dioxide molecules. The output voltage of the instrument was recorded on a selfbalancing potentiometric recorder.

We developed an infrared instrument for measuring fluctuations of atomospheric carbon dioxide concentration (Ohtaki and Matsui, 1982). Noise and drift

of the latest model of the carbon dioxide instrument were about 1.4 mg m^{-3} in peak to peak and 1.7 mg m^{-3} hour. The infrared instrument of carbon dioxide and a three dimensional sonic anemometer-thermometer (Kaijo Denki Co., DAT-310) were fixed at the bow of 10 m height above the sea surface. Output voltages of fast response instruments mentioned above were digitized and then stored on a floppy disk at the rate of 10 Hz under control of personal computer (NEC, PC9801F).

The routine wind speed data measured at the top of mast (23 m height above the sea surface) were used in a computation of carbon dioxide fluxes by the aerodynamic technique.

7.2.2 Carbon dioxide flux estimated by the aerodynamic technique

The upward flux of carbon dioxide is estimated from the working formula under near neutral conditions:

$$F = A \cdot U23\,(C5 - C23), \tag{7.2.1}$$

with

$$A = k^2(1 - U5/U23)/[\ln Z23 - \ln Z5]^2, \tag{7.2.2}$$

and

$$U5/U23 = [\ln Z5 - \ln Z_0]/[\ln Z23 - \ln Z_0], \tag{7.2.3}$$

where k is the von Kármán constant (0.4), and U5, U23 and C5, C23 are the wind speed and carbon dioxide concentration at two heights Z5 (5 m) and Z23 (23 m) above the sea surface. Z_0 is the roughness length of the sea surface. The value of Z_0 was assessed to be 0.01 to 0.1 cm over the sea water for moderate wind speed by many researchers (e.g., Kondo, 1977). Inserting values of Z_0 into Eq.(7.2.3), U5/U23 can be assessed to be 0.85 within errors of 5 per cent for moderate wind speed. Inserting parameters mentioned above into Eq.(7.2.2), we obtain the value of A, and then we can estimate the carbon dioxide flux. The above procedure involves an assumption that the vertical profiles of carbon dioxide and wind speed are both represented by a logarithmic law.

The cabon dioxide gradient between 5 and 23 m over the sea surface was measured from April 16 to 23 (leg 1), and May 1 to 10 (leg 2) with reliable operation of the infrared gas analyser around the fixed station (29°N, 135°E). During these periods the stratification of the air layer was unstable in the night-time and near neutral in the daytime.

Fig. 7.2.1 shows wind speed at 23 m height, carbon dioxide gradient and fluxes estimated with Eq. (7.2.1) for three-day period 2 to 4 May 1988. the wind speed is moderate during these three days. the gradient of carbon dioxide concentration becomes large in the nighttime under lapse conditions, and it reduces to near zero in the daytime under near neutral or inversion conditions. The observed upward flux of carbon dioxide is about 0.02 mg $m^{-2}s^{-1}$ in the daytime. At night, much higher values of upward flux result from a large gradient of carbon dioxide concentration.

The daily means of carbon dioxide flux (F), gradient (ΔC) between 5 and 23 m and wind speed (U) at 23 m above the sea surface are summarized in Table 7.2.1. It is interested to see that the carbon dioxide is transported upward throughout the present cruise, and fluxes range from 0.02 to 0.10 mg $m^{-2}s^{-2}$. These values of carbon dioxide fluxes are comparable with those obtained at Sable Island (0.022-0.035 mg $m^{-2}s^{-1}$, Jones and Smith, 1977), off the coast of Florida (0.05-0.35 mg $m^{-2}s^{-1}$, Wesely et al., 1982) and Seto Inland Sea (0.035-0.049 mg $m^{-2}s^{-1}$, Ohtaki, 1986).

Table 7.2.1 Daily means of carbon dioxide flux (F), gradient (ΔC) between 5 and 23 m, and longitudinal wind velocity measured routinely at 23 m height above the sea surface.

Day	No of runs	U m s^{-1}	ΔC mg m^{-3}	F mg m^{-2} s^{-1}
April				
16	10	3.0 ± 1.4	1.59 ± 0.91	0.041 ± 0.019
17	9	7.7 ± 1.4	0.62 ± 0.37	0.048 ± 0.028
18	6	13.5 ± 2.7	0.73 ± 0.30	0.100 ± 0.042
19	11	6.1 ± 2.2	1.19 ± 0.59	0.068 ± 0.034
20	10	3.0 ± 1.3	0.79 ± 0.43	0.023 ± 0.015
21	6	6.7 ± 1.7	0.71 ± 0.53	0.047 ± 0.033
22	9	8.5 ± 1.2	0.94 ± 0.89	0.080 ± 0.068
23	13	5.6 ± 1.3	0.75 ± 0.23	0.042 ± 0.010
May				
1	19	6.5 ± 2.6	0.59 ± 0.29	0.035 ± 0.015
2	14	5.6 ± 1.5	0.53 ± 0.57	0.028 ± 0.032
3	13	5.1 ± 1.8	0.68 ± 0.43	0.030 ± 0.016
4	15	4.3 ± 2.0	0.61 ± 0.28	0.026 ± 0.015
5	8	8.4 ± 2.7	0.60 ± 0.55	0.045 ± 0.036
6	7	5.0 ± 1.3	0.44 ± 0.24	0.023 ± 0.012
7	11	10.8 ± 2.8	0.25 ± 0.25	0.027 ± 0.031
9	8	7.5 ± 0.8	0.47 ± 0.28	0.036 ± 0.022
10	7	7.2 ± 0.8	0.31 ± 0.20	0.023 ± 0.015

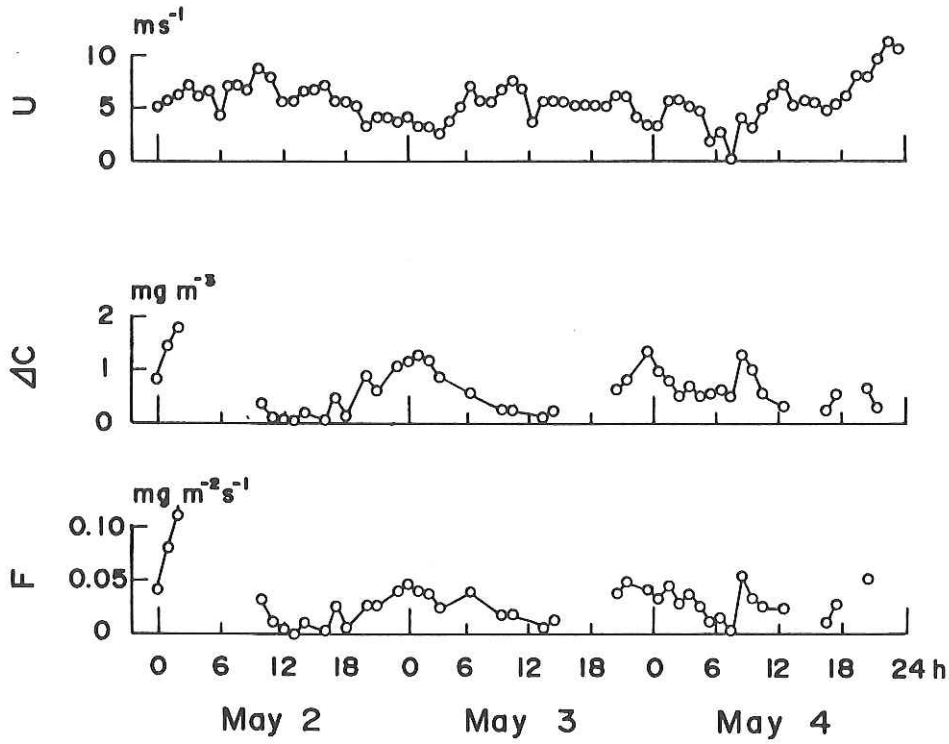

Fig. 7.2.1 Typical examples of diurnal variation of wind speed at 23 m above the sea surface, carbon dioxide difference between 5 and 23 m and flux estimated by the aerodynamic technique.

7.2.3 Carbon dioxide flux estimated by the eddy correlation technique

The vertical carbon dioxide flux, F, is directly estimated by the eddy correlation technique as follows:

$$F = \int_{n_L}^{n_H} Cwc(n)\, dn. \qquad (7.2.4)$$

Here, Cwc(n) is the cospectral density between vertical wind velocity (w) and carbon dioxide concentration (c). n is the frequency in Hz. The low frequency limit n_L is specified by the sampling time. The high frequency limit n_H should be sufficiently high to cover the highest frequencies contributing to the covariance $\overline{w'c'}$. Ohtaki and Matsui (1982) indicated that the low and high limiting frequencies were about $n_L = 0.002$ and $n_H = 2$ Hz for wc-cospectrum obtained over a wheat field.

The wc-cospectra are calcurated by Tuckey's scheme using data obtained

from May 3, 1988, and results are plotted in Fig. 7.2.2. The abscissa is the frequency n and the ordinate is the cospectral density multiplied by n. It is noted that the cospectra are limited nearly zero for almost all frequencies without a large positive peak for frequencies from 0.1 to 0.2 Hz. This peak represents the effect induced by pitching and rolling of the ship motion. During observation

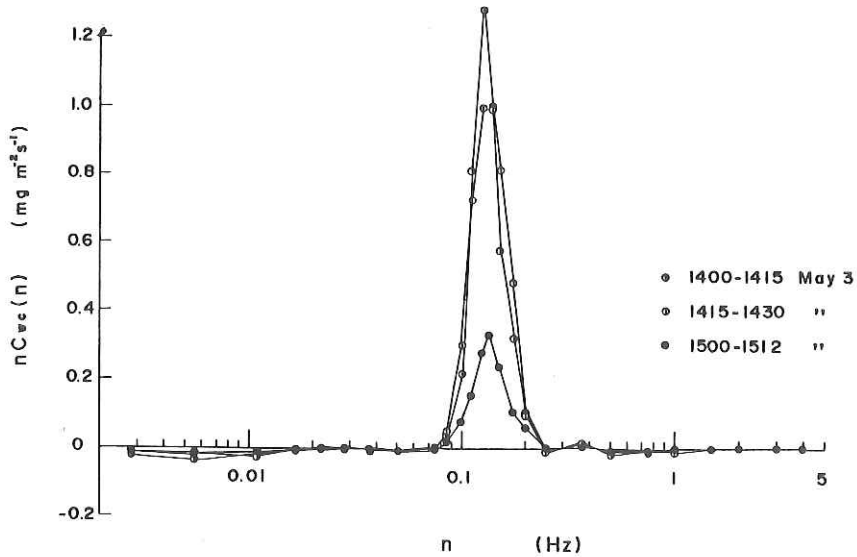

Fig. 7.2.2 Examples of wc-cospectral estimate. Large peak at 0.15 Hz represents the effects of ship motion induced by the ocean swell. The infrared carbon dioxide sensor was suspended from the boom during period of 1500-1512.

from 1500 to 1512, the infrared carbon dioxide sensor was suspended from the boom. The cospectrum shows that the swell effect is largely reduced compared with other examples. The carbon dioxide sensor should be mounted carefully for experiments abroad a ship. Mitsui and Fujitani (1974) proposed the scheme for correction of pitching and rolling effects. Unfortunately, the large components of wc-cospectra induced by ship motion can not be eliminated with correction in the present study.

We would like to notice here that if the sensor is fixed on a rigid platform over the sea water, the eddy correlation technique is useful to measure the carbon dioxide flux directly. During the autumn in 1986 and 1987, the same carbon dioxide sensor was mounted on a pier in conjunction with a sonic anemometer to measure the carbon dioxide flux over the ocean with the eddy correlation tech-

nique. The results showed that the infrared instrument of carbon dioxide was adequate in sensitivity and response time for measurements of carbon dioxide fluctuations.

7.2.4 Carbon dioxide flux estimated by the NIFTI technique

The cabon dioxide flux can be estimated by the NIFTI technique. This technique was first proposed by Hicks and Dyer (1972). Tsukamoto (1974) developed nomographs to estimate fluxes of momentum, sensible heat and latent heat by the NIFTI technique. Appling their ideas to carbon dioxide transport, we can estmate carbon dioxide flux from spectra of carbon dioxide and longitudinal wind velocity in the inertial subrange as

$$F = \frac{(2\pi k)^{\frac{2}{3}}}{\sqrt{\alpha_c\, \alpha_u\, \phi_N\, \phi_\varepsilon^{\frac{1}{3}}}} \sqrt{Sc(n)\, Su(n)} \left(\frac{z}{u}\right)^{\frac{2}{3}} n^{\frac{5}{3}},$$

$$= 2.68 \sqrt{Sc(n)\, Su(n)} \left(\frac{z}{u}\right)^{\frac{2}{3}} n^{\frac{5}{3}}. \qquad (7.2.5)$$

Here, k is the von Kármán constant, α_c and α_u are the Kolmogoroff constant for carbon dioxide and longitudinal wind velocity. We already proposed $\alpha_c = 0.89$ and $\alpha_u = 0.53$ in the previous paper (Ohtaki, 1982). ϕ_ϵ and ϕ_N are the dimensionless form of dissipation for kinetic energy and carbon dioxide variance. These two parameters are considered as 1 under near neutral conditions. Sc(n) and Su(n) are the spectral density of carbon dioxide and longitudinal wind velocity in the inertial subrange.

Fig. 7.2.3 shows the power spectral densities of carbon dioxide calculated using data obtained on 3 May, 1988. The spectral peak appears at about 0.15 Hz, corresponding to the period of ship motion induced by an ocean swell. This may be associated with the fact that stems of carbon dioxide sensor are a little bit distorted by the ship motion. We can see from Fig. 7.2.3 that power spectra show a -5/3 power law in high frequency regions above 0.01 Hz, though they are affected by the white noise of the sensor in high frequency regions above 0.5 Hz.

Fig. 7.2.4 shows the spectral densities of longitudinal wind velocity observed on 3 May, 1988. The spectral densities apparently show a -5/3 power law in high

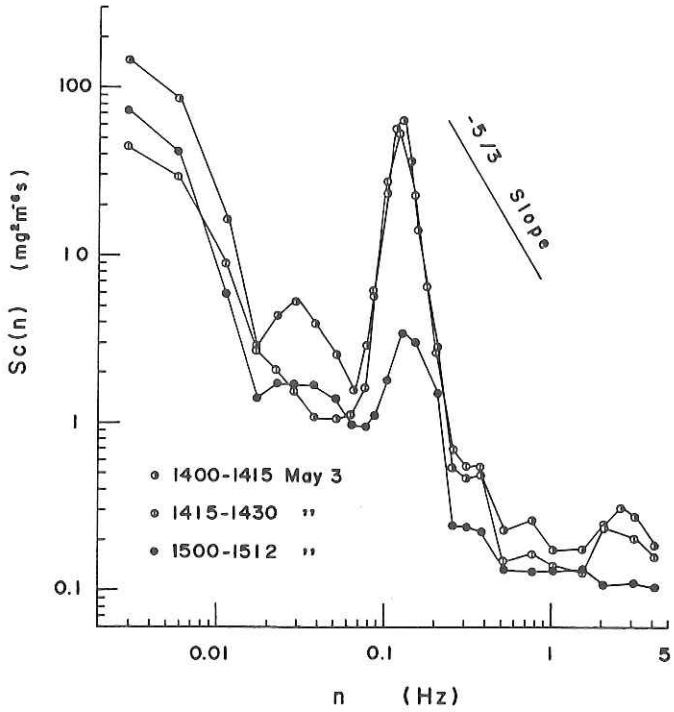

Fig. 7.2.3 Power spectral densities of carbon dioxide fluctuations. The spectral peak at about 0.15 Hz was caused by the distortion of the stems of the sensor due to ocean swell. The power spectral shapes represent that the carbon dioxide signal is affected by the white noise in high frequency ranges above 0.5 Hz.

frequencies, though the peak corresponding to the wind fluctuations induced by the ship motion is clearly seen arround 0.15 Hz.

The vertical flux of carbon dioxide can be calculated using the spectral intensity in an inertial subrange and wind speed. In the present study, we would like to use the spectral intensity at $n = 0.3$ Hz, because it is not significantly distorted at that fequency by the effects of swell and white noise. For the case of 1500-1512, May 3, the spectral intensity is about 0.2 mg^2 m^{-6} s for carbon dioxide and 0.03 m^2 s^{-1} for longitudinal wind velocity. The wind speed at that period was 5.5 m s^{-1} at 10 m height. Inserting these parameters into Eq.(7.2.5), we obtain the carbon dioxide flux being 0.04 mg m^{-2} s^{-1} This is about twice the value estimated by the aerodynamic technique (cf. Fig. 7.2.1). This discrepancy mainly comes from the uncertainty of spectral intensity of carbon dioxide in the inertial subrange. If we use the value of 0.03 mg^2 m^{-6} s, which corresponds to

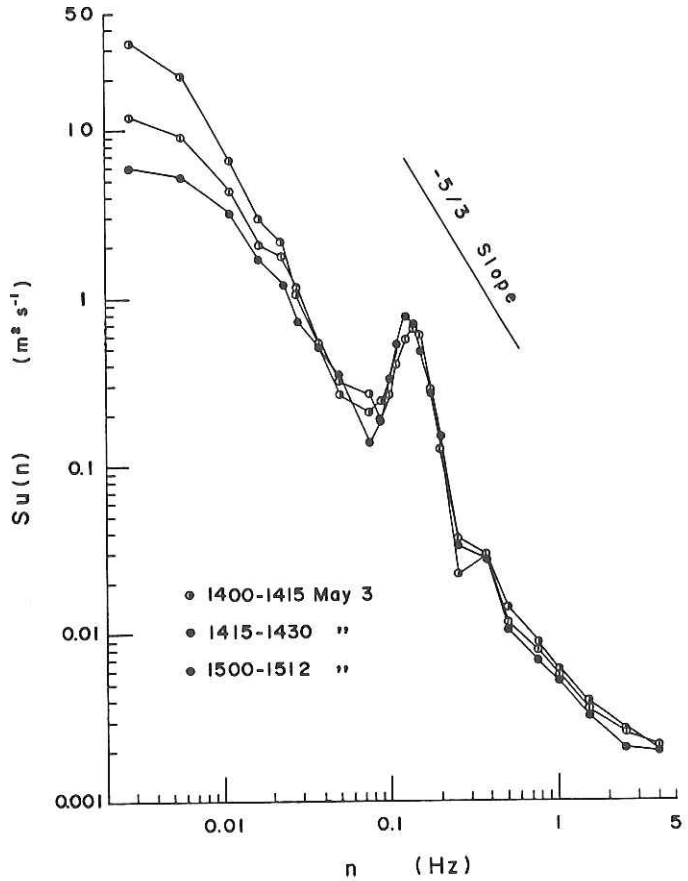

Fig. 7.2.4 Power spectral densities of longitudnal wind velocity fluctuations. The spectral peak at about .15 Hz was caused by the ship motion due to ocean swell.

the extrapolated value of spectral intensity from low frequency regions, the carbon dioxide flux is modified to be 0.02 mg m^{-2} s^{-1}. Similar values of carbon dioxide flux can be obtained from other runs by the NIFTI technique.

7.2.5 Concluding remarks

Three meteorological techniques are examined to measure the carbon dioxide flux over the ocean. The primary results we obtained are summarized as follows:
(1) The carbon dioxide gradient between 5 and 23 m above the sea surface is about 0.7 mg m^{-3}. This is measurable by the infrared gas analyser (URA-106). We convinced from the present study that the aerodynamic technique is applic-

able to measure the carbon dioxide flux abroad a ship.

(2) The power spectral estimate of carbon dioxide is affected by pitching and and rolling of the ship motion. This may be caused by the stem distortion of the carbon dioxide sensor due to ship motion. Effects of the ship motion are too large to obtain the significant fluxes of carbon dioxide in the present study.

(3) The NIFTI technique is applicable to measure the carbon dioxide flux over the ocean. the accuracy of the technique depends on the spectral shape of the carbon dioxide fluctuations in the intertial subrange.

References

Jones, E. P. and S. D. Smith, 1977: A first measurement of sea-air CO_2 flux by eddy correlation. J. Geophys. Res. 2, 5990-5992.

Hicks, B. B. and A. J. Dyer, 1972: The spectral density technique for the determination of eddy fluxes. Quart. J. Roy. Meteorol. Soc. **98**, 838-844.

Kondo, J. 1977: Geostrophic drag and the cross-isobar angle of the surface wind in a baroclinic convective boundary layer. J. Meteorol. Soc. Japan. **55**, 301-311.

Mitsuta, Y. and T. Fujitani, 1974: Direct measurement of turbulent fluxes on a cruising ship. Boundary-Layer Meteorol. **6**, 203-217.

Ohtaki, E. 1982: The Kolmogorov constant for carbon dioxide in the atmospheric surface layer over a paddy field. Boundary-Layer Meteorol. 23, 153-159.

Ohtaki, E. 1986: Measurements of carbon dioxide flux over a shallow coastal water. J. Meteorol. Soc. Japan. **64**, 161-166.

Ohtaki, E. and T. Matsui, 1982: Infrared device for simultaneous measurement of fluctuations of atmospheric carbon dioxide and water vapor. Boundary-Layer Meteorol. **24**, 109-119.

Tsukamoto, O. 1974: Application of NIFTI method for field measurment of turbulent fluxes. Bull. Disas. Prev. Res. Inst. Kyoto Univ. **24**, 281-293.

Wesely, M.L.D.R. Cook, R.L. Hart and R. M. Williams, 1982: Air-sea exchange of CO_2 and evidence for enhanced upward fluxes. J. Geophys. Res. **87**, 827-8832.

8. On-board quantitative wind-wave observations using a stop watch

Y. Toba, S. Kizu and N. Ebuchi
(Department of Geophysics, Tohoku University)

8.1 Introduction

For the on-board routine observation of ocean waves, estimates of the wave heights of wind waves and swells, or estimates of wind-wave and swell classes, are performed by the crew of the observation vessels. For special purposes, on-board pressure-sensor or sonic wave recorders are sometimes used for more quantitative wave observations. In this report, we present observations of significant wave period for wind waves by using a stop watch. The observations are rather easy by watching foam patches or other materials floating on the water surface. When the wave field consists essentially of wind waves, it will be shown that the significant wave height can also be obtained successfully from the significant wave period and the wind speed, by using the 3/2-power law of wind waves.

Fifteen years ago, one of the authors used this method effectively on-board the Hakuho Maru on her KH-69-3 and KH-70-3 Cruises, as part of a series of observations of wave breaking, whitecapping and droplet production on the sea surface (Toba and Chaen, 1973; Chaen, 1973). However, quantitative examination of the validity of the observed wave period by comparison with independently measured data was not done at that time.

Recently, a question of a significant dependence of the sea-surface wind stress on the wind waves characteristics was raised by our group (Toba et al., 1988). In order to consider the possibility of improvement of the method of simple routine wave observations, we have done some systematic examinations of the present method of wind-wave observations by using a stop watch, during the OMLET Cruise of the Hakuho Maru (KH-88-2). The stop watch data was compared with the data obtained by the Ocean Data Buoy off Shikoku (29°N, 135°E) which is operated by the Japan Meteorological Agency (JMA), and also with Wave Charts compiled from ships' reports by the JMA.

8.2 Measurement of wave period by using a stop watch

The principle of the method of observation is to watch some floating sub-

stance such as a foam patch, and to measure by a stop watch the period of two waves, that is, to measure a time interval between the moment when a foam patch comes to the top of a crest, and the moment when it comes to the top of the crest following the next crest, i.e., the time for two waves to pass. After repeating this procedure ten or twenty times, an average wave period can be obtained. We name this average value T_0, hereafter.

The reason why we measure the period of two waves is as follows. There is a possibility that T_0 values from two-wave periods will give a more useful average wave period than averages of one-wave periods, since the latter case we will have a tendency to watch only most dominant waves. Also, if we intend to measure three successive waves, we are apt to lose the third wave.

In Table 8.1 is shown an example of the measurement at about 8:40 of 18 April 1988. It contains a set of twenty measured two-wave periods, and T_0 values which have been obtained by averaging five original data, ten data and twenty data, respectively. It is seen from the table that the averages of ten original data are very close to the average of twenty original data. If we consider the standard deviations, we can say that the averaged values from twenty or ten original values are reliable ones.

Table 8.1 Example of wave period measurement

Two-wave period original data (s)	14.7	13.2	15.8	14.0	Other data
	12.5	15.8	15.0	15.8	Time: 8:30-8:45, 18 April 1988
	14.4	15.6	13.8	15.4	Position: 28°58'N, 133°35'E
	16.3	14.2	13.6	16.0	Ship heading: 134° (SE)
	15.0	17.5	13.2	14.6	Ship speed: 2.5kt
T from 5-data set	7.29	7.63	7.14	7.58	Relative wind: 10°, 22.0-19.5 m/s
	±0.61	±0.73	±0.48	±0.38	Wind direction: 144° (SE)
					Pressure: 1009.5mb
T from 10-data set	7.46±0.70		7.36±0.49		Air temp.: 19.0 °C
					Water temp.: 20.6 °C
T from 20-data set	7.41±0.60				

The above observation was done in a condition when a cyclone was approaching from the west, wind waves were growing, and swells were not significant compared to the wind waves. Table 8.2 contains all the data of our wave measurement during the present cruise, together with the wind data. As seen from Run nos. 1-6, as the cyclone approached the vessel site, changes in wind

direction affected the purity of wind waves, and caused the increase in the standard deviations of T_0 values. This is an inference from observation of the sea state by eye. Though we have no wave spectral data, it is inferred that the wave spectra should have been simplest at 8:40.

An effect of wind drift may influence the observation of the wave period. We can use the following relationship for the wind drift u_s proposed by Tokuda and Toba (1982):

$$u_s = 0.21\, u_*,$$

where u_* is the friction velocity of air. For the smallest reliable value of T_0 in Table 8.2; the linear phase speed of 1.5 s wave is 2.3 ms^{-1}, whereas under a 10 m wind speed of 6 ms^{-1}, u_s is of the order of 0.04 ms^{-1}, and the correction of T_0 that is needed is of the order of 2%. As T_0 becomes large, this effect becomes even smaller.

In order to examine quantitatively to what frequency the T_0 value corresponds of the wave energy spectrum, it is necessary to make a comparison of thus measured values with quantitative wave measurements at a site such as an oceanographic tower station. However, this time we will compare our data with data of Ocean Data Buoy of the JMA situated rather close to our vessel, and JMA's Wave Chart, in section 8.3

The above method of wave-period observation is also applicable for swell period, if we select a certain component of swells as the object of observation.

Table 8.2 Data of observation during the KH-88-2 Cruise

Run no.	Day	Time	Wind at 22m level		Observed wave period (wind waves)	Remarks
			Direction (from N)	Speed (m/s)	T_o(s)	
1	4/18	8:40	144.0	20.7	7.41+0.60	
2	18	10:27	165.0	14.3	7.86+0.87	
3	18	13:30	176.0	14.9	8.13+1.35	
4	18	14:18	--	--	---	Passage of front
5	18	15:00	310.0	13.3	not measurable	Swell: 7 8s
6	18	17:05	310.0	13.3	5.16+1.01	
7	19	8:40	315.0	7.8	not measurable	Swell: 7.66+0.80s
8	20	8:10	170.0	3.6	~1	
9	20	15:20	95.0	4.9	~1	
10	21	9:00	135.0	5.4	~1	
11	21	11:15	150.0	3.6	~1.5	
12	21	12:45	145.0	7.7	1.90+0.24	
13	21	15:00	145.0	9.7	2.92+0.26	
14	21	17:10	150.0	8.8	3.45+0.35	
15	22	10:00	325.0	7.6	2.78+0.36	Swell: 5.43+0.65s
16	22	13:20	25.0	6.5	3.48+0.50	
17	22	15:30	330.0	8.5	3.71+0.46	
18	23	9:05	340.0	7.2	1.86+0.27	Swell: 6.82+1.22s
19	23	12:30	330.0	5.4	not measurable	Swell: 6.6s
20	23	13:55	335.0	3.1	< 1	Swell: 5.8s
21	23	14:50	285.0	5.0	< 1	Swell: 6.6s
22	24	8:50	295.0	14.0	6.19+0.59	
23	24	9:55	300.0	17.1	6.34+0.37	
24	24	12:25	305.0	14.0	6.68+0.79	
25	24	13:50	305.0	10.2	7.46+1.03	
26	24	14:55	300.0	12.6	7.54+1.46	
27	24	17:15	310.0	8.9	6.79+1.31	
28	25	8:45	340.0	4.2	~1	Swell: 4s
29	25	12:15	300.0	5.2	1.46+0.23	
30	25	15:20	275.0	8.3	1.92+0.36	
31	25	17:30	260.0	11.1	2.70+0.53	
32	5/ 1	9:20	177.0	8.0	1.93+0.18	
33	1	12:45	174.0	9.8	2.84+0.22	
34	1	16:00	176.5	9.8	2.96+0.38	
35	2	8:30	251.0	7.7	1~1.5	
36	3	10:00	126.0	6.6	≲ 1	
37	3	15:15	90.0	4.9	< 1	
38	4	12:00	282.0	4.7	< 1	
39	4	15:00	214.0	5.8	< 1	
40	5	10:40	248.0	9.2	not measurable	
41	5	15:30	277.0	7.4	3.42+0.55	Swell: 6.27+0.76s
42	6	10:10	77.0	5.8	not measurable	Swell: 7.52+0.53s
43	6	14:50	99.0	3.1	< 1	Swell: 6.38+0.49s
44	7	12:00	187.0	10.5	3.87+0.45	
45	7	15:00	216.0	12.0	4.00+0.38	
46	7	16:10	217.0	14.8	4.52+0.34	
47	7	18:00	221.0	13.4	5.07+0.32	
48	8	11:55	28.0	14.1	6.90+0.85	
49	8	13:50	25.0	11.5	7.63+1.16	
50	8	16:00	40.0	11.3	7.07+1.50	
51	9	10:00	82.0	7.3	not measurable	
52	9	12:00	67.0	7.3	not measurable	Swell: 6.89+0.82s
53	9	14:00	35.0	8.3	not measurable	Swell: 6.21+0.70s
54	10	8:10	36.0	6.7	2.14+0.19	
55	10	11:00	81.0	5.1	not measurable	

Table 8.3 Significant wave period for wind waves T_s (=1.13T_o) and estimated wave height H_s from T_s by using the 3/2-power law.

Run no.	Day	Time	T_s(s)	H_s(m)	Run no.	Day	Time	T_s(s)	H_s(m)
1	4/18	8:40	8.37	5.5	27	4/24	17:15	7.67	2.9
2	18	10:27	8.88	4.8	29	25	12:15	1.65	0.2
3	18	13:30	9.19	5.2	30	25	15:20	2.17	0.4
6	18	17:05	5.83	2.4	31	25	17:30	3.05	0.8
12	21	12:45	2.15	0.4	32	5/ 1	9:20	2.18	0.4
13	21	15:00	3.30	0.8	33	1	12:45	3.21	0.8
14	21	17:10	3.90	1.0	34	1	16:00	3.34	0.8
15	22	10:00	3.14	0.6	41	5	15:30	3.86	0.9
16	22	13:20	3.93	1.0	44	7	12:00	4.37	1.3
17	22	15:30	4.19	1.1	45	7	15:00	4.52	1.5
18	23	9:05	2.10	0.3	46	7	16:10	5.11	2.0
22	24	8:50	6.99	3.3	47	7	18:00	5.73	2.3
23	24	9:55	7.16	3.8	48	8	11:55	7.80	3.9
24	24	12:25	7.55	3.7	49	8	13:50	8.62	4.0
25	24	13:50	8.43	3.6	50	8	16:00	7.99	3.5
26	24	14:55	8.52	4.2	54	10	8:10	2.42	0.4

8.3 Estimation of significant wave height from the significant wave period

For wind waves which are in local equilibrium with the wind, the following 3/2-power law holds (Toba, 1972; Toba, 1988):

$$gH_s/u_*^2 = B\,(gT_s/u_*)^{3/2},\ B = 0.062, \tag{8.1}$$

where g is the acceleration of gravity, H_s and T_s the significant wave height and period, respectively, u_* is the friction velocity of air, and B is considered as a universal constant. The logarithmic wind profile is applicable to the atmospheric boundary layer over the sea when the sea-air temperature difference is not large, especially under strong wind conditions:

$$U_z/u_* = (1/k)\ln(z/z_0), \tag{8.2}$$

where U_z is the wind speed at a height of z, k(=0.4) is the von Karman constant and z_0 is the roughness length. There is a new formula for Z_0 such as

$$z_0\,\sigma_p/u_* = \gamma,\quad \gamma = 0.025, \tag{8.3}$$

which was proposed by Toba and Koga (1986) and supported by Brutsaert and Toba (1986) and Toba et al. (1988), and where σ_p is the spectral peak frequency

of wind waves which can be related to T_S by

$$\sigma_P = 2\pi/1.05T_S \tag{8.4}$$

(cf. Mitsuyasu, 1968 and Toba, 1978).

Since the system of these equations are closed, we can estimate the significant wave height H_S from the observed wave period T_0 and wind speed obtained on-board the vessel. When swells are not significant compared to wind waves, that is, when the wave field is essentially of pure wind waves which are in local equilibrium with the wind. It is necessary to assume a relation between T_S and the observed T_0.

We will examine this procedure also in the next section, by comparing the deduced heights with other sources of data.

8.4 Comparison of the observed data with other sources of data

The Ocean Data Buoy of JMA was moored at 29°N, 135°E off Shikoku, and it became operated on 26 April 1988 (just after our leg 1 period). Consequently, only data obtained during leg 2 can be compered with the Buoy data. Although the exact location of the Hakuho Maru was not necessarily very close to the Buoy, she was generally in the same area off Shikoku; the largest separation was about 500 km. The other source of data is daily Wave Charts compiled from ships' records by the JMA. These are available during the whole period.

Fig. 8.1(a) and (b) show wind direction and wind speed, respectively, obtained from the routine meteorological data of the Hakuho Maru (dots, at 22 m level) and data of the Ocean Data Buoy (lines, at 7.5 m level).

Fig. 8.1(c) shows the observed wave period data as closed circles, but converted to values of T_S from T_0 by an assumption of

$$\overline{T} = T_0, \quad T_S = 1.13\overline{T}, \tag{8.5}$$

where $\overline{T}$ is the average wave period (cf. Toba et al., 1988). It also shows the value of T_S estimated from data of $\overline{T}$ of the Buoy by a continuous line. It is seen that the both data are very close on 8 May, when the wind speed was maximum.

Fig. 8.1(d) contains the significant wave height H_S, estimated from the Buoy's average wave height $\overline{H}$ data by using

$$H_S = 1.6\overline{H} \tag{8.6}$$

after Longuet-Higgins (1952) by the thick line. The thin line shows H_S which was estimated from the Buoy's T_S of Fig. 8.1(c) by using the method described in the last section together with the Buoy's wind speed. The open circles indicate H_S values obtained from our observed wave period data by using the method of the last section together with our wind data shown in Table 8.2. Triangles are H_S read from the daily Wave Charts; only values which exceeds 2 m are plotted since smaller wave height values are not reliable.

First it is seen from Fig. 8.1(d) that the thin line is coincident with the thick line of H_S only on 8 May, indicating that only on 8 May did the wind waves predominated, and that significant swells existed during the other periods. This observation is supported also by Fig. 8.1(c).

Moreover, open circles and triangles are all coincident with the Buoy's lines on 8 May, and not in other periods. This provides us with confidence for our method of wind-wave period observation by using a stop watch, as well as for the method of T_S-H_S conversion described in the last section.

Though there is no data from the Ocean Data Buoy for our leg 1, we twice had wind situations similar to that on 8 May, that is, on 18 April and on 24 April (indicated by arrows in Fig. 8.1(d)). On these days, open circles and triangles show an excellent coincidence. This also supports our conclusion obtained from the data of leg 2.

Fig. 8.1(e) shows the same data except for the values of the open circles. This case the open circles were obtained by an assumption of $T_0 = T_S$, instead of $T_0 = \overline{T}$. The smaller values of the open circles lead us to the conclusion that the former assumption of $T_0 = \overline{T}$ is better.

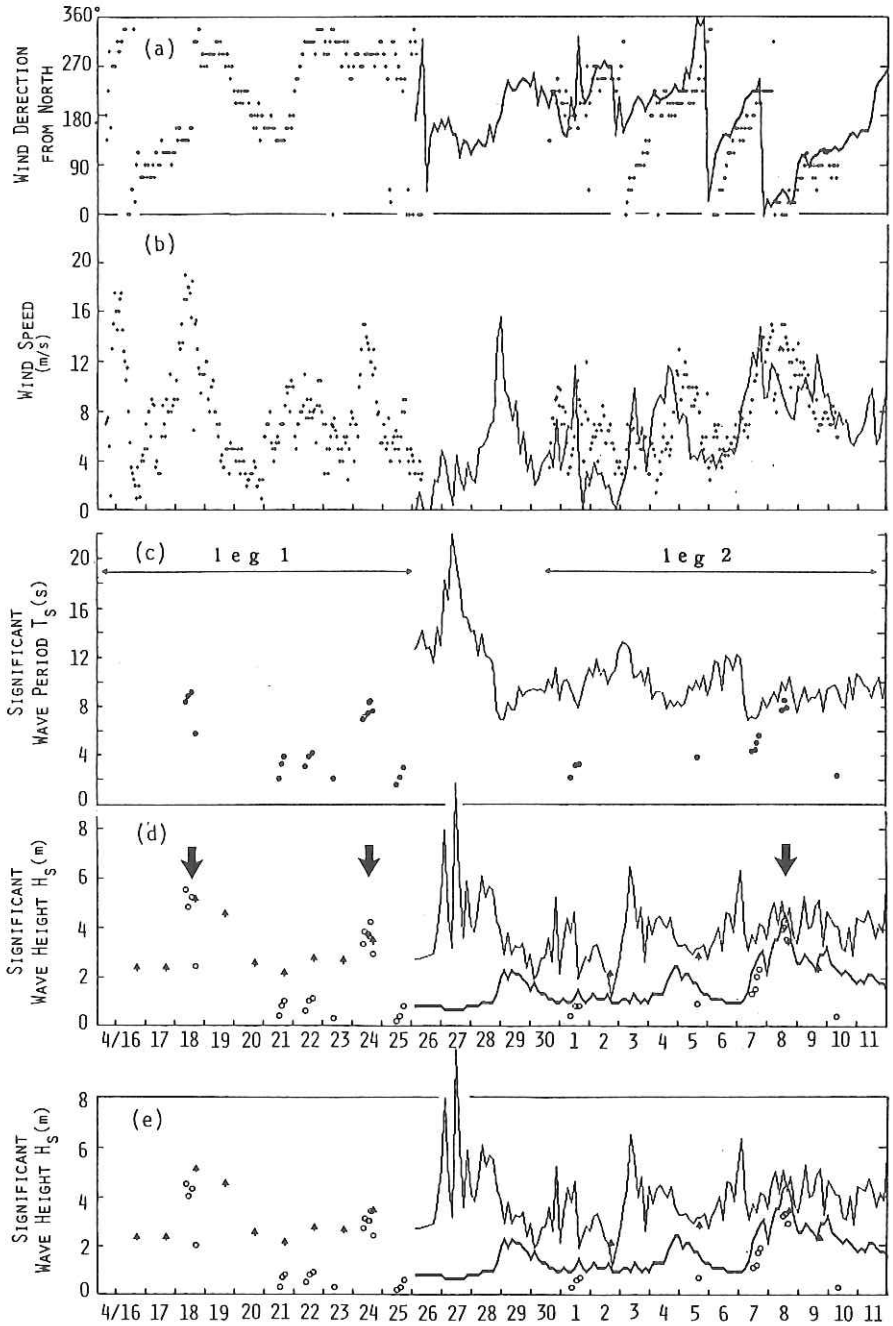

Fig. 8.1 Comparison of data of on-board measurement (dots and circles) with data from JMA's Ocean Data Buoy off Shikoku (lines) and with JMA's Wave Chart data (triangles). See the text for detailed explanation.

8.5 Conclusion

From the consideration presented in the preceeding sections, we can conclude as follows.

(1) We can measure the average wind-wave period on-board a vessel by using a stop watch with considerable acuracy, especially in situations when wind waves are developing.

(2) A conversion formula of $T_S = 1.1T_0$ is a good approximation.

(3) For the situation where the wave field is primarily of wind waves which are in local equilibrium with the wind, an estimation of significant wave height can be successfully made from the observed wind-wave period together with the wind speed, by using the 3/2-power law.

(4) The situation that leads to waves satisfying the condition of the item (3) is found when the wind speed due to a cyclone is approaching its maximum value.

(5) Such periods are rather restricted, and in other periods swells are a significant part of the wave field.

Acknowledgments

This work was performed as a part of the Ocean Mixed Layer Experiment (OMLET). The work was also supported by the Grant-in-Aid for Scientific Research of the Ministry of Education, Science and Culture. The data from the Ocean Data Buoy and Wave Charts during the observation period were provided by the Japan Meteorological Agency.

References

Brutsaert W. and Y. Toba (1986): A quasi-similarity between wind waves and solid surfaces in their roughness characteristics. J. Oceanogr. Soc. Japan, **42**, 166-173.

Chaen, M. (1973): Studies on the production of sea-salt particles on the sea surface. Mem. Fac. Fish., Kagoshima Univ., **22**, 49-107.

Longuet-Higgins, M.S. (1952): On the statistical distribution of the heights of sea waves. J. Mar. Res., **11**, 245-266.

Mitsuyasu, H. (1968): On the growth of the spectrum of wind-generated waves (I). Rep. Res. Inst. Appl. Mech., Kyushu Univ., **16**, 459-482.

Toba, Y. (1972): Local balance in the air-sea boundary processes I. On the growth process of wind waves. J. Oceanogr. Soc. Japan, **28**, 109-120.

Toba, Y. (1978): Stochastic form of the growth of wind waves in a single-parameter representation with physical implications. J. Phys. Oceanogr., 8, 494-507.

Toba, Y. (1988): Similarity laws of the wind wave and the coupling process of the air and water turbulent boundary layers. Fluid Dyn. Res., 2, 263-279.

Toba, Y. and M. Chaen (1973): Quantitative expression of the breaking of wind waves on the sea surface. Rec. Oceanogr. Works in Japan, 12, 1-11.

Toba, Y., N. Iida, H. Kawamura, N. Ebuchi and I.S.F. Jones (1988): Wave dependence of sea-surface wind stress. To be published.

Toba, Y. and M. Koga (1986): A parameter describing overall conditions of wave breaking, witecapping, sea-spray production and wind stress. E.C. Monahan and G. Mac Niocaill (eds.), Oceanic Whitecaps, D. Reidel, 37-47.

Tokuda, M. and Y. Toba (1982): Statistical characteristics of individual waves in laboratory wind waves II. Self-consistent similarity regime. J. Oceanogr. Soc. Japan, 38, 8-14.

9. Hydrographic Observation of Ocean Mixed Layer and the Subtropical Mode Water South of Honshu in Spring 1988

(The OMLET Hydrographic Observation Group in Spring 1988)

9.1 Introduction

In the cruise of the R/V Hakuho Maru KH-88-2, we made hydrographic observations focussing on the temporal variation and characteristics of ocean mixed layer and the distribution of the Subtropical Mode Water (henceforth, STMW) south of Honshu, Japan. During almost the same period, the cruise of the R/V Tansei Maru KT-88-6, belonging to Ocean Research Institute, University of Tokyo, also engaged in observation with the same purpose as that of KH-88-2.

In the present preliminary report, first the outline of these observations and participants will be described (Section 9.2). Next, based on the observed temperature sections and oxygen profiles, the description of the Subtropical Mode Water in spring 1988 will be given in Section 9.3. In Section 9.4, surface and subsurface conditions in spring 1988 will be discussed.

9.2 Participants, ship courses, observational points and items

Tables 9.1 and 9.2 are the list of the participants of KH-88-2 and KT-88-6, involved in the OMLET Hydrographic Observation Group in Spring 1988.

Figures 9.1(a), (b) and (c) show the ship courses of the R/V Hakuho Maru KH-88-2 LEG. 1 and LEG. 2, and that of the R/V Tansei Maru KT-88-6, respectively. For convenience, we will call A-line to D-line from the western north-south line to the eastern one as shown in the figures. On their courses, three kinds of hydrographic observations were made: XBT (T-7 probes) observation, CTD casts down to 1000m or bottom and CTD casts with the Rosette Multi Sampler (RMS). The observations at each station are summarized in Tables 9.3(a) through (d).

The whole data obtained are to be analyzed for the clarification of the mixed layer dynamics by the OMLET Group. Especially, the CTD data around the former OWS-T (29°N, 135°E) will be used for the estimation of geostrophic velocity fields by the Surface Mooring Group (see other chapters in this volume). Moreover, temporal variations of the mixed layer and dissipation rate within the mixed layer will be examined based on the CTD and XBT data at the fixed point

near 30°N, 141°13'E of KT-88-6.

As already mentioned in Introduction, the following two sections focus on the description of STMW south of Honshu in spring 1988.

Table 9.1 Participants of KH-88-2, involved in the OMLET Hydrographic Observation Group in Spring 1988.

KH-88-2 (Principal investigator : Prof. T. Asai)

K. Taira*,1, M. Fukasawa[1], M. Kawabe[2], S. Kitagawa[1], H. Otobe[3], S.-K. Yang[2], K. Uehara[1] and M. Hamatani[2]

(Ocean Research Institute, Unversity of Tokyo)

Y. Toba*,1, T. Suga[2] and S. Kizu[3],

(Faculty of Science, Tohoku University)

S. Mizuno*,3, A. Kaneko[3], N. Masumoto[2], M. Ishibashi[1], H. Mitsuyasu+, W. Koterayama+ and K. Marubayashi+,

(Research Institute for Applied Mechanics, Kyushu University)

A. Maeda*,+, S. Fujichika[1], T. Nishikido[2], F. Nakayama[1] and N. Nishihara[2]

(Faculty of Technology, Kagoshima University)

S. Watanabe*,3, S. Saito[3] and T. Todoroki[3]

(Faculty of Fishery, Hokkaido University)

* : Principal person of each university

\+ : not on board

1 : Researcher of LEG. 1

2 : Researcher of LEG. 2

3 : Researcher participating the whole cruise

Table 9.2 Participants of KT-88-6, involved in the OMLET Hydrographic Observation Group in Spring 1988.

KT-88-6 (Principal investigator : Prof. K. Taira)

K. Taira*

(Ocean Research Institute, University of Tokyo)

S. Kanari*, C. Kobayashi and T. Ishikawa

(Faculty of Science, Hokkaido University)

K. Hanawa*, S.-P. Xie, G. Yamanaka, Y. Yoshikawa and R. Suzuki**

(Faculty of Science, ** Faculty of Agriculture, Tohoku University)

Y. Sugimori*,+ and T. Takahashi

(Faculty of Marine, Tokai University)

H. Kozai*

(Kobe University of Merchantile Marine)

* : Principal person of each University

+ : not on board

Table 9.3(a). Summary of CTD observations in KH-88-2.

Station name*	Date	Time (JST)	Position Lat.(N)	Long.(E)	Remarks
KH-C-01	20 Apr.	11:00	28°46.9'	134°59.8'	bottom
KH-C-02	20 Apr.	16:42	28°58.8'	135°19.8'	1000m
KH-C-03	20 Apr.	18:09	28°58.8'	135°29.8'	1000m
KH-C-04	20 Apr.	19:45	28°58.8'	135°39.8'	1000m
KH-C-05	20 Apr.	21:17	28°58.8'	135°50.1'	1000m
KH-C-06	21 Apr.	17:02	29°08.8'	134°59.7'	bottom
KH-C-07	22 Apr.	08:00	28°58.6'	134°29.9'	1000m
KH-C-08	22 Apr.	09:42	28°58.7'	134°40.1'	bottom
KH-C-09	22 Apr.	13:38	28°58.6'	134°49.7'	1000m
KH-C-10	22 Apr.	15:14	28°58.7'	134°59.8'	1000m
KH-C-11	22 Apr.	17:37	28°58.7'	135°09.8'	1000m
KH-C-12	22 Apr.	18:35	28°58.9'	135°19.7'	RMS, no CTD data
KH-C-13	30 Apr.	17:35	33°00.2'	133°45.7'	bottom
KH-C-14	30 Apr.	21:20	32°30.0'	133°56.5'	bottom
KH-C-15	1 May	16:53	29°20.1'	135°20.0'	botoom
KH-C-16	2 May	06:43	29°59.8'	136°59.9'	RMS, 1000m
KH-C-17	2 May	15:23	29°00.0'	136°59.9'	RMS, 1000m
KH-C-18	2 May	22:09	27°59.9'	137°00.0'	RMS, 1000m
KH-C-19	3 May	04:01	26°59.6'	136°59.8'	RMS, 1000m
KH-C-20	3 May	11:30	26°00.0'	137°00.1'	RMS, 1000m
KH-C-21	3 May	21:57	24°59.8'	137°00.2'	RMS, 1000m
KH-C-22	5 May	18:33	28°40.0'	135°20.0'	1000m
KH-C-23	6 May	00:32	28°39.9'	135°20.0'	1000m
KH-C-24	6 May	06:28	28°40.0'	135°20.0'	1000m
KH-C-25	6 May	10:00	28°39.9'	135°19.6'	bottom
KH-C-26	6 May	16:11	28°47.1'	134°59.7'	1000m
KH-C-27	7 May	15:11	29°08.8'	134°55.3'	300m

* Tentative station names in this report.

Table 9.3(b). Summary of CTD observations in KT-88-6.

Station name*	Date	Time (JST)	Position Lat.(N)	Long.(E)	Remarks
KT-C-01	3 May	14:02	32°59.9'	137°00.1'	RMS, 1000m
KT-C-02	3 May	20;07	31°59.1'	137°00.6'	RMS, 1000m
KT-C-03	4 May	02:42	31°00.1'	137°00.1'	RMS, 1000m
KT-C-04	4 May	09:26	29°59.9'	137°00.0'	RMS, 1000m
KT-C-05	4 May	15:45	29°30.1'	137°59.1'	1000m
KT-C-06	4 May	21:49	28°59.5'	139°00.3'	1000m
KT-C-07	5 May	03:52	28°29.9'	140°00.1'	1000m
KT-C-08	5 May	09:45	27°59.9'	141°00.1'	1000m
KT-C-09	5 May	18:29	27°59.9'	141°50.6'	RMS, 1000m
KT-C-10	6 May	00:58	29°00.0'	141°31.9'	RMS, 1000m
KT-C-11	6 May	07:22	29°59.9'	141°12.8'	RMS, 1000m
KT-C-12	6 May	09:04	29°57.1'	141°07.1'	1000m
KT-C-13	6 May	11:03	30°05.8'	141°13.0'	1000m
KT-C-14	6 May	12:52	29°57.2'	141°18.2'	1000m
KT-C-15	6 May	14:09	30°00.1'	141°12.9'	1000m
KT-C-16	6 May	16:00	30°00.0'	141°12.4'	1000m
KT-C-17	6 May	18:00	29°59.5'	141°11.5'	1000m
KT-C-18	6 May	20:00	29°59.8'	141°13.0'	1000m
KT-C-19	6 May	22:00	29°59.0'	141°12.6'	1000m
KT-C-20	6 May	23:57	30°00.3'	141°12.6'	1000m
KT-C-21	7 May	01:56	30°00.0'	141°13.0'	1000m
KT-C-22	7 May	03:57	30°00.0'	141°12.6'	1000m
KT-C-23	7 May	05:58	29°59.5'	141°11.5'	no data 0-620m
KT-C-24	7 May	08:00	30°00.2'	141°12.5'	1000m
KT-C-25	7 May	10:00	30°00.1'	141°12.7'	1000m
KT-C-26	7 May	11:55	30°01.3'	141°12.0'	1000m
KT-C-27	7 May	18:01	30°59.9'	141°00.3'	RMS, 1000m

* Tentative station names in this report.

Table 9.3(c) Summary of XBT observations in KH-88-2.

Station name*	Date	Time (JST)	Position Lat.(N)	Long.(E)	Remarks
KH-X-01	24 Apr.	13:40	29°00.2'	135°19.1'	
KH-X-02	25 Apr.	09:13	31°57.3'	134°05.6'	
KH-X-03	25 Apr.	11:53	32°16.9'	134°00.3'	
KH-X-04	25 Apr.	14:31	32°36.2'	133°53.6'	
KH-X-05	25 Apr.	17:06	32°55.6'	133°46.5'	
KH-X-06	25 Apr.	19:11	33°10.8'	133°42.2'	
KH-X-07	1 May	01:24	32°00.0'	134°10.1'	
KH-X-08	1 May	03:57	31°30.0'	134°19.0'	
KH-X-09	1 May	06:33	31°00.1'	134°27.1'	
KH-X-10	1 May	09:11	30°30.1'	134°35.1'	
KH-X-11	1 May	11:54	30°00.1'	134°43.5'	
KH-X-12	1 May	14:36	29°30.0'	134°51.1'	
KH-X-13	2 May	11:36	29°30.1'	137°00.0'	
KH-X-14	2 May	18:37	28°29.9'	137°00.1'	
KH-X-15	3 May	01:14	27°30.1'	137°00.1'	
KH-X-16	3 May	08:04	26°20.4'	137°00.7'	
KH-X-17	3 May	17:36	25°29.1'	137°01.1'	
KH-X-18	4 May	01:13	25°30.3'	136°46.3'	
KH-X-19	4 May	05:00	26°00.0'	136°33.0'	
KH-X-20	4 May	07:36	26°29.9'	136°19.4'	
KH-X-21	4 May	16:03	27°02.1'	136°03.0'	
KH-X-22	4 May	19:40	27°30.0'	135°51.9'	
KH-X-23	4 May	23:43	28°00.0'	135°37.8'	
KH-X-24	5 May	03:42	28°30.2'	135°24.4'	
KH-X-25	6 May	18:15	29°00.3'	134°58.6'	
KH-X-26	7 May	08:20	29°07.4'	134°56.8'	
KH-X-27	8 May	22:59	30°52.0'	136°29.0'	
KH-X-28	9 May	03:20	31°23.6'	136°41.0'	
KH-X-29	9 May	08:44	31°55.7'	136°53.6'	
KH-X-30	9 May	14:00	32°34.1'	137°08.2'	

* Tentative station names in this report.

Table 9.3(d). Summary of XBT observations in KT-88-6

Station name*	Date	Time (JST)	Position Lat.(N)	Long.(E)	Remarks
KT-X-01	3 May	17:35	32°30.0'	137°00.0'	
KT-X-02	3 May	23:45	31°30.0'	136°59.8'	
KT-X-03	4 May	06:16	30°30.1'	136°58.6'	
KT-X-04	4 May	13:15	29°45.6'	137°00.6'	
KT-X-05	4 May	19:04	29°15.0'	138°30.2'	
KT-X-06	5 May	01:10	28°45.5'	139°30.0'	
KT-X-07	5 May	07:09	28°14.3'	140°30.2'	
KT-X-08	5 May	13:00	27°45.1'	141°30.0'	
KT-X-09	5 May	15:27	27°29.8'	142°00.2'	
KT-X-10	5 May	22:09	28°30.6'	141°41.6'	
KT-X-11	6 May	04:33	29°30.2'	141°22.6'	
KT-X-12	6 May	15:00	30°00.1'	141°12.7'	
KT-X-13	6 May	16:02	30°00.0'	141°12.4'	
KT-X-14	6 May	17:00	29°59.9'	141°11.9'	
KT-X-15	6 May	18:02	29°59.5'	141°11.5'	
KT-X-16	6 May	19:00	30°00.1'	141°13.3'	
KT-X-17	6 May	21:00	29°59.4'	141°12.8'	
KT-X-18	6 May	22:03	29°59.0'	141°12.6'	
KT-X-19	6 May	23:00	30°00.2'	141°13.0'	
KT-X-20	6 May	23:57	30°00.3'	141°12.5'	
KT-X-21	7 May	00:58	30°00.4'	141°12.2'	
KT-X-22	7 May	01:58	30°00.0'	141°13.0'	
KT-X-23	7 May	02:57	30°00.0'	141°12.8'	
KT-X-24	7 May	03:58	30°00.0'	141°12.6'	
KT-X-25	7 May	05:02	29°59.8'	141°12.1'	
KT-X-26	7 May	06:00	29°59.5'	141°11.5'	
KT-X-27	7 May	07:03	30°00.0'	141°13.2'	
KT-X-28	7 May	08:06	30°00.2'	141°12.4'	
KT-X-29	7 May	09:00	30°00.5'	141°11.8'	
KT-X-30	7 May	11:00	30°00.6'	141°12.3'	
KT-X-31	7 May	11:59	30°01.4'	141°11.9'	
KT-X-32	7 May	14:24	30°20.8'	141°08.7'	
KT-X-33	7 May	16:11	30°40.0'	141°04.6'	
KT-X-34	7 May	20:43	31°19.9'	140°53.3'	
KT-X-35	7 May	22:34	31°40.0'	140°46.8'	

* Tentative station names in this report.

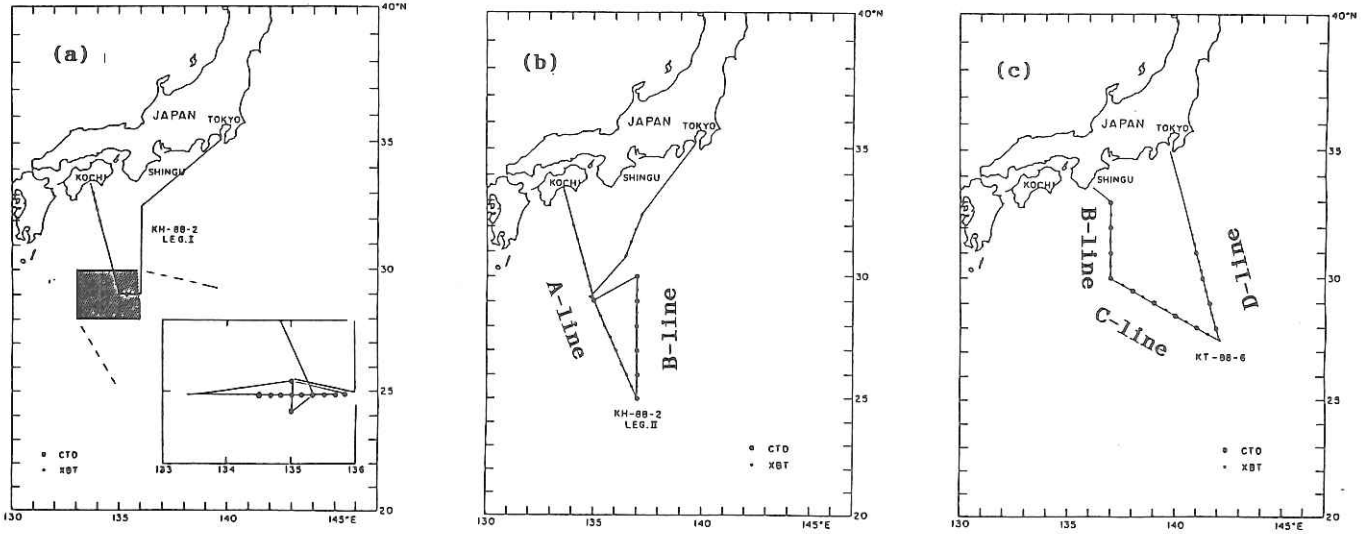

Fig. 9.1 Ship courses of the R/V Hakuho Maru KH-88-2 and the R/V Tansei Maru KT-88-6. (a) LEG. 1 of KH-88-2, (b) LEG. 2 of KH-88-2 and (c) KT-88-6. A-line through D-line are named tentatively in this report.

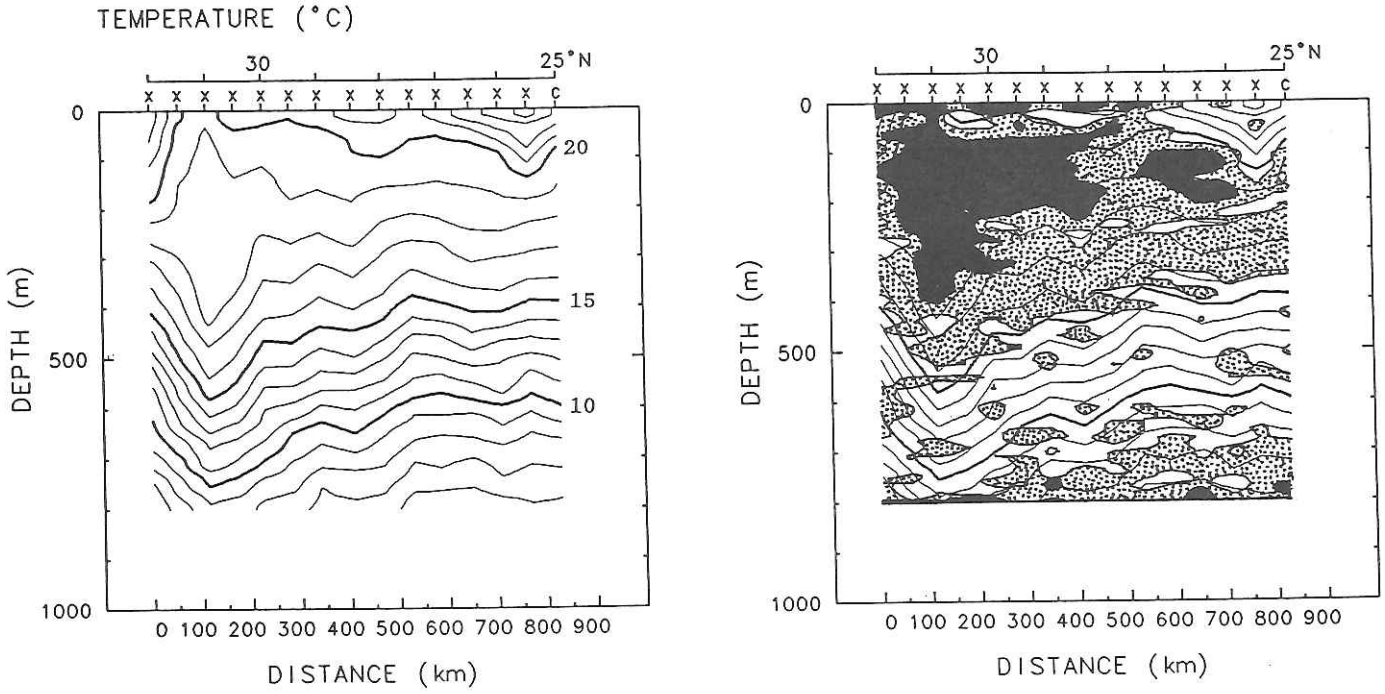

Fig. 9.2(a) Temperature vertical section along A-line (left panel) and layers with temperature gradient lower than 2×10^{-2} °Cm^{-1} (right). Blackened regions correspond to layers with temperature gradient lower than 10^{-2} °Cm^{-1}.

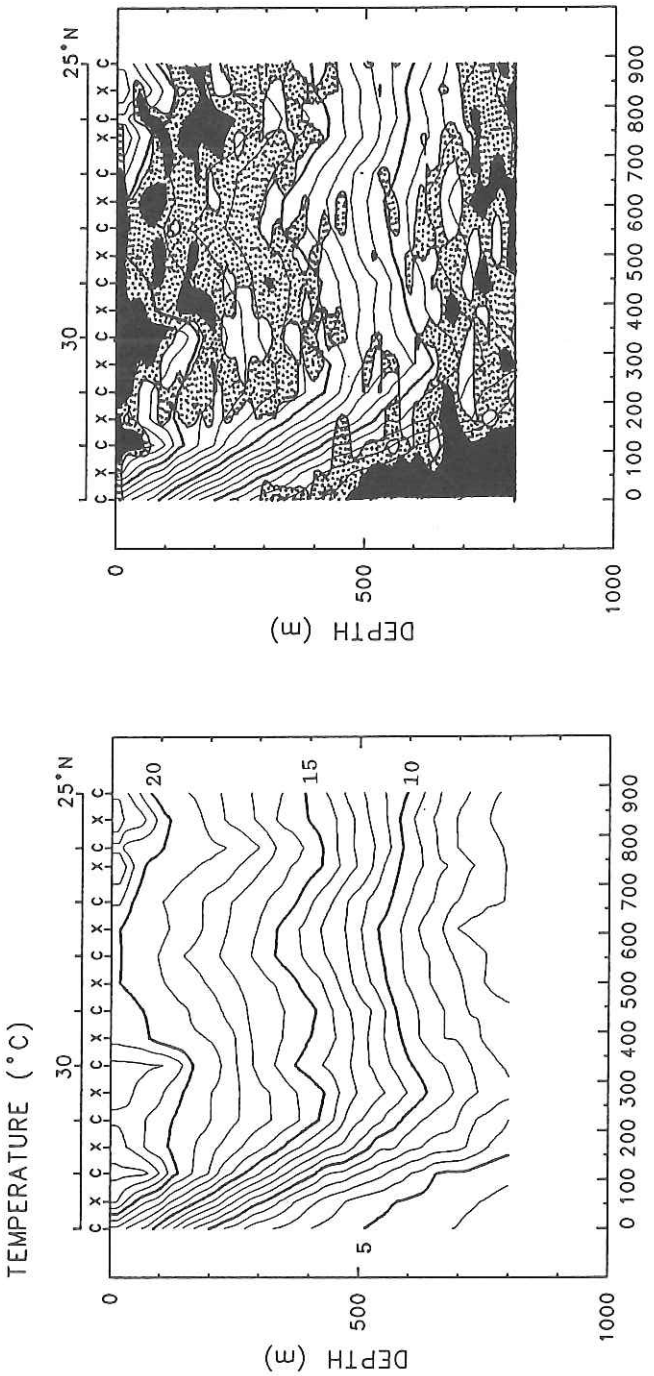

Fig. 9.2(b). As in Fig. 9.2(a) but for B-line.

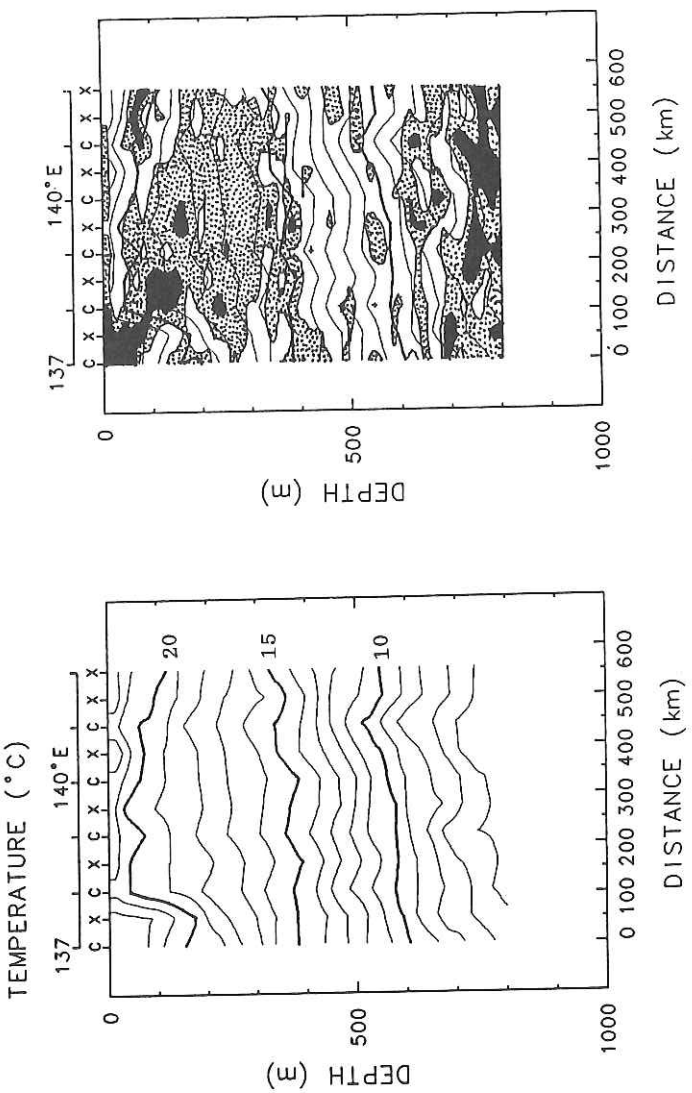

Fig. 9.2(c). As in Fig. 9.2(a) but for C-line.

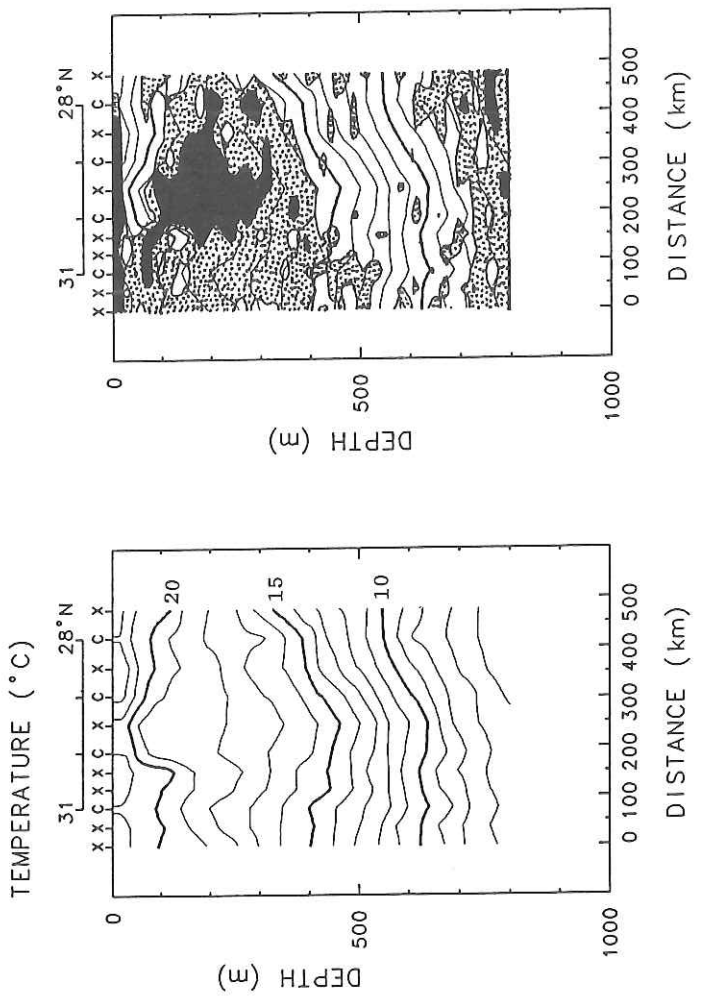

Fig. 9.2(d). As in Fig. 9.2(a) but for D-line.

9.3 STMW observed in four sections

Figures 9.2(a) through (d) show the temperature sections and the layers with temperature gradient lower than $2x10^{-2}$°Cm^{-1} along four lines. The temperature data from both CTD and XBT were used in construction of sections. The depths of XBT data were calculated by the empirical equation proposed by Hanawa and and Yoritaka (1987). As already pointed out by Hanawa et al. (1988b), the layers with temperature ranging from 16 to 19°C and with temperature gradient lower than $2x10^{-2}$°Cm^{-1} are approximately regarded as the layers of STMW. Figures 9.3(a) and (b) show the vertical profiles of the apparent oxygen utilization (AOU) along B-line and D-line. Suga et al. (1988) pointed out that the AOU can be used as an index of the age of STMW. Waters with AOU lower than about 0.5 ml/l observed in spring or summer can be regarded as those formed in the just previous winter.

A-line

Around 31°N, remarkable thermostad with temperature of 18°C appears from surface to 450m. In this period, the Kuroshio takes the large meander path and so-called "Warm Eddy off Shikoku" (Shikoku-oki-dansuikai) steadily exists around here. This thermostad centered in the "Warm Eddy off Shikoku" can be inferred to be formed locally in winter.

B-line

The STMW with AOU lower than 0.5ml/l can be found from 100 to 250m at 26°N and 150 to 200m at 25°N. Although temperature gradients are lower from the Kuroshio axis to 27°N, these layers are considered as STMW formed in winter 1987, because AOU in this layer are higher than 0.5 ml/l.

C-line

Layers with somewhat low temperature gradient extend from 136°E (29°30'N) to 141°E (28°N). Unfortunately, oxygen profiles were not measured along this line.

D-line

Remarkable thermostad with temperature of 18°C and AOU lower than 0.5 ml/l is found from 100 to 250m near 30°N. Waters of this layer can be regarded as STMW formed in the just previous winter, i.e., winter 1988. This STMW may be formed non-locally and may be advected or intrude to this section by the Kuroshio recirculation system or its own dynamics. To clarify this advective or movement process is a very important future work and to accumulate the data is desired.

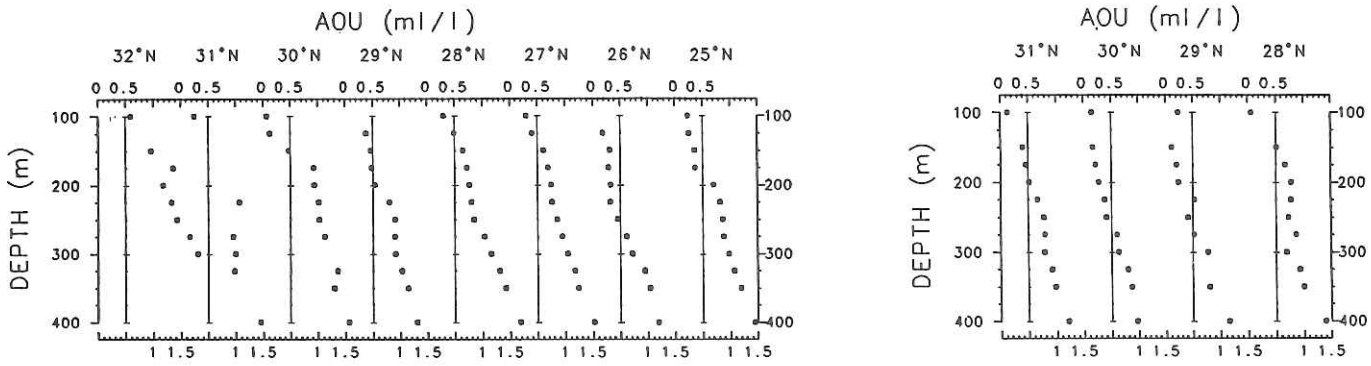

Fig. 9.3 AOU (apparent oxygen utilization) profiles along B-line (left panel) and along D-line (right).

9.4 Discussion - Surface and subsurface conditions in spring 1988 –

In this section, we will describe surface and subsurface thermal conditions in spring 1988, mainly using published temperature maps.

Figure 9.4 shows the monthly mean SST 16-19°C zones of March from 1986 through 1988, which can be regarded as the approximate outcrop/formation area of STMW (see, Hanawa, 1987). These were redrawn from "The Ten-Day Marine Report" regularly issued by the Japan Meteorological Agency (JMA). It is found that the 16-19°C zone in 1988 winter is narrow in latitude compared with that in winter 1986 and did not extend south of Honshu as same as that in winter 1987. We can also see the less evolution of STMW in winter 1988 from temperature distributions at depth of 100m shown in Fig. 9.5. These differences between those in winter 1986 and those in winters 1987 and 1988 suggest that the seas around Japan were considerably warmer in the latter two winters. Although we can not exactly say on the formation rate of STMW in winter 1988, it may be expected that the formation rate of STMW in winter 1988 was very smaller than that in winter 1986 and might be the same order as that in winter 1987.

As discussed in Hanawa et al. (1988a), SST in the midlatitudes of the western North Pacific is strongly affected by the winter-time east Asian Monsoon and in general, monsoon is weak in the ENSO year winter. Since the 1986/87/88 ENSO event terminated around February 1988, the winter of 1988 can be regarded as the ENSO year winter. Actually, the scatter plots of the seasonal mean Monsoon index (MOI) and the Southern Oscillation index (SOI) show the weak monsoon category as shown in Fig. 9.6

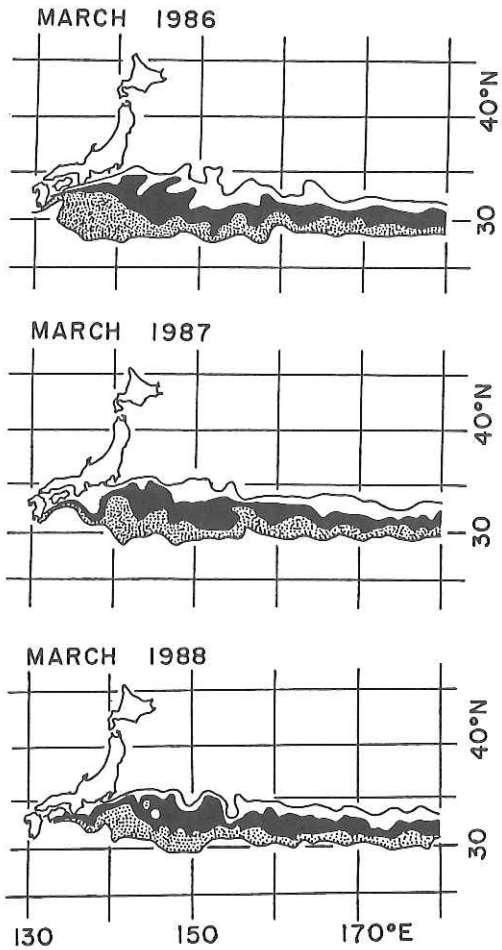

Fig. 9.4 Monthly mean SST 16-19°C zones of March in 1986, 1987 and 1988, which were redrawn from "The Ten-day Marine Report" by JMA (Nos, 1421 for 1986, 1457 for 1987 and 1483 for 1988).
Blackened and stippled areas indicate the 17-18 and 18-19°C zones, respectively.

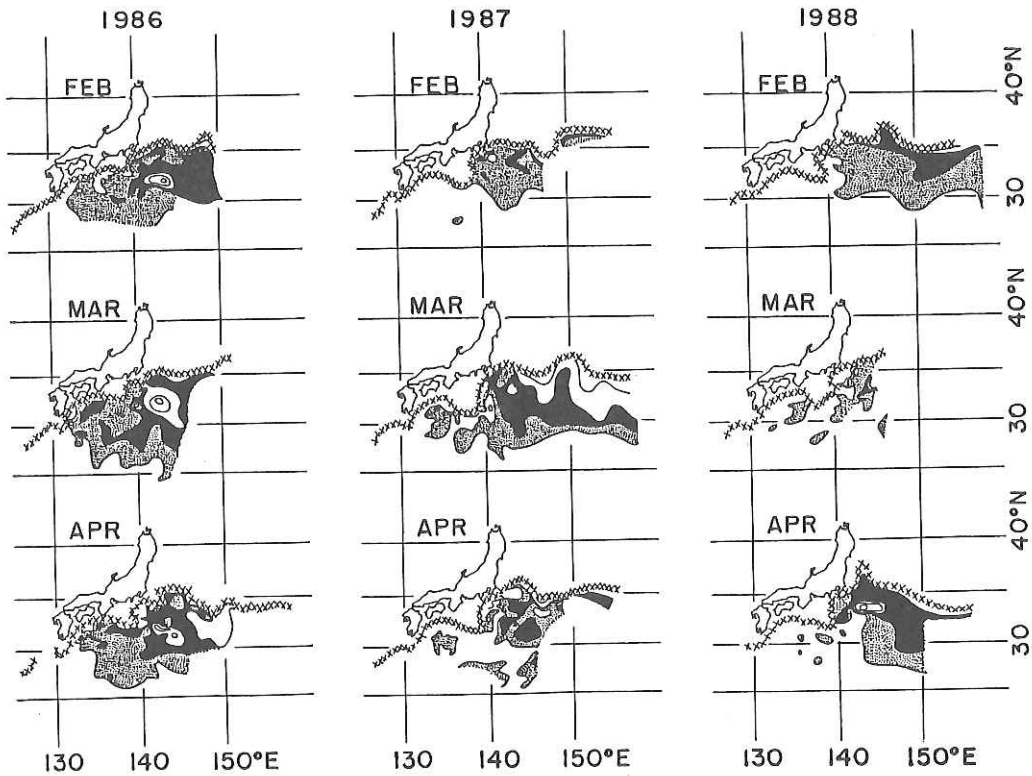

Fig. 9.5 Temperature distributions from February to April at depth of 100m. Symbols x denote the Kuroshio axis approximately. These were also redrawn from "The Ten-Day Marine Report" (Nos. 1419, 1422 and 1425 for 1986, Nos. 1455, 1458 and 1461 for 1987 and Nos. 1481, 1484 and 1487 for 1988).

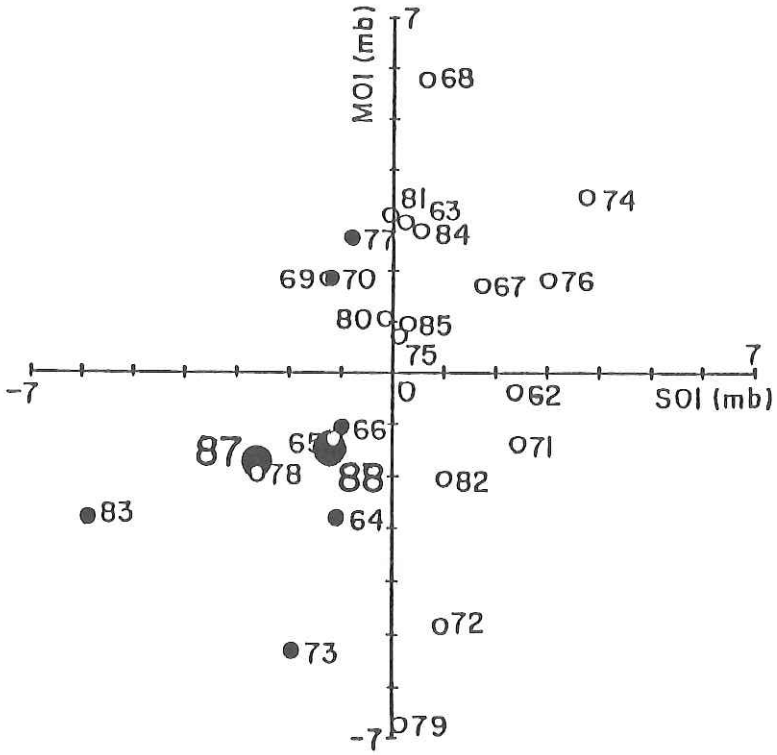

Fig. 9.6 Scatter plots of the seasonally mean monsoon index (MOI) and the Southern Oscillation index (SOI), which are averages from December to February (see Watanabe and Hanawa, 1988). Numerals in the figure denote year and closed circles correspond to the ENSO year winters: winters during the ENSO events.

References

Hanawa, K. (1987): ATMOSPHERE-OCEAN, **25**, 358-374.

Hanawa, K. and H. Yoritaka (1987): J. Oceanogr. Soc. Japan, **43**, 68-76.

Hanawa, K., T. Watanabe, N. Iwasaka, T. Suga and Y. Toba (1988a): J. Meteorol. Soc. Japan, **67**, 445-456.

Hanawa, K., N. Iwasaka, T. Watanabe, T. Suga and Y. Toba (1988b): Preliminary report of the R/V Hakuho Maru KH-87-1 (in press).

Suga, T., K. Hanawa and Y. Toba (1988): The subtropical Mode Water in the 137°E section. Submitted.

Watanabe, T. and K. Hanawa (1988): In preparation.

10. Surface mooring for observation of ocean mixed layer

K. Taira, M. Fukasawa, M. Kawabe, S. Kitagawa, H. Otobe,
S-K, Yang, K. Uehara, M. Hamatani,
(Ocean Research Institute, University of Tokyo)
T. Nishikido, Y. Fujichika, F. Nakayama and N. Nishihara
(Faculty of Technology, Kagoshima University)

Heat exchange between air and sea is carried out most actively over the Kuroshio, the intensified western boundary current of the subtropical gyre in the North Pacific. As a result of the air-sea exchange of heat momentum, a mixed layer where temperature is kept homogenous is formed in the upper layer. A co-operative research program, Ocean Mixed Layer Experiment (OMLET) is on-going to investigate the physical process governing formation of the mixed layer. Field program of OMLET is carried out in the vicinity of Station T (29° N, 135° E), located in the warm water region about 200 km away from the Kuroshio. Japan Meteorological Agency is keeping a discus buoy at Station T to collect marine meteorological data.

A surface mooring with thermometers and current meters was deployed on 20 April. Fig. 10.1 shows the surface mooring. Current meters were set at 50 m and 150 m, and thermometers were attached from the sea surface to 150 m. The mooring will be retrieved in October, and position of the buoy are watched by using the Argos system. Details of the mooring (OMLET#6) is shown in Table 10.1.

Two deep moorings of current meters were deployed in December 1987 from the R/V Hakuho Maru. An inverted echo sounder (IES) is also moored to monitor seasonal change of vertical profile of temperature. These moorings are to be retrieved in October 1988.

Table 10.1 Details of the moorings for Ocean Mixed Layer Experiment. The moorings are kept by Division of Physical Oceanography, Ocean Research Institute.

OMLET#2 6 December 1987-

28-58.5'N, 135-25.2'E, water depth 4990 m.

Current meters : 4470 m, 3670 m, 2070 m, 470 m.

IES : 4965 m

OMLET#5 9 December 1987-

28-59.9'N, 134-33.9'E, water depth 4580 m.

Current meters : 4160 m, 3760 m, 3360 m

OMLET#6 20 April 1988-

28-48.5'N, 135-01.2'E, water depth 4850 m.

Current meters : 150 m, 50 m

Thermometer : 0 m, 10 m, 20 m, 30 m, 40 m, 60 m, 80 m, 100 m

Depth recorder : 50 m, 150 m.

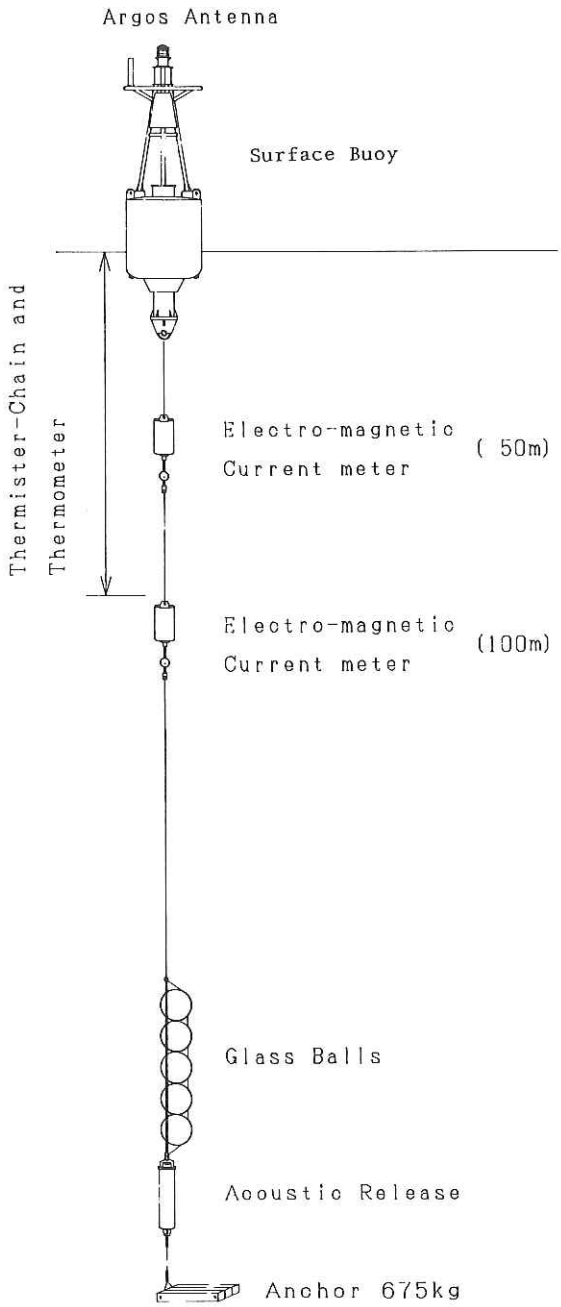

Fig. 10.1 The surface mooring for observations of the ocean mixed layer. The mooring line was deployed on 20 April at 28-48.4′N and 135-01.1′E, where water depth was 4840 m.

11. Surface Mooring and ADCP Experiments South of the Kuroshio

S. Mizuno, A. Kaneko, W. Koterayama,
Y. Masumoto, and H. Mitsuyasu
(Research Institute for Applied Mechanics, Kyushu University)

As part of OMLET, a surface mooring buoy (RIAM buoy) was deployed in an open ocean of 4700 m deep at St. (29°08'N, 134°58'E) near the OWS-T for 14 days from 23 April to 7 May, 1988. During the same period current profiles in the upper ocean were measured with an Acoustic Doppler Current Profiler (ADCP) along a square line a side 20 miles long around the RIAM buoy and along other several lines. The objective of the experiments is to measure the velocities and temperature in the upper ocean to examine the heat budget and current structure in the mixed layer and seasonal thermocline.

11.1 Surface Buoy Experiment

Figure 11.1 shows details of the mooring line of the RIAM buoy that consists of 7 Aanderaa current meters and 14 RMT thermometers to measure velocities and temperatures from the surface to a depth of 260 m. Records at the deepest current meter failed, and pressure records of the second and third current-meters from below indicated that the mooring line moved up and down rather largely, so that we confine our presentation here to the data within 100 m from the surface. Figures 11.2 and 11.3 show time series of water pressure and velocity stick diagrams for four current-meters from the surface. Figure 11.4 shows progressive vector diagrams that show the presence of a weak eddy during the first week and the northwestward current motion during the second week. From these diagrams the near-surface water appears to have moved about 100 km westward or northwestward during the mooring period. Time series of 11 water temperatures at an interval of 10 m to within 100 m (Fig. 11.5a) and of their depth-mean temperature (Fig. 11.5b) show an increase in temperature with time during the same period.

In this report we briefly consider the effect of horizontal advection on the heat budget to within 100 m. As shown in Fig. 11.4, the surface currents flowed northwestward consistently during the last 6 days of the mooring period. During

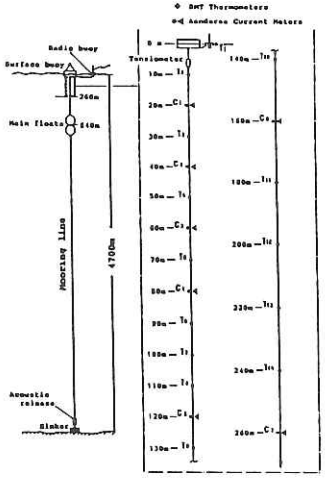

Fig. 11.1 RIAM Surface Buoy System

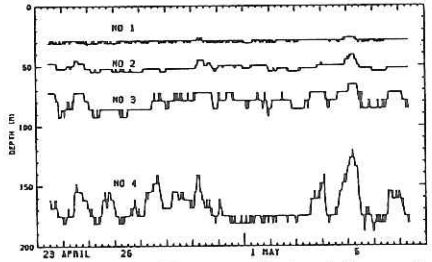

Fig. 11.2 Pressure Data at Tango in 1988.

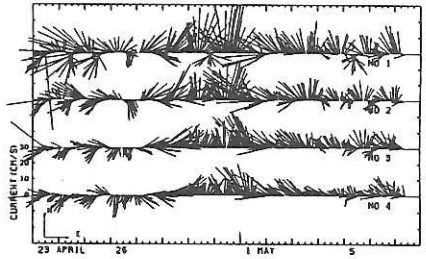

Fig. 11.3 Current Data at Tango in 1988

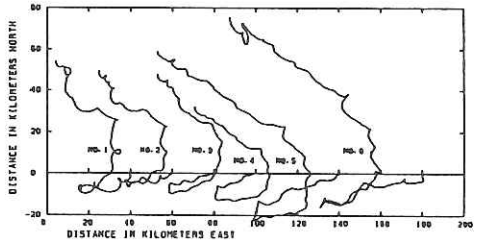

Fig. 11.4 Progressive Vector Diagrams for second omlet. The record period: 23 April – 7 May, 1988. A circle is plotted at 0:00 every day.

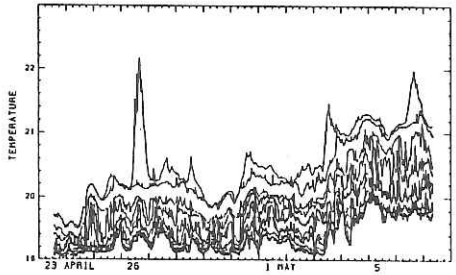

Fig. 11.5(a) Water temp. Data at Tango in 1988.

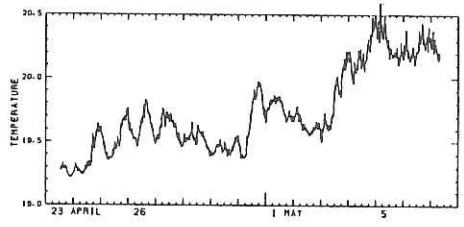

Fig. 11.5(b) Time series of mean temp. above 100 m.

this period the ship report of the R/V Hakuho Maru on sea surface temperature showns that there was the horizontal temperature gradient of about 0.6°C/130km along the *NNW* ship route, negative northward. Accordingly, the presence of the northwestward flow during this period suggests that a part of the increase in near-surface temperature shown in Fig. 11.5 is due to the horizontal heat advection. The 6-day mean current measured with the 6 current meters was about 10 cm/s northwestward, so that the heat advection in the NW direction gives about 200 W/m^2 for the upper 100 m layer. On the other hand, the daily-mean temperatures above 100 m were 19.7° and 20.2°C on May 1 and 6, respectively, so that the variation of the heat contents above 100 m during this period gives 450 W/m^2. It follows that the heat advection accounts for about 40% of the rate of increase in heat contents above 100 m during the last 6 days. Except this period, the currents flowed mostly westward or eastward, and the effect of horizontal heat advection did not appear to be important.

11.2 ADCP Experiment

11.2.1 Experimental site and method

Vertical current profiles in the upper ocean around the OMLET region were aquired with the ADCP mounted on a towed fish (Fig. 11.6), which moved horizontally with keeping a constant speed at 6 m below the surface (Kaneko & Koterayama, 1988). The data were collected on a square traverse line surrounding the RIAM buoy and on two other lines located at lower latitudes. The date of measurement, the position of stations in order of traverse and the range of ship speed for each survey are listed in Table 11.1.

The ADCP was adjusted to measure the current velocity relative to the ship with a sampling time of 60 s and a vertical spacing of 8 m. All the ADCP data were transferred to floppy disks of a HP-VECTRA computer on board through an RS-422 cable 100 m long. The data were converted into those relative to the sea bottom, using the ship speed estimated from a LORAC-C positioning. The LORAN-C data were sampled every 30 minutes after time-averaging over 30 minutes. The current velocity relative to the sea bottom was further smoothed out through a filter of depth interval 16 m and time interval 10 minutes.

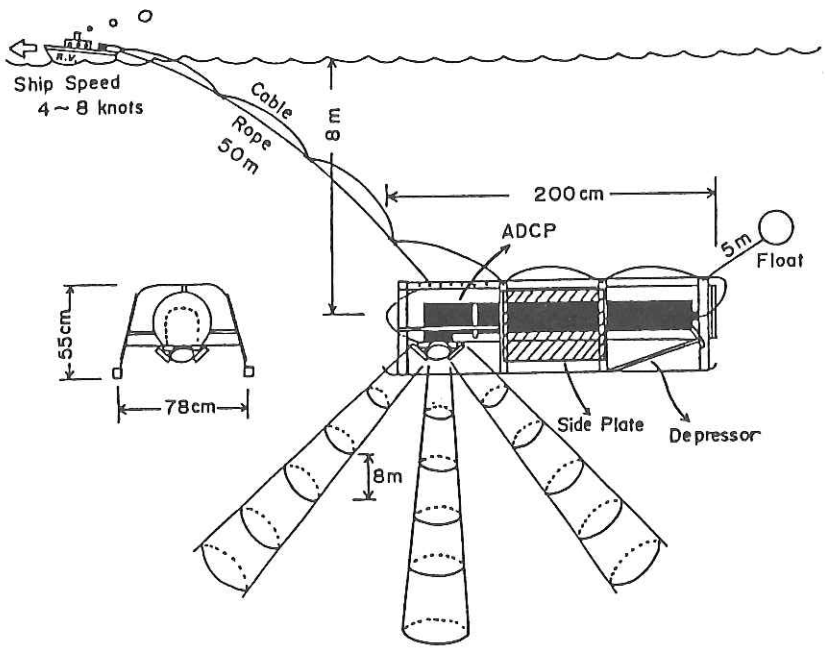

Fig. 11.6

Table 11.1 Date and Station of towed lines of ADCP.

Exp	Date	Stn.	Position N	Position E	Ship Speed (knots)
9	6 to 7 May 1988	AD91	29°00'	134°50'	7.6-8.3
		AD92	29°20'	134°50'	
		AD93	29°20'	135°10'	
		AD94	29°00'	135°10'	
7	4 May 1988	AD7S	26°35.01'	136°17.49'	8.5-9.0
		AD7F	26°49.64'	136°10.58'	
6	3 May 1988	AD6S	25°36.08'	137°01.46'	8.8-9.3
		AD6E	25°11.86'	137°00.20'	

11.2.2 Results and discussion

Figure 11.7 shows results obtained on the square traverse line surrounding the RIAM buoy on 6 to 7 May 1988. The current vectors measured are indicated in Fig. 11.7a as stick diagrams for 10 different depths. There are no velocity data near the corners of the square because of the lack of mean ship speed due to the change of ship heading. The results give us an overall view that the current vectors rotate clockwise like an intertial oscillation and that the current field has a small vertical shear. The wind data measured on board and the temperature data from a thermistor mounted on the ADCP are also presented in Fig. 11.7a. The rotating current mentioned above may have been induced by the strong northwestward wind of more than 8 m/s. The towed fish crossed a warm water mass that had a temperature higher by 1°C than in the ambient sea. The horizontal variation of vertical profiles of current speed is indicated in Fig. 11.7b as a stack diagram. There is no feature to notice except tht the current speed at depths of 250 to 350 m increased between Stns. AD93 and AD94. The mean current profile obtained as a function of depth by integrating the data for a fixed depth over the whole observation period is shown in Fig. 11.7c. The mean current has a small peak around 300 m (see Fig. 11.7b) and flows northwestward with a speed of 5 to 15 cm/s, indicating that the mean current measured with the ADCP is in rough agreement with that of the RIAM buoy during the same period.

Figure 11.8 shows results obtained on the traverse line lying between Stns. AD7S and AD7E on 4 May 1988. The stick diagrams indicate that the current flows westward from 11:00 to 11:30, and southwestward during the remaining time (Fig. 11.8a). Also, the stack diagram shows that the westward current remarkably speeds up between 100 and 300 m, while the southwestward current keeps a nearly uniform vertical profile (Fig. 11.8b). It may be concluded from a comparison with the CTD data that the intensive westward current observed here transfers part of the subtropical mode water.

Figure 11.9 shows results obtained on the line lying between Stns. AD6S and AD6E on 3 May 1988. An overall view of the stick diagram is that a state of weak current continued until 18:00 and then the current speed gradually increased, particularly in the upper layer (Fig. 11.9a). The mean current flowed southward over the whole depth observed. From the stack diagram (Fig. 11.9b), the flow field may be divided into the following three regions along the time axis:

· 1st region (16:47 – 17:30)

a sharp peak of current speed observed between 60 and 100 m

· 2nd region (17:30 – 18:40)

step-like structures observed through depths from the surface up to 300 m

· 3rd region (18:40 – 19:30)

intensive currents in the upper layer within 80 m from the surface and large velocity shear occurring just below this layer

It does not seem that the intensification of the surface current observed at the 3rd region was directly caused by the local wind stress because a weak wind was blowing. A close comparison of the ADCP and CTD data is desirable for more detailed analysis.

Finally, it is interesting to note that the direction of the near-surface mean current changed from northwestward (Fig. 11.7a) to southwestward (Figs. 11.8a and 9a). This result allows us to imagine that a divergence zone of current exists between the towed lines near 26 °N and another line at 29°N in latitude.

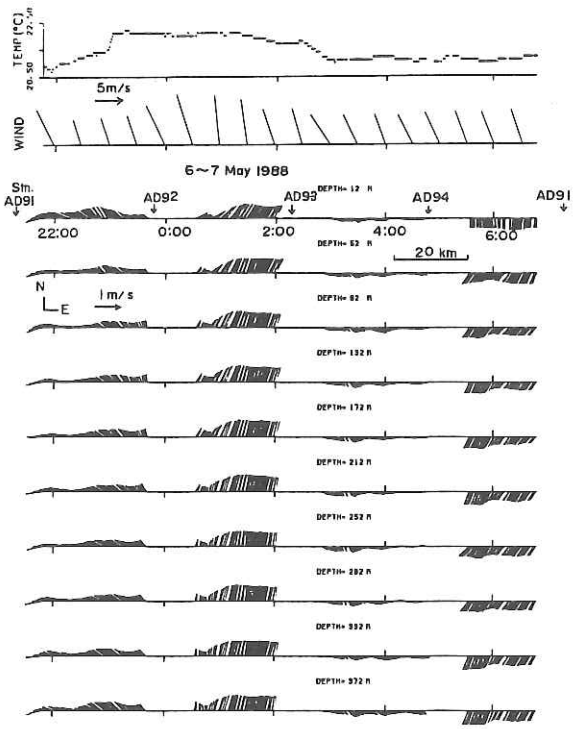

Fig. 11.7(a)

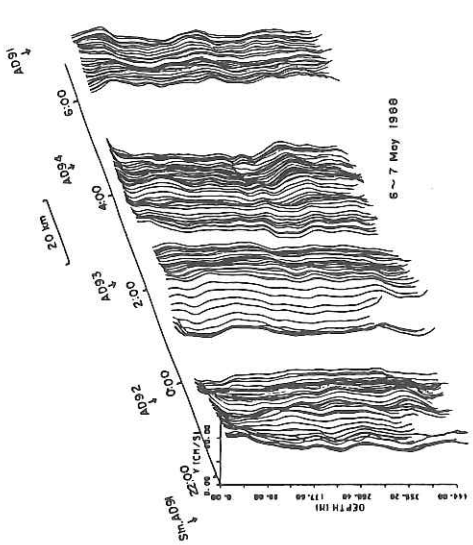

Fig. 11.7(b)

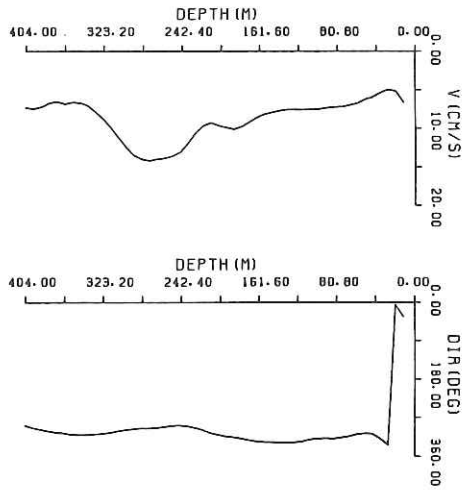

Fig. 11.7(c)

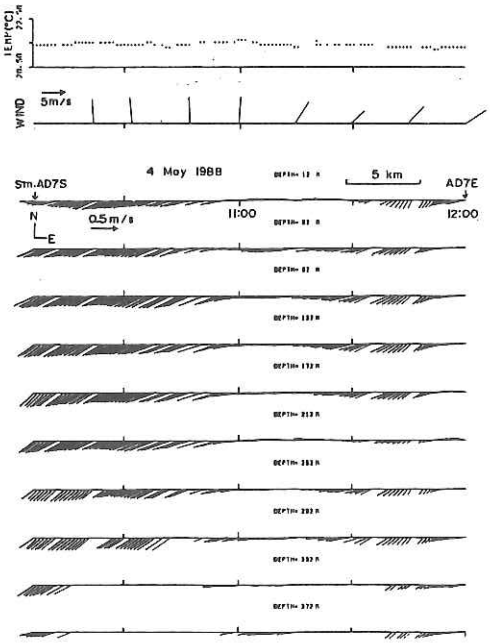

Fig. 11.8(a)

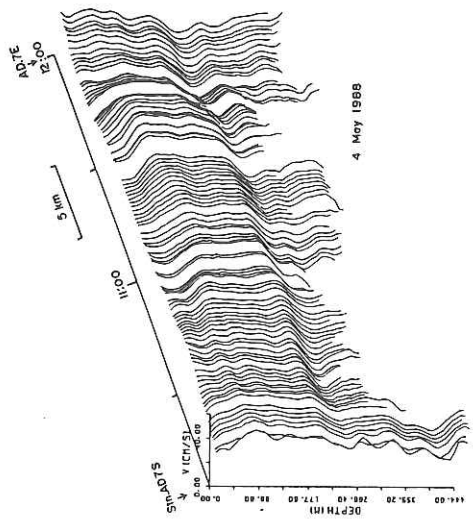

Fig. 11.8(b)

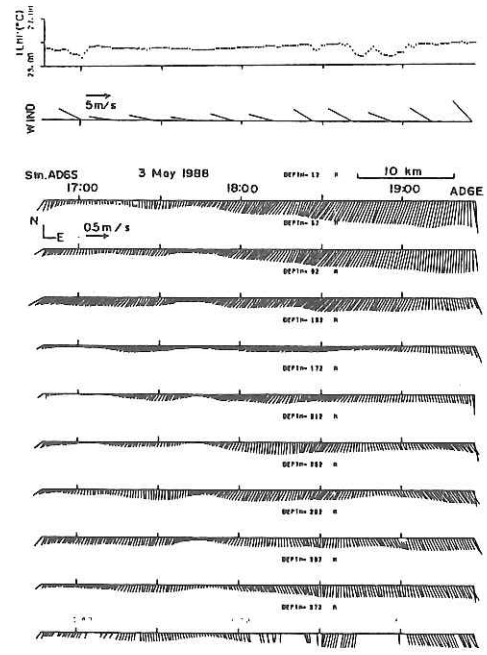

Fig. 11.9(a)

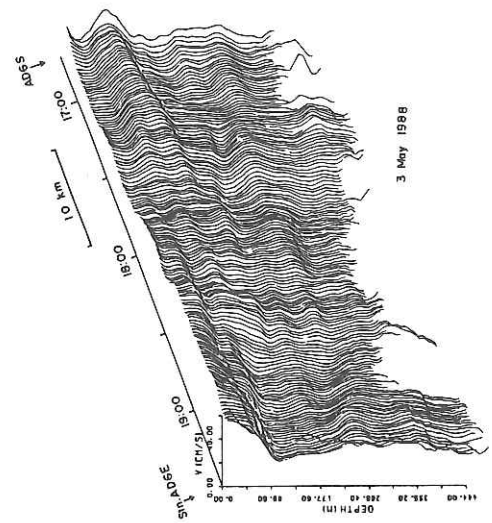

Fig. 11.9(b)

12. Release of Sofar floats and deployment of Sofar receivers

K. Taira, M. Fukasawa, M. Kawabe, S. Kitagawa, H. Otobe, S-K, Yang,
K. Uehara and M. Hamatani
(Ocean Research Institute, University of Tokyo)

Sound waves propagate long distance through a sound channel where sound speed is minimum. The channel is called as Sofar (sound fixing and ranging) channel, and located at about 1000 m depth. We track a neutral buoyancy float by acoustic signals through the sofar channel. The float is composed with an acoustic resonator and two glass balls, one contains electric circuit and the other the battery (Fig. 12.1). The float emitts a sound signal of 780 Hz two times everyday and the signal can be received at a distance of 600 km.

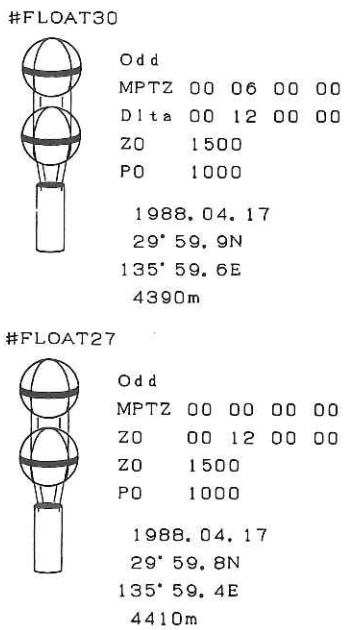

Fig. 12.1 Schematics of the Sofar floats and places of release.

During the cruise, we released two sofar floats at 30°N and 136°E. Each of them is adjusted its buoyancy to stay 1500 m depth and to follow the water motion at the layer. Buoyancy adjustment was made at laboratory within 0.2 g which is about 2 part per million of the weight of the float in the air, i.e., about 100 kg. The in-situ density was estimated by using CTD data collected in the sea area in 1985 from the R/V Hakuho Maru.

Sofar receivers were moored at three stations. The receiver records arrival time of the signals and their intensity on a magnetic tape. When the receivers are retrieved, the position of sofar floats will be determined. Mooring lines for the receivers and the positions are shown in Fig. 12.2. The hydrophone array is set at 1000 m depth where the sound channel is located in the sea area.

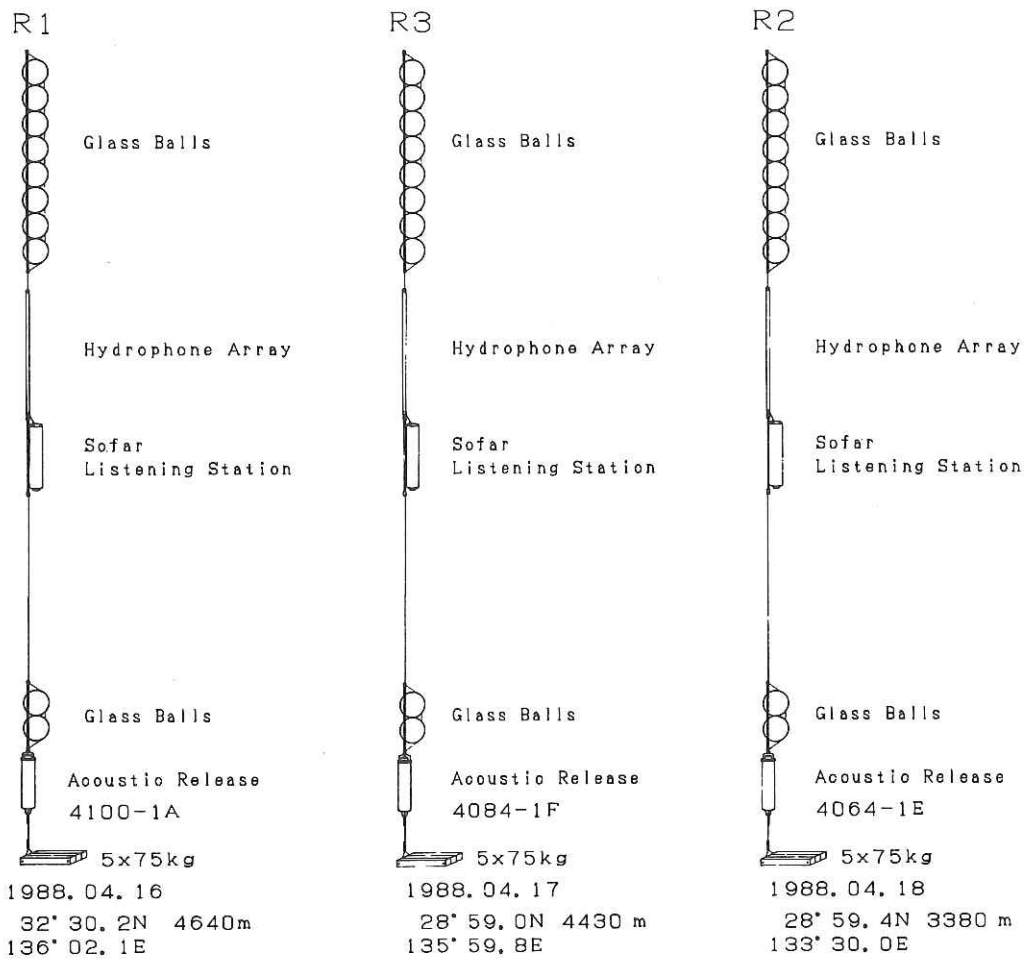

Fig. 12.2 Mooring lines of the Sofar receivers and moored places.

13. Study of maritime aerosol and ozone over the sea area at the south of Honshu

S. Kanamori and M. Tanaka
(Water Research Institute, Nagoya University)

The purpose of the present study is to observe the distribution of chemical composition and size distribution of maritime aerosol, and also, that of ozone concentration over the sea area from the coast of Honshu to the western North Pacific.

Samples were collected using three types of aerosol samplers.

1. Andersen low pressure impactor

Samples were separated into 12 size fractions (2 μm – 0.06 μm) and collected on polyethylene sheet with flow rate 20 l/min. Particles smaller than 0.06 μm were collected on a back up filter (Nuclepore Filter). This samples will be used to measure the heavy metal content.

2. Andersen high volume sampler

Samples were separated into 4 size fractions (7 μm – 1.1 μm) and collected on the quartz fiber filters with flow rate 566 l/min. Particles smaller than 1.1 μm were collected on a back up filter (Fluoropore Filter). This samples will be used to analyze the particulate carbon compounds.

3. High volume sampler

Total aerosol samples were collected on a Fluoropore filter with flow rate 1000 l/min.

4. The samples of gaseous substances which are expected to be the precursor of some atmospheric aerosols were collected. Filtered air was passed through a liquid nitrogen trap and the condensate was brought back keeping at $< -30°C$.

5. The continuous observations of atmospheric aerosol content and ozone concentration were carried out.

(1) In the first leg, unexpected high level of atmospheric aerosol content which is comparable with that in Tokyo bay (80 – 180 $\mu g/m^3$) was observed. This is thought to be due to Kosa phenomenon reported for the same period in Japan.

(2) Ozone concentration showed daily variation in Tokyo bay (0 – 50 ppb) that was high in daytime and low in night, but kept nearly constant level (60 – 70 ppb) over open sea.

The aerosol samples will be analyzed for heavy metal elements and their

distribution will be understood by comparison with observation of total aerosol and ozone distribution.

14. Chemical study in the western North Pacific Ocean

S. Watanabe, S. Saito and T. Todoroki
(Faculty at Fisheries, Hokkaido University)

14.1 Dimethyl sulfide in the ocean and the marine atmosphere

Dimethyl sulfide (DMS) is the major component of the reduced sulfur emitted from the marine surface water to the atmosphere. It is produced mainly by phytoplankton in the upper layers of the ocean. Variations in concentration of sea water are depended on time of day, season, location and depth. In this cruise we observed variations in concentration of surface sea waters and the atmosphere on time of day at 135°20°E, 28°40'N. DMS concentrations were measured on board vessel by FPD-gas chromatography immediately samples were collected. A part of the reslts are shown in table 14.1 and table 14.2. DMS concentrations of upper layer of the ocean at daytime are higher than these at night. This difference of DMS profiles can be related with activity of marine organism. The investigated behavior in the marine atmosphere will be explained with flux of DMS from sea surface and oxidation rate of DMS at the atmosphere.

14.2 Chlorofluoromethanes in the ocean

Chlorofluoromethanes (CFMs) are the useful tracers to investigate the water circulation in the upper ocean. CFMs are man-made and stable chemical compounds. CFMs are transported to ocean through atmosphere. CFMs distributions in the ocean result from mixing and advection of water. We collected 143 samples at eleven stations in this cruise. Trichlorofluoromethane (F-11) and dichlorodifluorometane (F-12) were extracted on board vessel from water and trapped in glass U-tube contained with Poracil C and Porapac T. Measurements of F-11 and F-12 contents with ECD-gas chromatography are underway.

14.3 Radiocarbon and tritium in the ocean

Data on ^{14}C and ^{3}H in the ocean are useful to investigate the general water circulation and the residence time of the ocean water. We collected nine samples at Sta. 9 for ^{14}C measurement and 39 samples at three stations (Sta. 7, S-2 and MW-1) for ^{3}H analysis. Analysis of ^{14}C and ^{3}H are underway with a liquid scintillation method. The water circulation in the western North Pacific Ocean will be understood with these results and other cruise data.

Table 14.1 Vertical distributions of DMS concentrations in the upper ocean at 135°20'E, 29°40'N.

Depth (m)	Temp. (°C)	Sal. (‰)	D.O. (ml/l)	Si (μgat/l)	DMS (ngS/l)
18:33-18:59 5th May					
0	21.2	34.729	5.16	1.3	20.1
2		34.715	5.19	1.4	8.74
11	21.0	34.731	5.17	1.8	8.00
21	20.8	34.769	5.20	1.6	4.26
30	20.5	34.802	5.17	1.3	6.29
40	20.5	34.816	5.22	1.3	2.62
50	20.5	34.816	5.14	1.5	1.20
60	20.4	34.823	5.10	1.9	1.16
80	20.3	34.823	5.06	2.0	0.141
100	20.1	34.837	5.02	1.6	0.029
150	19.7	34.866	4.96	2.0	0.008
249	18.9	34.890	5.05	2.4	0.006
501	13.9	34.566	4.34	14.5	
00:32-01:08 6th May					
0	21.2	34.742	5.16	1.5	14.1
2		34.738	5.20	1.2	9.01
10	21.0	34.737	5.14	1.4	
19	20.9	34.740	5.16	1.4	10.6
31	20.5	34.785	5.19	1.6	6.82
41	20.5	34.795	5.15	1.5	4.40
50	20.4	34.801	5.14	1.5	3.91
60	20.4	34.799	5.11	1.6	2.41
80	20.3	34.821	5.09	1.4	0.178
100	20.0	34.825	4.95	2.3	0.023
150	19.8	34.844	5.00	2.0	0.008
250	18.6	34.871	5.01	2.3	0.008
502	13.3	34.506		17.1	0.096
06:28-06:58 6th May					
0	21.1	34.733	5.06	1.7	19.4
2		34.729	5.11	1.5	17.2
10	21.0	34.730	5.09	1.5	21.5
20	21.0	34.733	5.11	1.5	18.5
30	20.9	34.745	5.07	1.6	33.4
40	20.7	34.761	5.10	1.6	11.3
49	20.5	34.789	5.09	1.7	11.4
61	20.5	34.801	5.04	1.6	2.93
80	20.2	34.825	5.11	1.6	0.94
100	20.2	34.825	4.99	1.7	0.027
150	19.8	34.840	5.04	2.1	0.006
250	18.9	34.869	4.96	2.4	0.006
503	14.0	34.560	4.25	14.9	0.004

Table 14.1 (continued)

Depth (m)	Temp. (°C)	Sal. (‰)	D.O. (ml/l)	Si (μgat/l)	DMS (ngS/l)
00:32-01:08	6th May				
0	21.6	34.731	5.07	1.7	10.9
2		34.722	5.07	1.8	12.7
10	21.4	34.722	5.07	1.6	9.30
21	21.0	34.744	5.10	1.8	32.1
30	20.9	34.741	5.08	1.6	31.4
40	20.8	34.746	5.11	1.6	10.7
50	20.6	34.793	5.13	1.8	4.53
60	20.4	34.792	5.15	2.4	2.45
79	20.3	34.819	4.87	2.3	0.31
100	20.1	34.821	4.95	2.8	0.063
150	19.7	34.850	4.89	2.9	0.012
249	18.8	34.863	4.73	3.4	0.084
500	13.4	34.518	4.17	17.0	0.040

Table 14.2 Diurnal variations in the concentration of DMS in air at 135°20′E, 29°40′N.

Sampling interval		DMS (ngS/m^3)
5th May	20:09-21:09	0.75
	21:16-23:35	2.04
6th May	00:00-01:01	1.05
	04:43-05:40	0.15
	05:48-06:50	0.12
	15:26-16:26	0.05
	17:21-18:21	0.13

Appendix I
Routine surface meteorological data during the period from 15 to 26 April (Leg I), and the period form 30 April to 10 May (Leg II).

Note:

1) Lat.: Latitude of position
2) Long.: Longitude of position
3) W.D.: Wind Direction
4) W.F.: Wind Speed (m/s)
5) F : Wind Force
   - 0: calm (wind spped 0.0-0.2 m/s)
   - 1: light air (0.3-1.5 m/s)
   - 2: light breeze (1.6-3.3 m/s)
   - 3: gentle breeze (3.4-5.4 m/s)
   - 4: moderate breeze (5.5-7.9 m/s)
   - 5: fresh breeze (8.0-10.7 m/s)
   - 6: strong breeze (10.8-13.8 m/s)
   - 7: high wind (13.9-17.1 m/s)
   - 8: gale (17.2-20.7 m/s)
   - 9: strong gale (20.8-24.4 m/s)
   - 10: whole gale (24.5-28.4 m/s)
   - 11: storm (28.5-32.6 m/s)
   - 12: hurricane (more than 32.7 m/s)
6) We : Weather
   - b: Blue sky, cloud amount 0-2
   - bc: Blue sky with detached cloud 3-7
   - c: Cloudy 8-10
   - d: Drizzing rain
   - e: Wet without rain
   - f: Fog
   - g: Gloomy
   - h: Hail
   - l: Lightning
   - m: Mist
   - o: Overcast sky
   - p: Passing shower
   - q: Squall
   - r: Rain
   - s: Snow
   - t: Thunder
   - u: Ugly weather
   - v: Unusual visibility
   - w: Dew
   - z: Haze
7) N : 10 grades cloud amount
8) Bar.: Surface pressure (hPa)
9) V : Visibility
   - 0: 0- 50 m Dense fog
   - 1: 50- 200 m Thin fog
   - 2: 200- 500 m Fog
   - 3: 500-1000 m Moderate fog
   - 4: 1- 2 km Thin fog or mist
   - 5: 2- 4 km Visibility poor
   - 6: 4- 10 km Moderate
   - 7: 10- 20 km Good
   - 8: 20- 50 km Very good
   - 9: more than 50 km Exceptional
10) Se : Sea condition
   - 0: Dead calm
   - 1: Very smooth
   - 2: Smooth
   - 3: Slight
   - 4: Moderate
   - 5: Rather rough
   - 6: Rough
   - 7: High
   - 8: Very high
   - 9: Phenomenal
11) Sw : Swell
   - 0: No swell
   - 1: Slight swell
   - 2: Moderate swell
   - 3: Rather rough swell
   - 4: Rough swell
   - 5: Heavy swell
   - 6: Very heavy swell
   - 7: Abnormal swell
12) A.T.: Atmospheric temperature (°C)
13) S.T.: Sea surface temperature (°C)

(4/15) KH-88-02 Meteorological data Sunrize 05:09 Sunset 18:15

J	Latitude	Longitude	W.D.	W.F.	F	We	N	Bar.	V	Se	Sw	A.T.	S.T.	T	Td
1															
2															
3															
4															
5															
6															
7															
8															
9															
10															
11															
12															
13															
14															
15														15.3	7.3
16			S	7.0	4									15.6	4.6
17			SE	7.2	4	b	2	1014.2	8	2	1	17.2	15.6	16.8	5.9
18			SW	7.5	4	b	2	1014.0	7	3	1	17.8	16.8	17.5	7.0
19	34°54.1'N	139°27.1'E	WNW	5.2	3	b	2	1015.4	7	3	1	17.2	18.0	16.7	7.0
20	34°48.5'N	139°17.5'E	SSE	1.2	1	b	1	1016.1	7	2	1	16.8	17.6	16.3	2.5
21	34°40.3'N	139°12.2'E	W	13.0	6	b	1	1016.5	7	4	1	16.2	17.4	15.8	3.0
22	34°33.5'N	139°04.6'E	W	15.0	7	b	1	1017.3	8	5	3	16.0	16.5	15.7	2.0
23	34°26.5'N	138°58.3'E	W	17.5	8	b	1	1017.4	8	5	3	16.1	18.4	16.0	3.8
24	34°18.9'N	138°50.3'E	W	16.0	7	b	2	1018.0	8	5	3	15.8	19.3	15.3	3.7

(4/16) KH-88-02 Meteorological data Sunrize 05:17 Sunset 18:26

J	Latitude	Longitude	W.D.	W.F.	F	We	N	Bar.	V	Se	Sw	A.T.	S.T.	T	Td
1	34°12.3'N	138°39.9'E	NW	14.5	7	b	2	1019.6	8	5	3	15.2	18.8	15.0	2.9
2	34°06.9'N	138°28.3'E	WNW	16.0	7	b	2	1020.0	8	5	3	15.0	18.7	14.7	3.0
3	34°00.8'N	138°16.8'E	WNW	17.0	7	b	2	1020.2	8	5	3	14.6	19.4	14.2	3.7
4	33°53.6'N	138°05.2'E	NW	17.5	8	b	1	1020.7	8	5	3	14.2	19.2	13.9	4.0
5	33°46.0'N	137°53.5'E	NW	14.5	7	b	2	1021.4	8	5	3	14.2	18.2	13.9	5.2
6	33°38.3'N	137°41.8'E	NNW	12.8	6	b	2	1022.2	8	5	3	13.9	17.2	13.7	6.2
7	33°30.0'N	137°30.0'E	NNW	12.0	6	b	2	1023.1	8	5	3	13.8	17.5	13.6	6.1
8	33°22.1'N	137°17.5'E	NNW	10.5	5	b	2	1023.9	8	4	3	13.8	17.4	13.8	5.0
9	33°14.2'N	137°05.9'E	N	11.5	6	b	2	1024.7	8	4	3	13.8	16.6	14.2	5.4
10	33°05.8'N	136°54.6'E	N	8.0	5	b	2	1025.6	8	4	3	14.7	17.0	15.1	5.6
11	32°52.8'N	136°43.8'E	N	5.5	4	bc	6	1025.5	8	3	3	14.8	17.1	15.1	5.0
12	32°49.9'N	136°31.1'E	NE	3.5	3	bc	3	1025.3	8	3	3	15.7	17.2	16.6	5.9
13	32°41.7'N	136°19.4'E	NE	3.0	2	bc	6	1024.9	8	3	3	16.6	18.6	17.0	7.0
14	32°34.1'N	136°07.5'E	NNW	2.5	2	c	8	1024.3	7	2	3	17.6	20.9	17.4	2.1
15	32°30.1'N	136°02.2'E	NNE	2.0	2	c	8	1024.1	7	2	3	17.4	19.1	17.2	1.9
16	32°30.0'N	136°02.3'E	E	1.0	1	o	10	1024.0	7	2	3	19.1	19.1	17.6	2.0
17	32°25.7'N	136°01.7'E	ESE	3.5	3	c	9	1023.4	8	2	1	17.3	19.2	17.0	4.5
18	32°11.5'N	136°01.2'E	ESE	2.0	2	c	8	1024.0	8	2	1	17.1	20.8	16.8	7.2
19	31°57.4'N	136°01.2'E	ENE	1.1	1	bc	7	1024.5	8	2	1	17.0	20.7	16.5	6.9
20	31°43.8'N	136°01.2'E	ENE	4.0	3	bc	3	1025.0	8	2	1	16.8	21.1	16.7	8.0
21	31°30.6'N	136°00.8'E	ENE	4.5	3	bc	3	1025.1	8	2	1	17.0	21.0	16.6	8.1
22	31°17.1'N	136°00.3'E	ENE	4.0	3	bc	3	1025.4	8	2	1	16.8	20.8	16.7	8.1
23	31°04.3'N	135°58.9'E	E	5.0	3	bc	3	1024.8	8	2	1	17.2	21.2	17.0	8.9
24	30°51.7'N	135°59.6'E	E	7.0	4	bc	3	1024.7	8	2	1	17.2	20.4	17.1	7.0

(4/17) KH-88-02 Meteorological data Sunrize 05:24 Sunset 18:27

J	Latitude	Longitude	W.D.	W.F.	F	We	N	Bar.	V	Se	Sw	A.T.	S.T.	T	Td
1	30°38.8'N	136°00.0'E	ENE	5.0	3	b	1	1024.6	8	2	1	17.8	21.1	17.2	8.1
2	30°26.3'N	135°59.9'E	E	8.0	5	bc	4	1024.0	8	2	2	17.6	20.0	17.2	11.0
3	30°13.7'N	135°59.0'E	ENE	8.0	5	bc	3	1023.6	8	3	2	17.7	19.2	17.3	11.9
4	30°01.0'N	135°59.9'E	ENE	6.0	4	bc	7	1023.5	8	3	2	18.0	19.4	17.6	12.0
5	29°56.0'N	135°59.2'E	ENE	9.0	5	o	10	1023.7	8	3	1	18.1	20.2	17.7	12.4
6	29°43.2'N	135°59.3'E	E	8.6	5	o	10	1023.5	8	3	1	18.4	19.8	18.0	12.8
7	29°30.4'N	135°59.4'E	ENE	8.5	5	bc	7	1023.9	8	3	1	18.4	19.1	18.2	13.0
8	29°17.7'N	135°59.8'E	ESE	3.5	3	c	8	1024.5	8	2	1	18.9	19.3	18.8	10.5
9	29°04.9'N	136°00.2'E	ESE	4.0	3	bc	4	1024.8	8	2	1	19.2	19.3	19.2	10.9
10	28°59.7'N	136°00.0'E	E	3.0	2	bc	7	1024.7	8	2	1	19.3	19.7	19.3	11.3
11	28°59.5'N	135°59.5'E	E	3.0	2	bc	7	1024.3	8	2	1	19.3	19.7	19.2	11.9
12	28°59.3'N	135°58.9'E	E	3.0	2	c	8	1023.8	8	2	1	19.3	19.7	19.3	12.4
13	28°59.1'N	135°57.2'E	SE	6.0	4	o	10	1023.0	8	2	1	19.5	19.7	19.6	12.0
14	28°59.0'N	135°59.8'E	ESE	8.5	5	c	9	1021.7	8	3	1	19.6	19.6	19.8	12.2
15	29°00.9'N	135°47.9'E	ESE	7.0	4	o	10	1021.4	8	3	1	20.4	19.5	19.3	12.0
16	29°04.3'N	135°33.5'E	ESE	6.0	4	c	8	1020.7	7	3	1	19.9	19.5	19.3	12.5
17	29°08.1'N	135°19.3'E	ESE	9.0	5	o	10	1020.9	8	3	1	19.8	19.5	18.9	12.2
18	29°11.9'N	135°05.2'E	ESE	8.0	5	o	10	1021.3	8	3	1	19.6	19.2	18.7	12.0
19	29°12.1'N	135°05.1'E	ESE	8.0	5	o	10	1021.1	7	3	1	19.2	19.6	18.9	13.3
20	29°12.3'N	135°04.7'E	ESE	11.0	6	o	10	1021.0	7	3	1	19.0	19.6	19.0	13.2
21	29°12.3'N	135°04.5'E	E	8.0	5	o	10	1021.3	7	3	1	19.0	19.6	18.6	13.4
22	29°12.2'N	135°04.4'E	ESE	8.5	5	o	10	1020.8	7	3	1	18.9	19.4	18.6	13.9
23	29°11.3'N	135°02.3'E	ESE	9.0	5	o	10	1020.2	7	3	1	18.9	19.2	18.7	14.2
24	29°10.3'N	135°00.6'E	ESE	9.0	5	o	10	1019.1	7	3	1	19.1	19.1	18.5	14.4

(4/18) KH-88-02 Meteorological data Sunrize 05:34 Sunset 18:35

J	Latitude	Longitude	W.D.	W.F.	F	We	N	Bar.	V	Se	Sw	A.T.	S.T.	T	Td
1	29°08.8'N	134°46.4'E	SSE	10.5	5	o	10	1017.6	7	3	1	19.1	19.3	18.6	14.8
2	29°06.5'N	134°32.8'E	SE	9.0	5	o	10	1015.8	7	3	1	19.3	20.6	19.0	15.0
3	29°05.4'N	134°19.1'E	SSE	13.5	6	o	10	1014.4	7	4	3	19.8	20.8	19.3	14.9
4	29°04.9'N	134°05.1'E	SSE	13.0	6	o	10	1013.4	7	4	3	19.8	20.1	19.4	14.7
5	29°03.4'N	133°51.2'E	SE	15.0	7	r	10	1012.3	7	4	3	19.7	20.4	19.2	15.2
6	29°00.9'N	133°37.4'E	SE	13.5	6	r	10	1011.9	6	4	3	19.2	20.6	18.3	16.4
7	29°00.2'N	133°29.6'E	SE	17.0	7	r	10	1010.5	6	5	3	18.8	21.2	18.4	16.9
8	28°58.7'N	133°32.4'E	SE	19.0	8	r	10	1010.0	5	5	3	18.6	21.0	18.0	16.5
9	28°58.0'N	133°35.0'E	SE	17.0	7	r	10	1009.5	6	5	3	19.0	20.6	18.9	17.0
10	28°56.7'N	133°37.8'E	SE	18.0	8	r	10	1008.8	6	6	3	19.2	20.6	18.5	17.8
11	28°55.7'N	133°41.0'E	SE	18.0	8	r	10	1007.7	6	6	3	19.7	20.1	19.5	18.4
12	28°55.0'N	133°44.3'E	SSE	17.5	8	r	10	1006.8	5	6	3	20.1	20.1	19.7	18.9
13	28°56.7'N	133°44.0'E	SSE	15.5	7	r	10	1005.6	5	6	3	20.1	20.1	20.0	19.6
14	28°59.7'N	133°40.4'E	SSE	18.5	8	r	10	1003.5	4	6	3	20.8	20.1	20.2	20.0
15	29°02.3'N	133°36.9'E	NW	6.5	4	r	10	1004.0	4	4	3	19.8	20.6	19.0	18.8
16	29°03.5'N	133°33.6'E	NW	15.0	7	o	10	1003.9	7	5	3	20.6	21.1	20.6	17.0
17	29°03.2'N	133°31.1'E	NW	15.3	7	pc	6	1005.0	7	5	3	20.8	21.6	20.6	12.8
18	29°02.1'N	133°29.0'E	NW	13.0	6	b	1	1005.9	7	5	3	20.5	21.7	20.1	11.5
19	29°02.1'N	133°27.0'E	WNW	11.5	6	b	1	1006.8	7	5	3	20.0	21.8	19.7	10.2
20	29°02.1'N	133°25.0'E	WNW	11.0	6	bc	3	1007.2	7	5	3	19.6	21.8	19.2	9.8
21	29°03.1'N	133°23.2'E	W	9.5	5	bc	3	1008.3	6	4	3	19.2	21.7	19.1	9.5
22	29°01.1'N	133°27.0'E	WNW	11.0	6	bc	3	1008.5	6	5	3	19.0	21.8	19.1	8.6
23	29°00.5'N	133°26.7'E	WNW	11.0	6	bc	3	1009.6	6	5	3	19.1	21.8	18.9	9.0
24	28°59.8'N	133°26.4'E	W	11.0	6	bc	4	1009.4	6	5	3	19.2	21.8	18.7	8.8

(4/19) KH-88-02 Meteorological data Sunrize 05:35 Sunset 18:29

J	Latitude	Longitude	W.D.	W.F.	F	We	N	Bar.	V	Se	Sw	A.T.	S.T.	T	Td
1	28°59.5'N	133°26.5'E	WNW	12.0	6	b	2	1009.6	6	5	3	18.8	19.7	18.6	9.0
2	28°59.3'N	133°26.5'E	W	12.0	6	b	2	1010.0	7	5	3	19.0	21.8	18.6	8.6
3	28°59.1'N	133°26.0'E	WNW	9.0	5	bc	3	1009.6	7	4	3	18.8	21.7	18.3	9.3
4	28°58.6'N	133°25.3'E	WNW	8.0	5	bc	4	1009.5	7	4	3	18.8	21.7	18.5	10.1
5	28°58.3'N	133°24.4'E	WNW	10.0	5	bc	4	1010.2	7	4	3	18.4	21.7	18.2	9.9
6	28°58.2'N	133°23.8'E	WNW	10.0	5	bc	7	1010.4	7	4	3	18.6	21.8	18.5	9.9
7	28°59.8'N	133°29.9'E	WNW	10.5	5	c	8	1011.1	7	4	3	18.4	21.3	18.3	10.0
8	29°00.7'N	133°29.4'E	WNW	8.0	5	c	9	1011.8	7	4	3	18.3	21.3	18.2	9.2
9	28°58.8'N	133°31.5'E	NW	8.0	5	o	10	1012.0	7	4	3	18.4	20.7	18.5	8.9
10	28°58.8'N	133°34.1'E	NW	7.0	4	o	10	1012.2	7	4	3	18.5	21.0	18.9	9.9
11	29°00.5'N	133°47.8'E	NW	6.0	4	o	10	1012.3	7	3	3	19.4	20.0	19.0	9.5
12	29°03.3'N	134°01.3'E	WNW	7.0	4	o	10	1012.3	7	3	3	19.6	20.4	19.0	9.1
13	29°04.5'N	134°15.4'E	NW	4.0	3	o	10	1011.4	6	3	3	19.4	20.1	19.0	9.8
14	29°06.8'N	134°29.5'E	WNW	4.5	3	o	10	1011.1	6	2	3	19.8	20.7	19.2	9.9
15	29°08.5'N	134°44.0'E	WNW	3.5	3	o	10	1011.1	6	2	3	19.6	20.2	19.1	10.0
16	29°10.9'N	134°57.8'E	WNW	3.5	3	o	10	1011.0	6	2	3	19.2	19.6	18.9	9.8
17	29°12.3'N	135°04.9'E	W	5.0	3	c	9	1011.3	6	2	3	19.2	19.4	18.9	10.0
18	29°12.5'N	135°04.7'E	WNW	5.0	3	b	2	1011.5	6	2	1	18.8	19.5	18.5	10.7
19	29°12.6'N	135°04.6'E	WNW	5.0	3	bc	3	1012.0	6	2	1	18.7	19.3	18.6	10.7
20	29°12.7'N	135°04.9'E	W	3.0	2	b	1	1012.2	6	2	1	18.7	19.3	18.3	11.1
21	29°12.8'N	135°04.8'E	WSW	5.5	4	b	1	1012.8	6	2	1	18.6	19.4	18.5	10.9
22	29°12.8'N	135°04.7'E	W	5.0	3	b	1	1013.1	6	2	1	18.8	19.3	18.4	11.6
23	29°12.5'N	135°05.3'E	W	5.0	3	b	1	1012.6	6	2	1	18.6	19.3	18.1	11.9
24	29°04.4'N	135°03.8'E	SW	5.0	3	b	1	1012.3	6	2	1	18.7	19.1	18.2	11.7

(4/20) KH-88-02 Meteorological data Sunrize 05:28 Sunset 18:28

J	Latitude	Longitude	W.D.	W.F.	F	We	N	Bar.	V	Se	Sw	A.T.	S.T.	T	Td
1	28°55.4'N	135°01.7'E	SSW	4.0	3	b	2	1012.6	6	2	1	18.6	19.1	18.2	12.0
2	28°49.4'N	135°00.5'E	SSW	4.0	3	b	2	1012.7	6	2	1	18.5	19.2	18.1	11.9
3	28°48.7'N	135°01.1'E	SW	5.0	3	b	2	1012.6	6	2	1	18.6	19.2	18.1	11.8
4	28°47.9'N	135°01.7'E	SW	4.0	3	bc	4	1012.6	6	2	1	18.6	19.1	18.0	12.3
5	28°47.4'N	135°02.1'E	SSW	3.0	2	bc	3	1012.8	6	2	1	18.6	19.0	18.0	13.0
6	28°46.9'N	135°02.3'E	SW	5.0	3	bc	3	1013.0	7	2	1	18.6	19.0	18.1	13.4
7	28°46.4'N	135°02.4'E	SSW	4.0	3	bc	7	1013.5	7	2	1	18.7	19.0	18.3	13.5
8	28°49.8'N	134°59.8'E	SW	4.0	3	c	8	1013.8	7	2	1	19.1	19.1	18.8	13.2
9	28°46.6'N	135°02.6'E	SW	3.0	2	o	10	1013.8	6	2	1	19.2	19.1	19.2	14.0
10	28°48.3'N	135°01.4'E	SW	2.0	2	o	10	1013.7	6	2	1	20.7	19.2	19.9	14.0
11	28°48.1'N	135°00.0'E	SW	2.5	2	o	10	1013.4	6	2	1	20.1	19.4	20.2	13.9
12	28°47.9'N	134°59.8'E	SSW	2.5	2	o	10	1013.3	6	2	1	20.3	19.1	20.0	14.1
13	28°47.8'N	134°59.5'E	S	3.0	2	o	10	1012.7	6	2	1	20.0	19.4	19.9	14.1
14	28°47.7'N	134°59.3'E	S	3.0	2	o	10	1012.3	6	2	1	20.0	19.3	19.8	14.2
15	28°47.9'N	135°02.1'E	S	3.0	2	o	10	1011.9	6	2	1	19.9	19.5	19.4	14.3
16	28°55.7'N	135°12.7'E	SSE	4.0	3	o	10	1011.6	6	2	1	19.4	19.5	19.2	14.9
17	29°00.2'N	135°20.0'E	S	3.5	3	c	9	1012.0	7	2	1	19.4	19.8	19.0	15.0
18	29°00.1'N	135°28.7'E	SSE	2.0	2	c	9	1012.9	6	2	1	19.4	19.6	18.8	14.5
19	29°00.5'N	135°30.3'E	S	2.0	2	c	9	1013.3	6	2	1	19.4	19.7	18.9	14.6
20	29°00.1'N	135°40.1'E	SSW	2.5	2	c	8	1013.8	6	2	1	19.1	19.5	18.7	14.6
21	29°00.1'N	135°47.6'E	SE	2.5	2	c	8	1013.5	6	2	1	19.0	19.4	18.5	14.1
22	28°59.8'N	135°50.6'E	S	1.0	1	c	8	1013.5	6	1	1	18.8	19.5	18.2	14.2
23	29°01.5'N	135°40.9'E	S	2.5	2	bc	7	1013.1	6	2	1	18.7	19.4	18.2	14.2
24	29°04.0'N	135°28.5'E	SSE	6.0	4	bc	7	1012.6	6	3	1	18.7	19.4	18.2	14.7

(4/21) KH-88-02 Meteorological data Sunrize 05:27 Sunset 18:32

J	Latitude	Longitude	W.D.	W.F.	F	We	N	Bar.	V	Se	Sw	A.T.	S.T.	T	Td
1	29°06.4'N	135°15.8'E	SSE	6.0	4	c	9	1011.7	6	3	1	18.8	19.3	18.2	15.0
2	29°09.2'N	135°03.5'E	SSE	7.0	4	o	10	1011.2	7	3	1	18.8	19.5	18.2	15.3
3	29°10.0'N	135°00.2'E	SSE	7.0	4	o	10	1011.0	6	3	1	18.7	19.4	18.1	15.8
4	29°09.9'N	134°59.9'E	SSE	7.0	4	o	10	1010.7	6	3	1	18.6	19.4	18.1	15.7
5	29°09.8'N	134°59.4'E	SSE	8.0	5	o	10	1011.5	7	3	1	18.9	19.4	18.3	15.9
6	29°09.8'N	134°58.7'E	S	5.5	4	o	10	1011.2	7	3	1	19.0	19.4	18.5	16.2
7	29°09.9'N	134°58.1'E	SSE	5.0	3	o	10	1011.5	7	3	1	19.1	19.4	18.7	16.2
8	29°09.9'N	134°57.4'E	SSE	4.0	3	o	10	1011.2	7	2	1	19.1	19.4	18.8	16.4
9	29°09.8'N	134°56.8'E	SSE	5.0	3	r	10	1011.2	6	2	1	19.2	19.3	18.9	16.8
10	29°09.9'N	134°58.9'E	SE	5.5	4	r	10	1010.6	6	3	1	19.1	19.3	18.9	17.0
11	29°10.1'N	134°59.9'E	SE	6.0	4	o	10	1010.3	6	3	1	19.2	19.1	19.0	17.1
12	29°10.5'N	135°00.3'E	SE	5.5	4	o	10	1009.8	6	3	1	19.5	19.2	19.3	17.6
13	29°10.9'N	135°01.1'E	SE	7.0	4	o	10	1009.1	6	3	1	19.4	19.2	19.2	17.6
14	29°09.8'N	134°57.2'E	SE	7.0	4	o	10	1008.0	6	3	1	19.6	19.2	19.2	17.9
15	29°10.1'N	134°57.2'E	SE	7.0	4	o	10	1007.6	6	3	1	20.2	19.4	19.8	18.0
16	29°10.1'N	134°57.5'E	SE	7.0	4	o	10	1007.5	6	3	1	20.1	19.5	19.9	18.2
17	29°09.9'N	134°59.9'E	SE	8.5	5	o	10	1007.0	6	3	1	19.7	19.8	19.1	18.2
18	29°09.9'N	134°59.4'E	SSE	10.0	5	o	10	1007.0	5	3	1	19.8	19.4	19.2	18.5
19	29°10.1'N	134°59.0'E	SSE	9.5	5	r	10	1006.9	6	3	1	19.6	19.3	19.0	18.6
20	29°10.1'N	134°58.8'E	SSE	10.0	5	r	10	1007.0	5	3	1	19.6	19.3	19.2	19.0
21	29°09.7'N	134°58.1'E	S	8.0	5	r	10	1007.2	6	3	1	20.2	19.2	19.5	19.0
22	29°06.3'N	134°48.7'E	SSE	10.5	5	o	10	1006.7	6	4	1	20.5	20.2	20.4	20.0
23	29°03.2'N	134°39.6'E	SSE	10.0	5	o	10	1006.7	6	4	1	21.0	20.1	20.2	20.0
24	29°00.0'N	134°30.8'E	S	10.0	5	o	10	1006.2	6	4	1	21.0	20.1	20.5	20.5

(4/22) KH-88-02 Meteorological data Sunrize 05:28 Sunset 18:32

J	Latitude	Longitude	W.D.	W.F.	F	We	N	Bar.	V	Se	Sw	A.T.	S.T.	T	Td
1	29°00.1'N	134°31.4'E	SW	6.0	4	o	10	1005.3	6	3	1	20.9	20.5	20.1	20.0
2	29°00.4'N	134°32.7'E	WSW	5.0	3	o	10	1005.2	6	3	1	21.0	20.4	20.2	20.0
3	28°59.3'N	134°32.5'E	WSW	7.0	4	bc	3	1005.0	6	3	1	20.6	20.4	20.1	19.0
4	28°56.8'N	134°32.3'E	WSW	7.0	4	bc	3	1004.9	7	3	1	20.4	20.4	20.3	19.3
5	28°56.3'N	134°33.7'E	W	8.0	5	c	9	1004.8	6	3	1	20.8	20.5	20.4	19.0
6	28°56.6'N	134°35.1'E	W	8.0	5	o	10	1005.0	7	3	1	20.8	20.4	20.4	18.7
7	28°55.7'N	134°35.5'E	WNW	8.0	5	o	10	1005.0	7	3	1	20.8	20.3	20.4	18.6
8	28°59.8'N	134°30.1'E	WNW	8.5	5	o	10	1005.6	7	3	1	21.0	20.4	20.4	18.9
9	28°59.3'N	134°32.5'E	NW	11.0	6	o	10	1006.4	6	4	1	20.2	20.5	19.9	19.0
10	28°59.6'N	134°40.4'E	NW	7.5	4	o	10	1006.6	6	3	1	20.6	20.5	20.2	18.5
11	28°59.2'N	134°40.5'E	NW	9.0	5	o	10	1006.7	7	3	1	20.4	20.8	20.2	18.3
12	28°59.0'N	134°40.5'E	NW	7.5	4	o	10	1006.1	7	3	3	20.4	20.8	20.1	18.1
13	28°58.9'N	134°43.1'E	NW	8.0	5	o	10	1006.1	7	3	1	20.6	20.6	20.8	17.9
14	28°59.6'N	134°49.9'E	NW	9.0	5	o	10	1006.1	7	3	1	20.6	20.9	20.4	17.7
15	29°00.1'N	134°58.1'E	NW	7.5	4	o	10	1005.6	7	3	1	21.0	19.7	20.5	17.8
16	28°59.8'N	135°00.2'E	NW	8.0	5	o	10	1006.1	7	3	1	20.2	19.8	19.9	17.6
17	28°59.9'N	135°10.0'E	NW	8.2	5	c	9	1006.6	7	3	1	20.3	19.4	19.7	17.4
18	29°00.0'N	135°14.2'E	WNW	5.5	4	c	9	1007.0	7	3	1	20.1	19.7	19.5	17.6
19	28°59.9'N	135°19.7'E	NNW	8.5	5	o	10	1007.7	7	3	1	19.4	19.6	19.2	16.0
20	28°59.7'N	135°19.1'E	NNW	10.5	5	o	10	1008.4	7	3	1	19.3	19.5	19.0	15.2
21	28°59.8'N	135°18.6'E	NNW	8.5	5	o	10	1009.1	7	3	1	19.1	19.5	18.9	14.5
22	29°00.5'N	135°16.0'E	NNW	10.5	5	o	10	1009.3	7	3	1	18.8	19.4	18.5	13.5
23	29°05.3'N	135°07.9'E	NNW	8.0	5	r	10	1009.5	7	3	1	18.2	19.4	18.0	12.0
24	29°09.9'N	135°00.1'E	NNW	7.0	4	o	10	1009.1	7	3	1	18.0	19.3	18.3	10.7

(4/23) KH-88-02 Meteorological data Sunrize 05:25 Sunset 18:31

J	Latitude	Longitude	W.D.	W.F.	F	We	N	Bar.	V	Se	Sw	A.T.	S.T.	T	Td
1	29°00.8'N	135°00.3'E	WNW	3.0	2	o	10	1009.1	7	3	1	18.4	19.3	18.1	12.0
2	29°08.0'N	135°00.7'E	NW	7.0	4	o	10	1009.0	7	3	1	18.1	19.2	17.7	12.8
3	29°07.8'N	134°59.6'E	WNW	5.0	3	o	10	1008.9	7	3	1	18.2	19.2	17.8	12.3
4	29°08.0'N	134°58.3'E	WNW	3.0	2	bc	6	1008.6	7	2	1	18.1	19.2	18.2	12.0
5	29°07.0'N	134°58.6'E	WNW	5.0	3	o	10	1008.8	7	2	1	18.1	19.1	17.9	13.0
6	29°05.8'N	134°58.7'E	NW	6.0	4	o	10	1009.2	7	2	1	18.2	19.1	17.8	13.2
7	29°04.7'N	134°58.7'E	NNW	7.0	4	o	10	1009.1	7	3	1	17.8	19.1	17.5	11.7
8	29°06.6'N	135°00.4'E	N	6.8	4	c	9	1009.0	7	3	1	17.8	19.2	17.5	11.1
9	29°07.1'N	134°58.8'E	NNW	7.5	4	r	10	1009.6	6	3	1	17.9	19.3	17.5	11.5
10	29°08.9'N	134°58.7'E	NW	6.5	4	r	10	1009.7	6	3	1	17.3	19.3	17.1	10.2
11	29°08.8'N	134°57.8'E	NW	6.0	4	r	10	1009.8	6	3	1	17.2	19.3	16.9	8.0
12	29°08.1'N	134°55.4'E	NW	5.0	3	r	10	1009.5	6	3	1	17.4	19.3	17.3	7.5
13	29°07.3'N	134°52.7'E	NW	4.0	3	r	10	1009.5	6	3	1	16.9	19.4	16.7	6.2
14	29°08.0'N	134°57.9'E	NW	4.0	3	o	10	1009.2	6	3	1	17.2	19.3	17.1	6.5
15	29°07.7'N	134°56.3'E	W	5.0	3	o	10	1009.0	6	3	1	17.2	19.4	17.2	8.5
16	29°09.7'N	134°58.2'E	W	4.0	3	o	10	1008.5	7	3	3	16.8	19.3	17.3	10.5
17	29°15.0'N	135°08.8'E	NW	6.0	4	o	10	1008.4	7	3	3	17.4	19.9	18.0	6.5
18	29°19.8'N	135°19.8'E	NW	5.5	4	r	10	1008.8	7	3	3	17.8	20.0	17.6	5.5
19	29°19.6'N	135°19.8'E	WNW	6.0	4	o	10	1009.3	7	3	3	17.8	20.0	17.8	5.0
20	29°19.4'N	135°19.6'E	NW	2.5	2	o	10	1009.4	7	2	3	18.2	20.0	18.2	6.8
21	29°18.8'N	135°18.5'E	W	5.0	3	o	10	1010.2	7	2	3	18.1	20.0	17.7	11.0
22	29°16.0'N	135°15.3'E	WSW	7.0	4	o	10	1010.3	7	3	3	17.8	20.0	17.5	11.2
23	29°09.4'N	135°08.6'E	WSW	8.0	5	o	10	1010.2	7	3	3	17.8	19.9	17.7	10.7
24	29°02.4'N	135°02.6'E	WSW	7.5	4	o	10	1010.0	7	3	3	18.0	19.3	18.0	10.5

(4/24) KH-88-02 Meteorological data Sunrize 05:24 Sunset 18:32

J	Latitude	Longitude	W.D.	W.F.	F	We	N	Bar.	V	Se	Sw	A.T.	S.T.	T	Td
1	28°59.4'N	135°00.7'E	W	4.0	3	o	10	1009.6	7	2	3	18.4	19.3	18.3	10.8
2	28°58.6'N	135°01.4'E	WNW	7.0	4	bc	4	1009.4	7	2	3	18.8	19.3	18.7	9.8
3	28°57.8'N	135°00.3'E	WNW	7.0	4	bc	5	1009.2	7	3	3	18.8	19.3	18.6	10.6
4	28°57.4'N	134°59.5'E	WNW	6.0	4	c	8	1009.5	7	3	3	19.2	19.2	19.2	10.6
5	28°56.1'N	135°00.6'E	WNW	10.0	5	o	10	1009.9	7	3	3	19.1	19.2	18.6	12.3
6	28°55.0'N	135°01.7'E	W	11.0	6	bc	7	1010.0	7	3	3	19.4	19.2	19.1	11.0
7	28°53.7'N	135°02.9'E	W	13.0	6	bc	5	1010.4	7	4	3	19.6	19.1	19.6	10.5
8	28°59.3'N	135°00.4'E	W	15.0	7	b	2	1010.3	7	4	3	19.8	19.2	20.0	10.0
9	28°59.0'N	134°58.1'E	W	15.0	7	b	1	1011.2	7	4	3	20.1	19.2	19.5	10.2
10	28°58.5'N	134°57.3'E	WNW	15.0	7	b	1	1011.8	7	4	3	18.8	19.2	18.7	11.0
11	28°57.2'N	134°55.2'E	WNW	14.0	7	b	1	1012.3	7	4	3	18.1	19.0	18.3	10.4
12	28°57.7'N	134°59.5'E	WNW	13.5	6	b	2	1012.3	7	4	3	18.4	19.3	18.3	10.5
13	28°59.4'N	135°13.3'E	WNW	13.0	6	c	9	1012.2	7	4	3	18.2	19.1	17.8	9.0
14	29°00.6'N	135°17.1'E	WNW	12.0	6	c	8	1012.1	7	5	3	18.6	19.6	18.8	8.0
15	29°01.9'N	135°11.7'E	WNW	12.0	6	o	10	1012.1	7	4	3	18.2	19.3	18.3	8.0
16	29°02.6'N	135°08.2'E	WNW	11.0	6	o	10	1012.6	7	4	3	18.0	19.2	18.0	8.4
17	29°05.1'N	135°02.4'E	WNW	13.0	6	o	10	1013.3	7	4	3	18.2	19.4	17.8	9.0
18	29°07.7'N	134°57.6'E	W	11.5	6	c	9	1013.9	7	4	3	17.8	19.7	17.7	8.3
19	29°17.0'N	134°54.2'E	WNW	8.8	5	c	9	1014.7	7	4	3	17.6	19.5	17.4	8.7
20	29°28.2'N	134°50.9'E	WNW	7.8	4	bc	5	1015.7	7	4	3	17.2	19.2	17.2	8.0
21	29°35.9'N	134°47.8'E	WNW	8.0	5	bc	3	1016.3	7	4	3	17.2	19.3	17.1	7.3
22	29°43.1'N	134°44.7'E	NW	5.5	4	bc	3	1016.7	7	3	3	17.2	19.4	17.2	7.8
23	29°54.8'N	134°41.4'E	NW	5.5	4	bc	7	1016.7	7	3	3	17.2	19.5	17.4	7.5
24	30°06.2'N	134°37.5'E	NW	5.5	4	bc	7	1016.3	7	3	3	17.0	19.6	16.9	8.3

(4/25) KH-88-02 Meteorological data Sunrize 05:23 Sunset 18:44

J	Latitude	Longitude	W.D.	W.F.	F	We	N	Bar.	V	Se	Sw	A.T.	S.T.	T	Td
1	30°16.3'N	134°33.9'E	WNW	7.0	4	b	2	1016.2	7	3	3	17.0	19.1	17.0	8.6
2	30°29.0'N	134°30.4'E	WNW	6.0	4	bc	3	1016.0	7	3	3	17.3	19.1	17.4	6.6
3	30°41.6'N	134°26.7'E	W	5.0	3	b	2	1015.9	7	3	3	17.4	18.8	17.4	7.8
4	30°54.5'N	134°24.8'E	WSW	5.5	4	bc	7	1016.0	7	3	3	17.5	18.5	17.3	8.4
5	31°07.5'N	134°21.8'E	WSW	7.5	4	c	9	1016.4	7	3	1	17.6	18.4	17.2	8.3
6	31°20.3'N	134°18.5'E	NE	4.0	3	bc	7	1017.2	7	3	1	16.4	18.6	15.8	11.6
7	31°32.7'N	134°14.7'E	NNE	4.0	3	bc	3	1018.0	8	3	1	17.3	19.5	17.0	8.6
8	31°45.1'N	134°09.6'E	NW	5.5	4	bc	3	1018.9	8	3	1	18.0	19.1	17.3	7.1
9	31°56.0'N	134°05.8'E	NW	6.0	4	b	1	1019.0	8	3	1	17.7	21.9	17.4	6.8
10	32°02.7'N	134°04.6'E	NW	5.0	3	b	1	1020.0	8	3	1	18.0	21.9	17.5	4.9
11	32°10.2'N	134°02.6'E	WNW	6.5	4	b	0	1019.7	8	3	1	17.8	22.0	17.2	5.9
12	32°17.7'N	134°00.1'E	WSW	6.0	4	b	1	1019.3	8	3	1	17.2	22.0	17.0	5.7
13	32°24.9'N	133°57.8'E	W	5.0	3	b	0	1018.9	8	2	1	16.0	22.4	17.1	5.8
14	32°32.2'N	133°55.4'E	W	4.0	3	b	1	1018.6	8	2	1	17.5	22.3	17.6	6.1
15	32°39.6'N	133°52.2'E	WSW	6.0	4	b	0	1017.9	8	2	1	18.0	21.6	18.0	6.8
16	32°47.3'N	133°49.7'E	WSW	8.0	5	b	1	1017.5	8	3	1	18.5	21.7	18.5	7.1
17	32°54.7'N	133°46.8'E	SW	9.0	5	b	1	1017.8	8	3	1	18.6	19.6	18.4	7.0
18	33°02.7'N	133°45.2'E	WSW	8.0	5	b	1	1017.8	8	3	1	18.3	18.2	17.8	10.5
19	33°10.0'N	133°42.5'E	WSW	9.0	5	b	1	1018.0	8	3	1	18.0	18.0	17.9	12.0
20	33°16.7'N	133°40.3'E	N	5.0	3	b	1	1019.0	8	2	1	17.6	18.2	17.0	9.7
21	33°17.8'N	133°39.7'E	NE	4.0	3	b	0	1019.8	8	2	1	17.4	18,6	16.9	9.6
22	33°17.5'N	133°40.3'E	N	3.0	2	b	0	1020.4	8	2	1	16.8	18.5	15.9	10.2
23	33°17.2'N	133°40.8'E	NW	5.0	3	b	0	1020.8	8	2	1	15.9	18.6	15.7	9.2
24	33°18.0'N	133°40.0'E	WNW	4.5	3	b	1	1020.3	8	2	1	16.4	18.2	16.1	6.5

(4/26) KH-88-02 Meteorological data Sunrize 05:23 Sunset 18:45

J	Latitude	Longitude	W.D.	W.F.	F	We	N	Bar.	V	Se	Sw	A.T.	S.T.	T	Td
1	33°17.9'N	133°40.2'E	N	4.0	3	b	1	1020.7	8	2	1	15.7	18.3	15.0	8.7
2	33°17.8'N	133°40.4'E	NNW	3.0	2	b	1	1020.9	8	2	1	15.0	19.0	14.7	8.0
3	33°17.6'N	133°40.5'E	NW	3.0	2	b	1	1020.9	8	2	1	15.7	18.7	15.4	8.0
4	33°17.6'N	133°40.5'E	WNW	1.0	1	bc	3	1021.0	8	1	1	15.6	19.3	15.3	7.0
5	33°15.5'N	133°40.8'E	N	3.0	2	bc	2	1021.2	8	1	1	14.7	18.8	14.0	8.6
6	33°17.8'N	133°39.7'E	N	4.0	3	b	1	1021.7	8	1	1	14.6	19.5	14.2	7.6
7	33°24.9'N	133°36.5'E	N	2.5	2	b	1	1022.5	8	1	1	15.0	19.0	14.6	7.1
8			N	3.0	2	b	2	1022.9	8	1	1	14.2	17.4	14.0	5.6
9				0.0	0	bc	3	1022.6	8	1	1	15.3	17.3	14.9	6.5
10															
11															
12															
13															
14															
15															
16															
17															
18															
19															
20															
21															
22															
23															
24															

(4/30) KH-88-02 Meteorological data Sunrize 05:19 Sunset 18:46

J	Latitude	Longitude	W.D.	W.F.	F	We	N	Bar.	V	Se	Sw	A.T.	S.T.	T	Td
1															
2															
3															
4															
5															
6															
7															
8															
9															
10															
11															
12															
13															
14															
15	33°28.2'N	133°36.1'E	SE	3.5	3	bc	5	1006.7	8	1	1	20.6	19.0	20.6	14.3
16	33°16.8'N	133°40.1'E	SE	5.5	4	bc	7	1006.3	8	2	1	21.2	19.7	21.2	15.8
17	33°05.0'N	133°44.0'E	SW	7.5	4	o	10	1006.8	7	2	1	20.6	20.5	20.1	17.0
18	33°00.4'N	133°45.7'E	SW	7.5	4	o	10	1007.5	7	2	1	20.6	20.3	20.1	16.9
19	33°55.6'N	133°47.6'E	SW	7.0	4	o	10	1008.2	7	2	1	20.9	19.0	20.5	16.3
20	32°43.9'N	133°51.8'E	SW	9.0	5	c	9	1008.9	7	3	1	22.2	21.1	21.9	16.4
21	32°32.8'N	133°54.7'E	SSW	9.2	5	o	10	1010.0	7	3	3	22.5	23.2	22.1	16.4
22	32°30.4'N	133°58.0'E	WSW	10.0	5	o	10	1010.6	7	4	3	22.6	23.5	22.2	17.9
23	32°28.6'N	134°02.1'E	SW	8.5	5	c	9	1010.4	7	4	3	22.8	23.2	22.2	18.0
24	32°16.4'N	134°04.4'E	SW	9.8	5	c	9	1010.5	7	4	3	22.4	23.2	21.8	19.2

(5/01) KH-88-02 Meteorological data Sunrize 05:18 Sunset 18:36

J	Latitude	Longitude	W.D.	W.F.	F	We	N	Bar.	V	Se	Sw	A.T.	S.T.	T	Td
1	32°04.4'N	134°07.5'E	SSW	7.0	4	o	10	1010.4	6	3	1	22.0	22.0	21.3	19.9
2	31°52.7'N	134°11.6'E	SSW	8.4	5	o	10	1010.3	6	3	1	21.2	21.8	20.8	18.9
3	31°41.0'N	134°15.2'E	SSW	7.0	4	o	10	1010.3	6	3	1	20.5	20.8	19.7	18.2
4	31°29.6'N	134°19.1'E	S	8.0	5	o	10	1010.3	6	3	1	20.0	20.0	19.6	17.5
5	31°18.0'N	134°22.0'E	SW	5.5	4	o	10	1011.2	6	3	1	19.9	19.8	19.2	17.7
6	31°06.5'N	134°25.0'E	SSW	3.0	2	o	10	1011.7	6	2	1	19.6	19.6	19.1	18.0
7	30°55.1'N	134°28.2'E	SSE	3.5	3	o	10	1011.9	6	2	1	19.6	19.0	19.1	18.2
8	30°43.5'N	134°30.9'E	SSE	3.5	3	o	10	1012.4	7	2	1	19.9	19.0	19.6	18.5
9	30°32.3'N	134°34.3'E	SSE	4.5	3	o	10	1012.6	7	2	1	21.0	19.8	20.9	19.9
10	30°21.4'N	134°38.0'E	S	5.0	3	o	10	1013.0	7	2	1	21.4	21.1	21.0	20.0
11	30°10.4'N	134°40.3'E	S	6.0	4	o	10	1012.5	7	3	1	21.2	21.6	20.7	19.4
12	29°59.2'N	134°43.8'E	S	8.0	5	r	10	1012.6	7	3	1	20.4	21.6	20.1	19.2
13	29°48.0'N	134°47.2'E	S	10.0	5	r	10	1012.0	7	3	1	20.6	20.0	20.1	19.0
14	29°36.8'N	134°49.2'E	SSE	10.5	5	r	10	1012.0	6	3	1	20.5	20.2	20.0	19.1
15	29°28.0'N	134°55.9'E	SSE	9.0	5	r	10	1012.0	6	3	1	20.6	19.7	20.0	19.2
16	29°23.6'N	135°09.2'E	SSW	8.5	5	r	10	1012.3	6	3	1	20.4	19.9	19.9	19.2
17	29°20.0'N	135°20.1'E	SSW	7.0	4	o	10	1013.2	6	3	1	20.4	20.0	20.1	19.4
18	29°20.4'N	135°20.3'E	SW	4.0	3	r	10	1013.2	7	2	1	20.2	20.3	19.8	19.1
19	29°20.8'N	135°20.4'E	SSW	4.0	3	r	10	1013.1	7	2	1	20.3	20.3	19.8	19.1
20	29°21.8'N	135°21.6'E	SSW	8.0	5	r	10	1012.8	7	3	1	20.2	20.8	19.9	19.2
21	29°25.8'N	135°32.0'E	S	12.0	6	r	10	1011.7	7	3	1	20.8	22.0	20.2	19.6
22	29°29.6'N	135°42.1'E	W	7.4	4	o	10	1014.9	7	3	1	20.9	20.4	20.7	19.3
23	29°33.8'N	135°52.4'E	NE	2.1	2	o	10	1013.8	7	2	1	21.0	21.9	20.9	19.2
24	29°38.0'N	136°03.0'E	SSW	5.0	3	o	10	1013.6	7	2	1	21.2	20.8	20.5	19.5

(5/02) KH-88-02 Meteorological data Sunrize 05:08 Sunset 18:29

J	Latitude	Longitude	W.D.	W.F.	F	We	N	Bar.	V	Se	Sw	A.T.	S.T.	T	Td
1	29°42.7'N	136°13.6'E	SW	5.5	4	o	10	1013.6	7	2	1	21.0	22.1	20.9	19.4
2	29°46.2'N	136°24.2'E	WSW	6.0	4	o	10	1012.8	7	2	1	21.2	22.2	21.1	19.7
3	29°49.6'N	136°34.6'E	W	7.0	4	o	10	1013.1	7	2	1	21.4	22.3	21.2	19.5
4	29°53.4'N	136°44.6'E	W	6.0	4	o	10	1012.8	7	2	1	21.4	22.3	21.3	19.3
5	29°57.5'N	136°54.4'E	W	6.5	4	o	10	1013.8	7	2	1	21.5	22.2	21.2	19.1
6	30°00.1'N	137°00.3'E	WSW	4.0	3	o	10	1013.7	7	2	1	21.7	22.2	21.2	19.2
7	29°59.8'N	136°59.7'E	WSW	7.0	4	o	10	1014.9	7	2	1	21.7	22.3	21.5	18.9
8	29°59.7'N	136°59.5'E	SW	7.0	4	o	10	1015.0	7	3	1	21.7	22.2	21.5	19.0
9	29°58.3'N	136°57.0'E	WSW	6.5	4	o	10	1014.7	8	3	1	22.0	22.2	21.9	18.7
10	29°47.7'N	136°57.7'E	WSW	8.5	5	o	10	1015.5	8	3	1	21.9	22.2	21.7	18.9
11	29°36.9'N	136°59.0'E	WSW	7.7	4	o	10	1015.8	8	3	1	21.7	21.6	21.7	19.6
12	29°25.1'N	136°59.8'E	WSW	5.5	4	o	10	1015.8	8	3	1	21.4	20.8	21.0	19.6
13	29°12.9'N	136°59.9'E	WSW	5.5	4	o	10	1015.2	8	3	1	21.1	20.6	21.0	19.4
14	29°01.4'N	137°00.0'E	W	6.5	4	o	10	1015.2	8	3	1	21.5	21.5	21.9	19.6
15	29°01.6'N	136°58.0'E	W	6.5	4	o	10	1015.0	8	3	1	22.2	21.5	22.0	19.6
16	28°59.9'N	136°59.9'E	W	7.0	4	o	10	1015.0	8	3	1	21.7	21.0	21.5	19.7
17	28°51.3'N	137°00.5'E	WSW	5.5	4	o	10	1015.0	8	3	1	21.2	20.8	20.8	19.8
18	28°38.1'N	136°59.5'E	WSW	5.5	4	o	10	1015.1	8	3	1	21.1	20.9	20.3	19.5
19	28°25.2'N	137°00.2'E	WSW	5.0	4	o	10	1015.5	7	2	1	20.8	20.2	20.2	19.6
20	28°13.6'N	137°00.3'E	SW	3.0	2	o	10	1016.2	7	2	1	20.7	20.3	20.2	19.7
21	28°12.2'N	136°57.4'E	SW	4.0	3	o	10	1017.3	7	2	1	20.6	20,4	20.2	19.6
22	28°00.6'N	137°00.0'E	SW	4.0	3	o	10	1017.3	7	2	1	20.6	20.4	20.1	19.8
23	27°59.4'N	137°00.4'E	WSW	3.5	3	o	10	1017.1	7	2	1	20.8	20.7	20.3	19.8
24	27°46.4'N	137°00.0'E	WSW	4.0	3	o	10	1016.9	7	2	1	20.8	20.6	20.2	19.7

(5/03) KH-88-02 Meteorological data Sunrize 05:12 Sunset 18:25

J	Latitude	Longitude	W.D.	W.F.	F	We	N	Bar.	V	Se	Sw	A.T.	S.T.	T	Td
1	27°33.4'N	137°00.2'E	W	3.0	2	o	10	1016.3	7	2	1	20.6	20.5	20.3	19.7
2	27°20.5'N	136°59.9'E	W	3.0	2	o	10	1015.8	7	2	1	20.6	20.6	20.1	19.7
3	27°07.3'N	136°59.9'E	NW	2.5	2	o	10	1015.7	7	2	1	20.6	20.6	20.0	19.7
4	26°59.6'N	136°59.8'E	NW	3.5	3	bc	4	1015.3	7	2	1	20.8	21.2	20.3	19.6
5	26°58.1'N	137°00.0'E	N	5.0	3	b	2	1016.2	7	2	1	20.7	21.6	20.2	19.3
6	26°44.9'N	137°00.0'E	NNE	7.0	4	c	9	1016.7	7	2	1	20.9	21.2	20.5	19.6
7	26°32.0'N	137°00.4'E	NE	5.5	4	bc	7	1017.2	8	2	1	21.1	21.0	21.0	19.5
8	26°20.2'N	137°00.6'E	ENE	5.5	4	bc	7	1017.2	8	2	1	21.5	22.5	22.0	19.1
9	26°21.8'N	137°03.2'E	NE	6.5	4	bc	7	1017.5	8	3	1	22.2	22.5	22.0	18.8
10	26°17.0'N	137°03.7'E	NE	7.5	4	bc	6	1017.6	8	3	1	22.3	22.3	22.4	19.0
11	26°04.9'N	137°01.1'E	ENE	6.7	4	c	9	1017.0	8	3	1	22.5	22.6	22.3	19.1
12	25°59.9'N	137°00.0'E	ENE	3.5	3	bc	7	1016.5	8	2	1	22.2	22.6	22.2	19.0
13	25°52.0'N	136°59.5'E	E	5.5	4	c	8	1016.2	8	2	1	22.4	22.4	22.6	19.0
14	25°40.5'N	137°00.0'E	E	5.5	4	bc	7	1015.1	8	2	1	22.8	23.7	23.3	19.6
15	25°40.9'N	137°01.3'E	E	5.5	4	b	2	1014.3	8	2	1	23.2	24.1	23.5	19.6
16	25°41.7'N	137°01.8'E	E	5.0	3	b	2	1014.0	9	2	1	22.6	23.7	22.7	18.6
17	25°34.3'N	137°01.4'E	E	5.0	3	bc	3	1013.8	8	2	1	23.2	24.5	22.9	19.8
18	25°25.8'N	137°00.8'E	E	5.0	3	bc	6	1013.8	8	2	1	23.2	24.0	23.0	20.0
19	25°16.6'N	137°00.2'E	ESE	5.0	3	bc	7	1014.0	8	2	1	23.2	24.6	23.0	20.3
20	25°07.3'N	137°00.4'E	E	6.0	4	c	8	1014.5	8	2	1	23.4	24.7	23.5	21.3
21	25°05.8'N	137°01.5'E	SE	6.0	4	bc	7	1015.0	6	3	1	23.8	25.2	23.6	22.0
22	24°59.8'N	137°00.2'E	ESE	4.5	3	o	10	1015.0	7	3	1	24.0	24.2	23.7	22.2
23	25°02.9'N	136°59.1'E	ESE	3.0	2	c	9	1014.3	7	2	1	24.0	24.4	23.6	22.3
24	25°14.8'N	136°53.5'E	SE	3.0	2	c	9	1014.1	7	2	1	24.3	24.8	23.6	22.6

(5/04) KH-88-02 Meteorological data Sunrize 05:14 Sunset 18:32

J	Latitude	Longitude	W.D.	W.F.	F	We	N	Bar.	V	Se	Sw	A.T.	S.T.	T	Td
1	25°27.4'N	136°47.5'E	S	5.5	4	c	9	1013.3	7	2	1	24.2	24.6	23.6	22.7
2	25°39.5'N	136°42.4'E	S	5.5	4	c	9	1012.5	7	2	1	24.2	24.8	23.7	22.9
3	25°37.6'N	136°43.3'E	S	5.0	3	bc	7	1012.3	7	2	1	24.2	24.8	23.6	22.9
4	25°47.6'N	136°38.4'E	SW	4.5	3	o	10	1012.3	8	2	1	24.3	24.4	23.5	23.3
5	26°00.0'N	136°33.0'E	SW	1.5	1	o	10	1012.8	7	2	1	23.6	23.9	23.1	22.3
6	26°12.0'N	136°28.0'E	SSW	2.5	2	o	10	1013.0	8	2	1	23.8	24.2	23.2	22.2
7	26°23.1'N	136°22.7'E		0.0	0	o	10	1013.1	7	1	1	22.9	22.0	22.3	21.4
8	26°33.3'N	136°18.2'E	SSW	4.0	3	o	10	1013.0	7	2	1	22.8	22.9	22.5	21.4
9	26°31.1'N	136°19.1'E	S	3.0	2	m	2	1012.9	6	2	1	23.2	22.9	23.7	21.8
10	26°34.2'N	136°17.9'E	S	4.8	3	m	1	1012.3	5	2	1	24.4	22.3	23.5	21.9
11	26°41.9'N	136°14.2'E	S	6.0	4	c	9	1011.5	6	2	1	24.3	22.5	23.1	21.8
12	26°49.7'N	136°10.6'E	SW	7.0	4	c	9	1011.6	8	3	2	23.9	22.2	22.9	21.5
13	26°53.7'N	136°08.6'E	SW	5.0	3	o	10	1012.0	7	2	2	23.2	22.2	22.5	21.0
14	26°53.4'N	136°08.9'E	SW	5.5	4	f	10	1010.9	3	2	1	22.0	22.5	22.8	21.5
15	26°51.3'N	136°08.3'E	SSW	5.5	4	f	10	1010.2	2	2	1	22.9	22.2	22.8	21.7
16	27°01.6'N	136°03.1'E	S	4.5	3	b	1	1009.5	7	2	1	22.9	22.2	22.5	21.4
17	27°10.3'N	136°00.1'E	SSW	5.0	3	bc	7	1009.9	7	2	1	22.9	21.9	22.6	21.4
18	27°17.8'N	135°57.0'E	S	6.0	4	b	1	1009.7	7	2	1	22.6	21.7	21.9	21.6
19	27°25.2'N	135°54.0'E	SSW	8.0	5	bc	3	1009.7	7	3	1	22.4	21.6	21.8	21.4
20	27°31.6'N	135°51.1'E	SSW	8.0	5	bc	7	1010.0	7	3	1	22.4	21.4	21.7	21.7
21	27°29.6'N	135°50.6'E	S	9.5	5	bc	3	1010.1	7	3	1	22.6	21.3	22.0	19.8
22	27°39.4'N	135°46.6'E	SSW	11.3	6	c	8	1009.5	6	3	1	22.4	21.5	21.7	21.6
23	27°51.3'N	135°41.4'E	SSW	11.0	6	o	10	1009.4	6	3	1	22.5	21.6	21.8	21.8
24	28°03.2'N	135°36.4'E	SSW	13.0	6	m	9	1008.8	4	4	1	22.4	21.6	21.7	21.7

(5/05) KH-88-02 Meteorological data Sunrize 05:15 Sunset 18:38

J	Latitude	Longitude	W.D.	W.F.	F	We	N	Bar.	V	Se	Sw	A.T.	S.T.	T	Td
1	28°15.0'N	135°31.3'E	SSW	9.0	5	o	10	1008.1	7	3	1	22.2	21.2	21.6	21.4
2	28°25.8'N	135°26.7'E	SSW	9.0	5	f	10	1007.1	3	3	1	22.2	21.0	21.6	21.4
3	28°23.2'N	135°25.4'E	SSW	10.0	5	f	10	1007.1	3	3	1	22.2	21.0	21.6	21.6
4	28°33.7'N	135°22.9'E	SW	11.0	6	o	10	1006.8	6	3	3	22.2	21.3	21.6	21.5
5	28°40.0'N	135°19.6'E	SW	12.0	6	o	10	1006.6	6	4	3	22.2	21.2	21.5	21.4
6	28°38.8'N	135°18.4'E	SW	11.0	6	o	10	1006.3	7	4	3	22.2	20.9	21.6	20.6
7	28°39.3'N	135°19.6'E	SW	10.0	5	o	10	1006.8	7	4	3	22.2	20.9	21.7	21.4
8	28°39.7'N	135°21.0'E	SSW	10.0	5	o	10	1007.2	6	4	3	22.0	21.0	21.6	21.0
9	28°37.7'N	135°20.4'E	SSW	10.0	5	o	10	1007.5	6	4	3	22.8	21.0	22.5	21.3
10	28°37.5'N	135°21.5'E	SSW	8.5	5	o	10	1007.4	6	4	3	22.4	21.0	22.5	21.5
11	28°39.4'N	135°20.5'E	SW	10.0	5	o	10	1007.8	6	4	3	22.3	21.0	21.8	21.3
12	28°37.6'N	135°19.2'E	SSW	8.5	5	o	10	1007.8	6	4	3	22.6	21.0	22.3	21.3
13	28°37.6'N	135°20.1'E	SW	9.0	5	r	10	1007.6	6	4	3	22.2	21.0	21.8	21.4
14	28°40.0'N	135°19.9'E	SW	10.0	5	r	10	1007.1	6	4	3	22.1	21.0	21.7	21.3
15	28°38.5'N	135°17.6'E	SW	9.5	5	r	10	1007.1	6	4	3	22.2	21.0	21.4	21.1
16	28°39.4'N	135°19.9'E	WSW	8.0	5	r	10	1007.0	5	4	3	21.9	21.1	21.3	20.8
17	28°38.9'N	135°20.3'E	WSW	8.0	5	r	10	1007.0	5	4	3	21.2	21.1	20.7	20.3
18	28°38.4'N	135°17.3'E	W	5.5	4	r	10	1007.3	6	3	3	21.1	21.0	20.6	19.9
19	28°40.2'N	135°20.1'E	SW	6.0	4	r	10	1008.2	6	3	3	21.0	21.0	20.7	19.9
20	28°39.8'N	135°20.3'E	SW	5.0	3	o	10	1008.4	6	3	3	21.0	21.0	20.8	20.2
21	28°38.5'N	135°17.6'E	WSW	4.0	3	bc	17	1009.4	6	3	3	21.2	21.0	20.7	20.2
22	28°38.3'N	135°17.8'E	WSW	6.0	4	c	19	1010.1	6	3	3	21.2	21.0	20.8	20.6
23	28°40.5'N	135°21.1'E	NW	9.5	5	m	10	1010.8	5	3	3	21.2	21.0	20.7	20.1
24	28°42.3'N	135°19.4'E	NW	3.5	3	bc	17	1011.0	6	3	3	21.0	21.0	20.6	20.1

(5/06) KH-88-02 Meteorological data Sunrize 05:14 Sunset 18:39

J	Latitude	Longitude	W.D.	W.F.	F	We	N	Bar.	V	Se	Sw	A.T.	S.T.	T	Td
1	28°39.8'N	135°20.0'E	NNW	2.5	2	c	9	1011.2	6	2	3	21.0	21.0	20.6	20.0
2	28°39.5'N	135°19.5'E	NNW	4.0	3	bc	6	1010.8	7	2	3	21.0	21.1	20.7	19.9
3	28°41.5'N	135°17.8'E	NNW	4.5	3	c	9	1011.2	7	2	3	20.8	21.0	20.4	19.6
4	28°41.7'N	135°17.1'E	N	6.0	4	c	8	1011.3	7	2	3	20.7	21.0	20.2	19.6
5	28°41.5'N	135°16.7'E	N	7.0	4	bc	7	1011.8	7	3	3	20.6	20.9	20.1	19.3
6	28°41.2'N	135°16.7'E	N	6.5	4	c	8	1012.3	7	3	3	20.6	20.9	20.3	19.1
7	28°40.0'N	135°20.0'E	N	6.0	4	bc	4	1013.4	7	3	3	20.6	21.3	20.4	18.1
8	28°40.2'N	135°19.5'E	N	7.0	4	bc	4	1014.3	8	3	3	20.6	21.0	21.7	16.3
9	28°42.5'N	135°20.8'E	NE	5.0	3	bc	5	1014.4	8	3	3	22.0	21.0	21.9	16.5
10	28°39.9'N	135°19.6'E	NE	4.0	3	b	2	1014.8	9	2	3	21.4	21.3	22.0	17.0
11	28°39.8'N	135°19.7'E	NE	3.5	3	bc	4	1014.8	9	2	3	21.7	21.4	22.0	16.7
12	28°39.8'N	135°19.8'E	NE	5.0	3	bc	3	1014.7	9	2	3	21.7	21.6	21.9	17.5
13	28°39.7'N	135°18.9'E	ENE	4.5	3	bc	5	1014.3	9	2	3	21.6	21.7	22.3	17.4
14	28°44.0'N	135°08.7'E	ENE	4.5	3	bc	5	1014.2	9	2	3	21.7	21.6	22.8	17.2
15	28°44.2'N	135°11.2'E	E	6.0	4	b	1	1013.7	9	3	3	23.1	21.6	22.8	17.1
16	28°47.4'N	135°01.4'E	ESE	4.5	3	b	2	1013.3	9	3	3	23.1	21.5	22.9	17.4
17	28°47.2'N	135°59.4'E	ESE	5.0	3	b	2	1013.8	9	3	3	22.7	21.8	21.8	17.6
18	28°57.7'N	134°58.6'E	ESE	5.5	4	bc	3	1013.8	8	2	1	21.6	21.3	21.2	17.7
19	28°59.9'N	134°53.7'E	ESE	5.5	4	bc	7	1014.2	8	2	1	21.3	21.3	20.9	18.0
20	28°59.4'N	134°48.7'E	SE	5.0	3	bc	7	1014.5	8	2	1	21.1	21.1	20.6	17.7
21	28°58.6'N	134°51.3'E	ESE	6.0	4	b	2	1014.7	8	3	1	21.2	21.1	20.5	17.7
22	29°03.3'N	134°49.9'E	SSE	7.0	4	b	2	1015.2	8	3	1	20.9	21.0	20.5	17.9
23	29°11.1'N	134°50.0'E	SSE	5.9	4	b	2	1015.5	8	3	1	20.9	21.3	20.3	17.9
24	29°18.7'N	134°50.1'E	SSE	6.0	4	bc	5	1015.1	8	3	1	20.9	22.0	20.3	17.7

(5/07) KH-88-02 Meteorological data Sunrize 05:13 Sunset 18:40

J	Latitude	Longitude	W.D.	W.F.	F	We	N	Bar.	V	Se	Sw	A.T.	S.T.	T	Td
1	29°20.1'N	134°57.7'E	SSE	8.0	5	bc	4	1014.2	8	3	1	20.8	22.0	20.3	17.8
2	29°20.1'N	135°06.8'E	SE	7.5	4	bc	5	1013.8	8	3	1	20.7	21.7	20.1	17.8
3	29°15.5'N	135°09.9'E	SSE	7.5	4	bc	5	1013.7	8	3	1	20.6	21.4	20.2	18.0
4	29°07.6'N	135°09.7'E	SE	7.5	4	bc	5	1012.5	8	3	1	20.6	21.1	20.2	18.7
5	28°59.9'N	135°09.9'E	SE	6.5	4	bc	6	1012.5	7	3	1	20.8	21.0	20.4	19.4
6	29°00.0'N	135°01.2'E	SSE	7.0	4	o	10	1012.7	7	3	1	21.0	21.0	20.4	19.7
7	29°00.0'N	134°52.5'E	S	7.0	4	o	10	1012.3	7	3	1	21.2	21.0	20.4	19.7
8	29°04.8'N	134°54.7'E	S	6.0	4	o	10	1012.1	7	3	1	21.2	21.0	20.7	19.8
9	29°08.2'N	134°57.2'E	SSE	7.0	4	o	10	1011.7	7	3	1	21.2	20.9	20.8	19.9
10	29°08.3'N	134°57.3'E	SSE	8.0	5	o	10	1010.9	7	3	1	21.4	21.0	20.8	20.1
11	29°08.9'N	134°57.1'E	SSE	9.0	5	r	10	1010.0	6	3	1	21.5	21.1	20.8	20.6
12	29°09.7'N	134°57.0'E	S	9.0	5	o	10	1009.2	6	3	1	21.6	21.1	21.4	20.9
13	29°10.2'N	134°57.4'E	S	10.5	5	o	10	1008.1	6	3	1	21.8	21.2	21.5	21.0
14	29°10.6'N	134°57.6'E	S	10.5	5	o	10	1007.7	6	3	1	22.0	21.2	22.4	21.2
15	29°08.8'N	134°55.4'E	SSW	11.0	6	o	10	1006.3	6	4	1	22.8	21.2	21.8	21.5
16	29°09.5'N	134°55.0'E	SW	12.0	6	o	10	1006.3	6	4	1	22.2	21.2	21.8	21.6
17	29°10.5'N	134°54.8'E	SW	13.0	6	o	10	1005.2	6	4	1	22.4	21.2	22.0	21.5
18	29°09.0'N	134°54.0'E	SSW	13.0	6	o	10	1005.0	6	4	1	22.2	21.1	21.8	21.6
19	29°06.6'N	134°52.5'E	SSW	14.0	7	o	10	1005.3	6	4	3	22.6	21.0	22.0	21.4
20	29°04.3'N	134°51.0'E	SW	14.0	7	o	10	1005.7	6	4	3	22.6	21.0	22.4	21.3
21	29°05.8'N	134°53.0'E	SW	14.0	7	o	10	1005.4	6	4	3	23.0	21.0	22.5	21.7
22	29°02.7'N	134°49.2'E	SW	12.0	6	o	10	1005.4	6	4	3	23.0	21.0	22.8	21.7
23	29°09.5'N	134°56.9'E	SW	13.0	6	r	10	1005.3	6	4	3	23.1	21.0	22.2	21.6
24	29°11.9'N	134°59.2'E	SW	13.0	6	r	10	1003.8	6	4	3	23.2	21.0	22.3	21.6

(5/08) KH-88-02 Meteorological data Sunrize 05:12 Sunset 18:38

J	Latitude	Longitude	W.D.	W.F.	F	We	N	Bar.	V	Se	Sw	A.T.	S.T.	T	Td
1	29°09.5'N	134°58.1'E	SW	13.5	6	r	10	1003.7	6	4	3	22.7	20.9		
2	29°07.0'N	134°56.4'E	SW	14.0	7	r	10	1002.8	6	4	3	22.5	20.7		
3	29°04.5'N	134°54.2'E	SW	15.0	7	r	10	1003.1	6	5	3	22.4	20.9		
4	29°02.4'N	134°51.7'E	SW	14.5	7	r	10	1003.9	6	5	3	22.2	20.9	21.5	21.1
5	29°02.8'N	134°52.5'E	NW	9.0	5	r	10	1003.3	5	5	3	21.0	20.8	20.6	20.1
6	29°07.7'N	134°59.2'E	N	9.5	5	r	10	1004.7	6	4	3	20.3	20.8	19.6	19.1
7	29°08.7'N	135°02.9'E	NNE	8.0	5	o	10	1005.7	6	4	3	20.2	20.9	19.8	18.9
8	29°07.5'N	135°03.0'E	NNE	11.0	6	o	10	1006.3	7	4	3	20.4	20.9	20.1	17.5
9	29°07.5'N	135°02.3'E	NNE	13.0	6	o	10	1007.2	7	4	3	20.4	20.9	20.0	16.4
10	29°16.6'N	135°09.4'E	NNE	13.2	6	o	10	1007.5	7	4	3	20.2	22.2	20.1	14.0
11	29°24.4'N	135°17.4'E	N	15.0	7	o	10	1007.8	7	5	3	20.0	22.5	19.7	14.2
12	29°31.3'N	135°24.9'E	N	13.0	6	o	10	1007.9	7	5	3	20.4	22.5	19.9	13.9
13	29°37.6'N	135°32.9'E	N	15.0	7	o	10	1008.2	7	5	3	20.3	22.5	19.6	13.0
14	29°45.0'N	135°40.3'E	N	14.0	7	o	10	1008.8	7	5	3	19.6	21.6	19.4	12.7
15	29°53.0'N	135°46.8'E	N	13.5	6	bc	3	1008.5	8	5	3	19.8	21.9	19.9	13.9
16	30°00.3'N	135°55.5'E	NNE	13.0	6	bc	7	1008.5	8	5	3	20.0	22.3	19.7	12.0
17	30°08.5'N	136°04.5'E	NE	12.0	6	c	9	1009.4	8	5	3	19.5	21.9	19.0	11.5
18	30°16.6'N	136°12.1'E	NNE	10.0	5	bc	6	1010.0	8	5	3	19.3	22.3	19.1	8.0
19	30°22.6'N	136°17.2'E	NNE	12.0	6	bc	6	1010.7	8	5	3	19.2	22.3	18.9	8.0
20	30°29.9'N	136°20.4'E	NNE	13.0	6	bc	6	1012.2	8	5	3	18.7	22.1	18.2	8.8
21	30°44.7'N	136°26.7'E	NNE	11.0	6	b	2	1012.5	8	4	3	18.6	22.2	18.1	9.0
22	30°44.7'N	136°26.7'E	NNE	11.0	6	bc	3	1013.0	8	4	3	18.5	22.4	18.2	11.2
23	30°52.1'N	136°29.0'E	ENE	12.2	6	bc	4	1013.4	8	4	3	18.7	22.7	18.1	12.9
24	30°59.4'N	136°31.3'E	NE	13.5	6	c	9	1013.4	8	4	3	19.2	23.4	18.7	11.6

(5/09) KH-88-02 Meteorological data Sunrize 05:01 Sunset 18:36

J	Latitude	Longitude	W.D.	W.F.	F	We	N	Bar.	V	Se	Sw	A.T.	S.T.	T	Td
1	31°06.9'N	136°34.7'E	ENE	11.0	6	c	8	1013.8	8	4	3	18.9	23.3	18.5	10.9
2	31°14.7'N	136°37.7'E	ENE	12.0	6	c	8	1013.8	8	4	3	18.8	21.9	18.1	10.2
3	31°21.5'N	136°40.2'E	ENE	11.0	6	c	8	1014.2	8	4	3	18.4	21.9	17.9	9.8
4	31°27.7'N	136°42.6'E	ENE	12.0	6	bc	3	1014.2	8	4	3	18.2	22.2	17.9	8.5
5	31°33.9'N	136°45.1'E	E	11.5	6	bc	4	1015.1	8	4	3	18.1	22.1	17.7	7.8
6	31°39.9'N	136°47.3'E	E	10.5	5	bc	5	1015.6	8	3	3	18.3	21.9	17.8	8.0
7	31°45.5'N	136°49.7'E	ESE	10.0	5	bc	6	1016.0	8	4	3	18.4	23.6	18.1	8.8
8	31°51.3'N	136°52.1'E	ESE	11.0	6	bc	7	1016.6	8	4	3	18.5	23.6	18.2	8.8
9	31°57.4'N	136°54.2'E	E	8.5	5	bc	6	1017.7	8	4	3	18.7	23.6	19.0	8.7
10	32°03.8'N	136°57.0'E	E	9.5	5	bc	3	1017.6	8	4	3	18.8	23.0	19.4	8.8
11	32°10.7'N	136°59.9'E	E	9.6	5	bc	4	1018.2	8	4	3	18.8	22.6	19.3	8.3
12	32°18.1'N	137°02.4'E	ENE	8.0	5	bc	3	1018.0	8	4	3	18.5	22.3	18.6	7.7
13	32°26.0'N	137°05.4'E	E	8.0	5	bc	3	1018.0	8	4	3	18.3	21.5	17.6	10.8
14	32°34.1'N	137°08.2'E	ENE	7.5	4	bc	4	1018.1	8	3	3	17.4	21.0	17.3	10.7
15	32°41.4'N	137°17.6'E	NE	9.0	5	c	8	1017.7	8	4	3	17.8	21.7	17.8	9.8
16	32°49.3'N	137°29.6'E	E	6.5	4	o	10	1017.6	8	3	3	17.3	17.8	16.7	9.7
17	32°58.0'N	137°40.8'E	E	7.0	4	o	10	1019.0	8	3	3	17.2	18.2	16.8	9.0
18	33°06.2'N	137°52.4'E	E	7.0	4	o	10	1019.5	8	3	3	17.2	17.7	16.8	8.8
19	33°14.5'N	138°03.7'E	E	7.0	4	c	9	1020.0	8	3	3	17.3	18.0	16.9	8.3
20	33°23.0'N	138°15.6'E	E	7.5	4	c	8	1020.2	8	3	3	17.4	19.0	17.0	9.7
21	33°24.9'N	138°16.8'E	ESE	8.0	5	bc	3	1020.6	8	3	3	17.4	19.0	16.9	10.1
22	33°25.4'N	138°16.0'E	ESE	8.0	5	b	2	1020.5	8	3	3	17.2	19.1	16.9	9.3
23	33°25.9'N	138°14.9'E	ESE	8.0	5	b	1	1020.6	8	3	3	17.2	19.2	16.7	9.0
24	33°28.7'N	138°18.8'E	ESE	7.5	4	b	2	1020.6	8	3	3	17.1	19.1	16.6	8.2

(5/10) KH-88-02 Meteorological data Sunrize 04:46

J	Latitude	Longitude	W.D.	W.F.	F	We	N	Bar.	V	Se	Sw	A.T.	S.T.	T	Td
1	33°35.9'N	138°31.2'E	E	7.0	4	b	2	1020.5	8	3	3	17.0	19.4	16.7	7.4
2	33°44.0'N	138°43.6'E	E	7.0	4	b	2	1019.5	8	3	3	17.1	21.8	16.6	7.0
3	33°51.8'N	138°56.6'E	ENE	7.0	4	bc	6	1020.1	8	3	3	17.1	22.2	16.5	6.7
4	34°02.0'N	139°07.5'E	E	8.5	5	c	9	1019.6	8	3	3	16.9	22.2	16.2	6.5
5	34°13.2'N	139°17.9'E	E	7.5	4	o	10	1019.9	8	3	3	16.6	21.2	16.1	6.0
6	34°24.7'N	139°25.4'E	E	8.0	5	c	9	1020.6	8	3	3	16.2	20.5	16.0	6.4
7	34°36.2'N	139°31.2'E	ENE	6.0	4	o	10	1021.5	8	3	1	15.7	19.3	15.3	7.1
8	34°47.7'N	139°37.0'E	E	6.0	4	c	8	1022.1	8	3	1	15.7	17.8	15.3	6.7
9														15.8	8.0
10															
11															
12															
13															
14															
15															
16															
17															
18															
19															
20															
21															
22															
23															
24															

Appendix II

Aerological data by Omega-sonde system during the period from 09 JST 21 April to 21 JST 24 April in Leg I, and from 09 JST 1 May to 15 JST 8 May in Leg II.

Note:

1) P: Pressure (hPa)
2) A: Geopotential (m)
3) T: Temperature (°C)
4) C: Potential temperature (K)
5) U: Relative humidity (%)
6) S: Specific humidity (g/kg)
7) X: Mixing ratio (g/kg)
8) CS: Saturation equivalent potential temperature (K)
9) CX: Equivalent potential temperature (K)
10) U: Eastward component of wind velocity (m/s)
11) V: Northward component of wind velocity (m/s)

09 JST APRIL 21

NO	P(MB)	A(GPM)	T(C)	C(K)	U(%)	S	X	CS(K)	CX(K)	U(M/S)	V(M/S)
1	1000	95	18.2	291.4	85	11.1	11.2	325.2	319.9	2.1	2.1
2	850	1475	13.2	300.0	22	2.4	2.4	330.2	306.3	3.7	5.0
3	700	3086	5.0	308.1	89	6.9	7.0	330.1	327.6	8.3	1.9
4	500	5760	-9.2	322.1	92	3.5	3.5	333.6	332.7	10.7	7.0
5	400	7453	-19.9	329.4	87	1.7	1.7	335.6	334.7	14.4	6.4
6	300	9522	-35.7	335.5	66	0.4	0.4	337.2	336.4	28.7	1.5
7	250	10766	-44.5	340.4	56	0.2	0.2	340.9	340.5	41.1	7.2
8	200	12218	-57.1	342.9	42	0.0	0.0	342.6	342.4	49.2	8.7
9	150	13980	-64.8	359.1	29	0.0	0.0	358.5	358.4	49.0	-9.5
10	100	16431	-70.9	391.7	23	0.0	0.0	390.8	390.7	26.1	1.4
11	70	18516	-69.0	438.0	27	0.0	0.0	436.9	436.7	20.3	-9.5
12	50	20548	/////	/////	///	////	////	/////	/////	/////	/////

15 JST APRIL 21

NO	P(MB)	A(GPM)	T(C)	C(K)	U(%)	S	X	CS(K)	CX(K)	U(M/S)	V(M/S)
1	1000	62	19.1	292.3	91	12.6	12.8	328.2	324.8	-2.6	6.4
2	850	1451	13.6	300.5	63	7.2	7.3	331.4	319.5	3.3	10.1
3	700	3066	5.7	308.9	84	6.9	6.9	332.0	328.2	9.2	4.5
4	500	5755	-7.9	323.6	19	0.8	0.8	336.5	325.8	13.3	-3.1
5	400	7450	-20.1	329.2	5	0.1	0.1	335.2	329.2	13.5	-6.9
6	300	9511	-37.1	333.5	6	0.0	0.0	334.9	333.1	21.1	-2.6
7	250	10745	-47.4	336.1	13	0.0	0.0	336.3	335.6	29.2	0.5
8	200	12190	-56.2	344.3	30	0.0	0.0	344.1	343.8	51.7	4.5
9	150	13974	-64.2	360.2	8	0.0	0.0	359.6	359.4	51.0	-1.8
10	100	16410	-70.3	392.8	3	0.0	0.0	391.9	391.8	27.8	-3.9
11	70	18498	-72.9	429.6	3	0.0	0.0	428.4	428.3	23.8	-10.6
12	50	20522	-62.6	497.5	2	0.0	0.0	496.7	495.8	0.3	-4.9

21 JST APRIL 21

NO	P(MB)	A(GPM)	T(C)	C(K)	U(%)	S	X	CS(K)	CX(K)	U(M/S)	V(M/S)
1	1000	58	19.4	292.6	98	13.8	14.0	329.2	328.4	-1.7	12.2
2	850	1450	14.0	300.9	100	11.8	11.9	332.7	332.7	14.2	8.5
3	700	3067	5.1	308.3	92	7.2	7.3	330.4	328.5	11.8	6.3
4	500	5749	-8.5	322.9	30	1.2	1.2	335.1	326.3	13.9	2.7
5	400	7448	-19.6	329.8	5	0.1	0.1	336.2	329.8	12.5	3.1
6	300	9511	-37.1	333.5	9	0.0	0.0	334.9	333.2	17.8	3.8
7	250	10742	-47.3	336.2	55	0.1	0.1	336.5	336.1	24.6	6.1
8	200	12183	-57.1	342.9	42	0.0	0.0	342.6	342.4	32.5	-0.6
9	150	13974	-62.8	362.6	10	0.0	0.0	362.0	361.8	53.7	-2.8
10	100	16413	-71.8	389.9	5	0.0	0.0	389.0	388.9	32.3	-4.0
11	70	18503	-71.3	433.0	5	0.0	0.0	431.9	431.7	17.8	-10.3
12	50	20538	-62.5	497.7	3	0.0	0.0	497.0	496.0	3.7	3.5
13	30	23775	/////	/////	///	////	////	/////	/////	/////	/////

03 JST APRIL 22

NO	P(MB)	A(GPM)	T(C)	C(K)	U(%)	S	X	CS(K)	CX(K)	U(M/S)	V(M/S)
1	1000	38	20.8	294.0	89	13.7	13.9	334.1	329.4	7.3	-0.4
2	850	1427	15.0	301.9	47	5.9	5.9	336.0	317.4	10.1	3.7
3	700	3050	8.1	311.6	33	3.2	3.2	339.0	320.2	11.7	2.1
4	500	5735	-10.6	320.3	35	1.2	1.2	330.7	323.7	14.6	5.0
5	400	7427	-18.9	330.7	2	0.0	0.0	337.5	330.5	15.6	2.2
6	300	9494	-36.8	333.9	20	0.1	0.1	335.4	333.8	18.9	1.0
7	250	10727	-47.4	336.1	37	0.1	0.1	336.3	335.8	18.9	2.0
8	200	12173	-54.7	346.7	15	0.0	0.0	346.5	346.1	28.6	-5.0
9	150	13989	-62.6	362.9	7	0.0	0.0	362.4	362.2	45.8	-4.0
10	100	16429	-69.6	394.2	5	0.0	0.0	393.3	393.1	31.0	-2.2
11	70	18524	-72.8	429.8	5	0.0	0.0	428.6	428.5	13.0	-6.9
12	50	20540	/////	/////	///	////	////	/////	/////	/////	/////

09 JST APRIL 22

NO	P(MB)	A(GPM)	T(C)	C(K)	U(%)	S	X	CS(K)	CX(K)	U(M/S)	V(M/S)
1	1000	49	19.8	293.0	95	13.7	13.9	330.6	328.6	5.8	-7.7
2	850	1438	17.5	304.5	19	2.8	2.8	344.8	311.7	5.2	-7.4
3	700	3063	6.5	309.8	14	1.2	1.2	334.3	313.0	11.8	-0.2
4	500	5752	-7.8	323.8	4	0.2	0.2	336.7	324.0	17.8	0.9
5	400	7451	-19.8	329.6	33	0.7	0.7	335.8	331.4	25.2	3.1
6	300	9516	-36.1	334.9	52	0.3	0.3	336.5	335.5	27.7	-3.4
7	250	10753	-46.8	337.0	50	0.1	0.1	337.3	336.9	34.0	-10.4
8	200	12197	-57.8	341.8	41	0.0	0.0	341.5	341.3	49.0	-13.1
9	150	13987	-64.4	359.8	22	0.0	0.0	359.2	359.1	44.9	-11.2
10	100	16426	-72.2	389.1	5	0.0	0.0	388.2	388.1	29.3	-4.1
11	70	18517	-72.2	431.1	4	0.0	0.0	429.9	429.8	20.4	0.7
12	50	20532	/////	/////	///	////	////	/////	/////	/////	/////

15 JST APRIL 22

NO	P(MB)	A(GPM)	T(C)	C(K)	U(%)	S	X	CS(K)	CX(K)	U(M/S)	V(M/S)
1	1000	45	21.4	294.6	78	12.4	12.6	336.3	326.6	3.9	-7.9
2	850	1427	14.1	301.0	40	4.7	4.7	333.0	313.3	8.2	-2.5
3	700	3047	7.4	310.8	29	2.7	2.7	336.9	318.0	11.4	2.6
4	500	5746	-7.5	324.1	61	2.6	2.6	337.4	332.0	23.2	-2.0
5	400	7448	-19.4	330.1	52	1.1	1.1	336.5	333.3	27.4	0.0
6	300	9525	-34.2	337.6	42	0.3	0.3	339.6	338.2	29.7	-6.9
7	250	10772	-44.6	340.2	42	0.1	0.1	340.8	340.2	40.5	-2.8
8	200	12224	-57.2	342.7	37	0.0	0.0	342.4	342.2	40.3	-7.8
9	150	14004	-63.4	361.6	32	0.0	0.0	361.0	360.8	45.6	-9.7
10	100	16435	-72.1	389.3	6	0.0	0.0	388.4	388.3	36.6	-5.1
11	70	18522	-71.8	431.9	6	0.0	0.0	430.8	430.6	17.7	-5.1
12	50	20531	-64.6	492.7	4	0.0	0.0	491.8	491.1	9.6	-0.8

21 JST APRIL 22

NO	P(MB)	A(GPM)	T(C)	C(K)	U(%)	S	X	CS(K)	CX(K)	U(M/S)	V(M/S)
1	1000	72	18.9	292.1	74	10.1	10.2	327.5	317.9	6.8	-8.7
2	850	1448	11.4	298.1	18	1.8	1.8	324.8	302.7	10.9	-6.8
3	700	3049	5.6	308.8	23	1.9	1.9	331.8	313.8	15.0	8.0
4	500	5741	-7.6	324.0	86	3.7	3.7	337.2	335.2	25.4	15.8
5	400	7443	-18.5	331.3	79	1.7	1.7	338.2	336.7	33.1	16.8
6	300	9530	-33.4	338.7	70	0.5	0.5	341.0	340.2	34.0	6.6
7	250	10780	-44.4	340.5	62	0.2	0.2	341.1	340.7	38.1	4.7
8	200	12232	-56.5	343.9	49	0.0	0.0	343.6	343.4	43.1	0.0
9	150	14017	-62.8	362.6	36	0.0	0.0	362.0	361.9	47.1	-7.5
10	100	16465	-73.3	387.0	10	0.0	0.0	386.1	386.0	35.4	-0.6
11	70	18528	/////	/////	///	////	////	/////	/////	/////	/////

03 JST APRIL 23

NO	P(MB)	A(GPM)	T(C)	C(K)	U(%)	S	X	CS(K)	CX(K)	U(M/S)	V(M/S)
1	1000	71	17.3	290.5	69	8.5	8.6	322.4	312.1	4.8	-3.4
2	850	1432	7.2	293.7	67	5.0	5.0	313.7	306.9	11.3	0.0
3	700	3027	5.3	308.5	96	7.6	7.7	330.9	330.0	21.2	4.1
4	500	5712	-8.5	322.9	72	2.9	2.9	335.1	331.6	34.0	6.0
5	400	7411	-19.7	329.7	81	1.6	1.6	336.0	334.7	33.0	5.2
6	300	9478	-35.9	335.2	67	0.4	0.4	336.8	336.1	38.1	2.0
7	250	10721	-45.4	339.1	63	0.2	0.2	339.5	339.1	43.1	5.3
8	200	12183	-53.3	348.9	15	0.0	0.0	348.8	348.4	53.8	4.7
9	150	14000	-61.9	364.1	15	0.0	0.0	363.6	363.4	46.7	-1.6
10	100	16439	-73.8	386.0	7	0.0	0.0	385.1	385.0	33.9	-4.2
11	70	18524	-71.3	433.0	8	0.0	0.0	431.9	431.7	22.6	-1.2
12	50	20505	/////	/////	///	////	////	/////	/////	/////	/////

09 JST APRIL 23

NO	P(MB)	A(GPM)	T(C)	C(K)	U(%)	S	X	CS(K)	CX(K)	U(M/S)	V(M/S)
1	1000	78	17.2	290.4	61	7.5	7.5	322.1	309.3	1.6	-6.7
2	850	1437	6.3	292.8	57	4.0	4.0	311.5	303.3	8.9	-3.1
3	700	3019	3.5	306.5	99	6.9	7.0	326.2	326.0	26.9	5.2
4	500	5695	-7.8	323.8	94	4.0	4.0	336.7	335.9	32.0	13.6
5	400	7393	-19.6	329.8	87	1.7	1.7	336.2	335.3	43.2	17.5
6	300	9466	-35.0	336.5	61	0.4	0.4	338.3	337.4	44.0	10.2
7	250	10712	-44.1	341.0	51	0.2	0.2	341.6	341.0	59.4	7.3
8	200	12176	-51.6	351.6	32	0.1	0.1	351.6	351.2	58.4	1.0
9	150	14001	-60.3	366.9	22	0.0	0.0	366.4	366.2	47.7	5.0
10	100	16471	-70.7	392.0	22	0.0	0.0	391.1	391.0	32.4	2.8
11	70	18548	/////	/////	///	////	////	/////	/////	/////	/////

09 JST APRIL 24

NO	P(MB)	A(GPM)	T(C)	C(K)	U(%)	S	X	CS(K)	CX(K)	U(M/S)	V(M/S)
1	1000	91	18.9	292.1	49	6.7	6.7	327.5	308.9	13.8	-4.0
2	850	1454	5.9	292.4	70	4.8	4.8	310.6	305.0	14.1	-2.2
3	700	3016	-1.8	300.6	5	0.2	0.2	313.9	301.1	17.2	-6.3
4	500	5630	-15.1	314.9	5	0.1	0.1	321.9	315.0	44.5	4.7
5	400	7302	-20.0	329.3	32	0.6	0.6	335.4	331.0	57.2	24.3
6	300	9379	-33.4	338.7	17	0.1	0.1	341.0	338.7	73.8	14.3
7	250	10633	-43.9	341.3	29	0.1	0.1	341.9	341.1	72.0	16.6
8	200	12101	-52.2	350.7	5	0.0	0.0	350.6	350.1	69.8	9.8
9	150	13925	-60.7	366.2	2	0.0	0.0	365.7	365.4	56.5	11.0
10	100	16391	-66.5	400.2	1	0.0	0.0	399.4	399.1	37.4	15.9
11	70	18511	-69.8	436.2	1	0.0	0.0	435.1	434.9	22.7	4.4
12	50	20526	/////	/////	///	////	////	/////	/////	/////	/////

15 JST APRIL 23

NO	P(MB)	A(GPM)	T(C)	C(K)	U(%)	S	X	CS(K)	CX(K)	U(M/S)	V(M/S)
1	1000	75	16.5	289.7	50	5.9	5.9	319.9	304.4	4.3	-1.6
2	850	1427	3.7	290.1	70	4.1	4.1	305.6	300.8	4.9	-7.8
3	700	3000	2.6	305.5	97	6.4	6.4	324.0	323.4	24.2	8.3
4	500	5674	-9.9	321.2	94	3.4	3.4	332.1	331.4	36.8	21.2
5	400	7357	-20.8	328.3	44	0.8	0.8	333.9	330.6	41.7	25.1
6	300	9430	-34.3	337.4	47	0.3	0.3	339.5	338.2	52.2	13.0
7	250	10681	-44.1	341.0	33	0.1	0.1	341.6	340.8	60.1	8.4
8	200	12147	-52.9	349.6	11	0.0	0.0	349.5	349.0	64.0	9.0
9	150	13958	-61.6	364.7	11	0.0	0.0	364.1	363.9	57.1	6.0
10	100	16433	-70.3	392.8	7	0.0	0.0	391.9	391.8	36.5	9.1
11	70	18517	-70.0	435.8	8	0.0	0.0	434.7	434.5	14.5	5.3

15 JST APRIL 24

NO	P(MB)	A(GPM)	T(C)	C(K)	U(%)	S	X	CS(K)	CX(K)	U(M/S)	V(M/S)
1	1000	104	18.6	291.8	57	7.6	7.7	326.5	311.0	11.1	-7.8
2	850	1459	4.8	291.2	53	3.3	3.3	308.0	300.0	12.9	-3.5
3	700	3033	0.1	302.7	10	0.5	0.5	318.1	304.1	18.2	-0.3
4	500	5648	-14.7	315.3	5	0.1	0.1	322.7	315.5	39.1	-0.7
5	400	7317	-20.9	328.1	74	1.3	1.3	333.8	332.2	57.6	23.3
6	300	9391	-34.0	337.9	64	0.5	0.5	340.0	339.0	66.5	19.1
7	250	10641	-43.7	341.6	57	0.2	0.2	342.2	341.7	70.0	22.7
8	200	12106	-53.3	348.9	23	0.0	0.0	348.8	348.4	74.4	15.8
9	150	13918	-61.1	365.5	6	0.0	0.0	365.0	364.8	58.1	21.1
10	100	16393	-67.5	398.2	3	0.0	0.0	397.4	397.2	41.5	8.8
11	70	18519	-73.5	428.3	2	0.0	0.0	427.1	427.0	20.0	11.5

21 JST APRIL 23

NO	P(MB)	A(GPM)	T(C)	C(K)	U(%)	S	X	CS(K)	CX(K)	U(M/S)	V(M/S)
1	1000	82	17.4	290.6	50	6.2	6.2	322.7	306.1	6.5	0.7
2	850	1439	6.4	292.9	24	1.7	1.7	311.7	297.3	10.3	-5.3
3	700	3007	1.6	304.4	5	0.3	0.3	321.5	305.1	23.5	-0.8
4	500	5658	-11.4	319.4	92	2.9	2.9	329.0	328.2	42.5	18.9
5	400	7334	-21.8	327.0	54	0.9	0.9	332.1	329.6	50.9	21.6
6	300	9401	-35.0	336.5	43	0.3	0.3	338.3	337.0	59.0	13.6
7	250	10652	-42.7	343.1	40	0.1	0.1	343.9	343.1	69.2	9.7
8	200	12123	-52.2	350.7	26	0.0	0.0	350.6	350.2	72.3	10.2
9	150	13940	-60.8	366.0	19	0.0	0.0	365.5	365.3	57.4	5.0
10	100	16418	-69.1	395.1	15	0.0	0.0	394.3	394.1	37.8	10.1
11	70	18511	/////	/////	///	////	////	/////	/////	/////	/////

21 JST APRIL 24

NO	P(MB)	A(GPM)	T(C)	C(K)	U(%)	S	X	CS(K)	CX(K)	U(M/S)	V(M/S)
1	1000	134	16.3	289.5	48	5.5	5.6	319.3	303.4	8.0	-2.3
2	850	1483	3.6	290.0	80	4.6	4.7	305.4	302.2	10.2	-1.8
3	700	3046	-3.0	299.3	23	1.0	1.0	311.4	301.9	17.7	-1.9
4	500	5652	-17.5	311.9	22	0.4	0.4	317.7	313.0	33.4	1.2
5	400	7301	-22.8	325.7	2	0.0	0.0	330.4	325.4	56.1	16.1
6	300	9354	-35.2	336.2	28	0.2	0.2	338.0	336.4	71.2	25.9
7	250	10603	-43.8	341.6	58	0.2	0.2	342.1	341.6	75.6	27.5
8	200	12067	-52.7	349.9	15	0.0	0.0	349.8	349.3	77.1	16.4
9	150	13902	-58.0	370.9	3	0.0	0.0	370.5	370.1	/////	/////

03 JST APRIL 24

NO	P(MB)	A(GPM)	T(C)	C(K)	U(%)	S	X	CS(K)	CX(K)	U(M/S)	V(M/S)
1	1000	76	18.4	291.6	58	7.7	7.7	325.9	310.9	7.4	0.6
2	850	1438	6.5	293.0	60	4.3	4.3	312.0	304.2	11.7	-4.3
3	700	3001	-1.0	301.5	32	1.6	1.6	315.6	305.9	21.9	-2.3
4	500	5632	-10.4	320.6	56	1.9	1.9	331.1	326.3	44.8	17.2
5	400	7314	-19.6	329.8	50	1.0	1.0	336.2	332.8	57.1	20.8
6	300	9392	-33.0	339.3	27	0.2	0.2	341.6	339.6	62.0	13.2
7	250	10652	-42.3	343.7	28	0.1	0.1	344.5	343.5	73.9	15.7
8	200	12132	-50.3	353.7	10	0.0	0.0	353.8	353.1	70.5	16.3
9	150	13951	-61.1	365.5	7	0.0	0.0	365.0	364.8	61.0	6.4
10	100	16415	-69.1	395.1	5	0.0	0.0	394.3	394.1	35.2	21.2
11	70	18532	-71.5	432.6	4	0.0	0.0	431.5	431.3	17.7	9.0

09 JST MAY 01

NO	P(MB)	A(GPM)	T(C)	C(K)	U(%)	S	X	CS(K)	CX(K)	U(M/S)	V(M/S)
1	1000	104	20.0	293.2	97	14.2	14.4	331.3	330.0	5.4	5.2
2	850	1493	13.4	300.2	84	9.5	9.6	330.8	325.7	6.4	7.1
3	700	3106	4.8	307.9	86	6.6	6.6	329.6	326.4	11.6	6.4
4	500	5770	-11.1	319.7	36	1.2	1.2	329.6	323.1	15.3	2.7
5	400	7449	-20.1	329.2	74	1.4	1.4	335.2	333.5	33.5	7.7
6	300	9525	-33.7	338.3	57	0.4	0.4	340.5	339.3	39.0	20.8
7	250	10775	-44.2	340.8	50	0.1	0.1	341.4	340.9	47.7	19.3
8	200	12229	-56.7	343.5	38	0.0	0.0	343.3	343.0	57.7	13.3
9	150	13994	-67.8	354.0	29	0.0	0.0	353.3	353.2	61.8	3.2
10	100	16451	-71.1	391.3	6	0.0	0.0	390.4	390.3	30.1	9.8
11	70	18577	-69.0	436.0	5	0.0	0.0	436.9	436.6	18.4	4.3
12	50	20607	/////	/////	///	////	////	/////	/////	/////	/////

15 JST MAY 01

NO	P(MB)	A(GPM)	T(C)	C(K)	U(%)	S	X	CS(K)	CX(K)	U(M/S)	V(M/S)
1	1000	95	20.1	293.3	92	13.6	13.7	331.6	328.3	1.8	9.1
2	850	1497	15.3	302.2	61	7.8	7.8	337.0	322.9	6.0	3.6
3	700	3114	4.2	307.3	80	5.9	5.9	328.0	323.7	14.4	-5.8
4	500	5787	-8.3	323.2	93	3.8	3.8	335.6	334.7	23.0	20.0
5	400	7490	-18.0	331.9	85	2.0	2.0	339.2	338.1	27.0	19.6
6	300	9582	-32.7	339.7	72	0.6	0.6	342.2	341.3	29.3	16.2
7	250	10838	-42.5	343.4	60	0.2	0.2	344.2	343.6	29.7	17.1
8	200	12303	-55.6	345.3	42	0.0	0.0	345.1	344.8	30.9	17.1
9	150	14073	-70.8	348.8	26	0.0	0.0	348.1	348.1	51.5	4.5
10	100	16497	-67.6	398.1	22	0.0	0.0	397.2	397.0	25.3	5.4
11	70	18615	-67.5	441.2	25	0.0	0.0	440.2	439.9	9.6	2.8
12	50	20640	/////	/////	///	////	////	/////	/////	/////	/////

15 JST MAY 02

NO	P(MB)	A(GPM)	T(C)	C(K)	U(%)	S	X	CS(K)	CX(K)	U(M/S)	V(M/S)
1	1000	129	22.1	295.3	89	14.8	15.1	338.9	333.8	6.1	-1.9
2	850	1522	14.7	301.6	68	8.4	8.4	335.0	323.8	10.9	-3.3
3	700	3138	5.0	308.1	62	4.8	4.8	330.1	321.5	14.3	0.2
4	500	5807	-10.5	320.5	14	0.5	0.5	330.9	321.7	19.7	-0.3
5	400	7489	-21.7	327.1	17	0.3	0.3	332.3	327.7	25.1	2.2
6	300	9549	-34.1	337.7	63	0.4	0.4	339.8	338.9	32.0	25.0
7	250	10800	-43.7	341.6	53	0.2	0.2	342.2	341.7	43.9	24.3
8	200	12258	-56.5	343.9	32	0.0	0.0	343.6	343.3	51.0	18.6
9	150	14032	-64.7	359.3	18	0.0	0.0	358.7	358.6	44.4	14.4
10	100	16460	-70.4	392.6	7	0.0	0.0	391.7	391.6	29.0	5.1
11	70	18576	-69.3	437.3	5	0.0	0.0	436.2	436.0	19.1	3.4
12	50	20594	/////	/////	///	////	////	/////	/////	/////	/////

21 JST MAY 01

NO	P(MB)	A(GPM)	T(C)	C(K)	U(%)	S	X	CS(K)	CX(K)	U(M/S)	V(M/S)
1	1000	100	19.7	292.9	93	13.4	13.5	330.2	327.4	2.6	13.3
2	850	1503	17.1	304.1	51	7.3	7.4	343.3	323.4	3.2	2.3
3	700	3131	6.7	310.0	71	6.2	6.2	334.8	327.4	11.4	-6.3
4	500	5816	-8.5	322.9	96	3.8	3.9	335.1	334.6	26.3	15.8
5	400	7516	-18.9	330.7	89	1.9	1.9	337.5	336.7	23.8	16.6
6	300	9598	-33.2	339.0	73	0.6	0.6	341.3	340.6	29.5	15.7
7	250	10852	-43.4	342.0	60	0.2	0.2	342.7	342.2	34.8	14.0
8	200	12310	-56.7	343.5	48	0.0	0.0	343.3	343.1	38.5	8.2
9	150	14071	-69.3	351.4	36	0.0	0.0	350.7	350.7	51.1	-1.8
10	100	16486	-70.6	392.2	30	0.0	0.0	391.3	391.2	27.6	7.9
11	70	18568	/////	/////	///	////	////	/////	/////	/////	/////

21 JST MAY 02

NO	P(MB)	A(GPM)	T(C)	C(K)	U(%)	S	X	CS(K)	CX(K)	U(M/S)	V(M/S)
1	1000	144	19.9	293.1	93	13.5	13.7	330.9	328.1	4.1	-2.2
2	850	1538	14.7	301.6	69	8.5	8.6	335.0	324.2	5.9	-3.0
3	700	3160	7.1	310.5	29	2.6	2.6	336.0	317.5	7.2	-3.8
4	500	5837	-9.6	321.6	6	0.2	0.2	332.8	322.0	17.4	-3.7
5	400	7519	-21.9	326.8	2	0.0	0.0	332.0	326.6	20.1	-8.5
6	300	9570	-36.1	334.9	63	0.4	0.4	336.5	335.8	34.0	6.6
7	250	10816	-44.8	339.9	55	0.2	0.2	340.5	340.0	40.5	16.4
8	200	12269	-57.2	342.7	43	0.0	0.0	342.4	342.3	49.9	13.4
9	150	14046	-63.3	361.7	29	0.0	0.0	361.2	361.0	43.8	10.9
10	100	16491	-71.8	389.9	8	0.0	0.0	389.0	388.9	28.8	4.0
11	70	18599	/////	/////	///	////	////	/////	/////	/////	/////

03 JST MAY 02

NO	P(MB)	A(GPM)	T(C)	C(K)	U(%)	S	X	CS(K)	CX(K)	U(M/S)	V(M/S)
1	1000	113	20.6	293.8	90	13.7	13.9	333.4	329.2	8.3	-1.5
2	850	1500	13.1	299.9	79	8.7	8.8	329.9	323.3	6.4	0.7
3	700	3110	7.5	310.9	52	4.8	4.8	337.2	324.2	10.0	9.3
4	500	5786	-9.8	321.3	92	3.3	3.3	332.3	331.4	21.4	5.7
5	400	7478	-19.3	330.2	91	1.9	1.9	336.7	336.1	26.4	17.8
6	300	9557	-33.5	338.6	72	0.5	0.5	340.8	340.0	38.4	23.1
7	250	10808	-44.3	340.7	59	0.2	0.2	341.3	340.8	43.4	20.2
8	200	12260	-57.3	342.6	47	0.0	0.0	342.3	342.1	40.9	14.1

03 JST MAY 03

NO	P(MB)	A(GPM)	T(C)	C(K)	U(%)	S	X	CS(K)	CX(K)	U(M/S)	V(M/S)
1	1000	134	19.7	292.9	92	13.2	13.4	330.2	327.0	2.8	-4.5
2	850	1529	15.5	302.4	65	8.4	8.5	337.7	324.8	3.5	-1.6
3	700	3156	7.8	311.2	27	2.5	2.5	338.1	318.1	4.1	-3.7
4	500	5841	-8.6	322.8	6	0.2	0.2	334.9	323.3	13.1	-2.5
5	400	7532	-21.2	327.7	13	0.2	0.2	333.2	328.2	12.6	-7.9
6	300	9586	-37.0	333.6	5	0.0	0.0	335.1	333.3	26.5	-3.7
7	250	10821	-46.0	338.2	8	0.0	0.0	338.5	337.7	32.5	1.7
8	200	12274	-56.0	344.7	32	0.0	0.0	344.4	344.1	41.6	11.2
9	150	14050	-63.9	360.7	28	0.0	0.0	360.1	360.0	39.5	4.1
10	100	16494	-69.0	395.3	8	0.0	0.0	394.5	394.3	23.5	-0.8
11	70	18599	/////	/////	///	////	////	/////	/////	/////	/////

09 JST MAY 02

NO	P(MB)	A(GPM)	T(C)	C(K)	U(%)	S	X	CS(K)	CX(K)	U(M/S)	V(M/S)
1	1000	126	20.6	293.8	84	12.8	12.9	333.4	326.6	8.0	0.6
2	850	1515	13.5	300.3	72	8.2	8.3	331.1	322.1	9.0	3.3
3	700	3129	5.2	308.4	57	4.5	4.5	330.7	320.8	17.3	6.6
4	500	5787	-11.5	319.3	35	1.1	1.1	328.8	322.4	17.3	2.1
5	400	7459	-21.2	327.7	76	1.3	1.3	333.2	331.8	30.1	10.9
6	300	9526	-34.5	337.2	63	0.4	0.4	339.1	338.2	36.9	26.8
7	250	10773	-44.2	340.8	58	0.2	0.2	341.4	341.0	46.3	24.6
8	200	12228	-57.0	343.1	41	0.0	0.0	342.8	342.6	49.8	19.1
9	150	13992	-62.8	362.6	28	0.0	0.0	362.0	361.9	46.0	10.6
10	100	16448	-68.9	395.5	7	0.0	0.0	394.7	394.5	27.2	13.3
11	70	18570	-69.0	438.0	4	0.0	0.0	436.9	436.6	15.7	6.3
12	50	20606	/////	/////	///	////	////	/////	/////	/////	/////

09 JST MAY 03

NO	P(MB)	A(GPM)	T(C)	C(K)	U(%)	S	X	CS(K)	CX(K)	U(M/S)	V(M/S)
1	1000	145	20.5	293.7	84	12.7	12.8	333.0	326.3	-5.4	-2.8
2	850	1540	15.8	302.8	59	7.8	7.8	338.7	323.4	2.5	-1.2
3	700	3165	7.6	311.0	20	1.9	1.9	337.5	316.0	2.3	-0.4
4	500	5855	-6.6	325.2	3	0.1	0.1	339.5	325.4	9.0	0.2
5	400	7552	-20.3	328.9	4	0.1	0.1	334.9	328.8	14.9	-3.4
6	300	9610	-36.6	334.2	7	0.0	0.0	335.7	333.9	22.8	-8.7
7	250	10845	-45.8	338.5	6	0.0	0.0	338.9	338.0	23.9	-7.3
8	200	12292	-58.1	341.3	14	0.0	0.0	341.0	340.7	28.8	-7.2
9	150	14072	-63.9	360.7	7	0.0	0.0	360.1	359.9	33.1	1.2
10	100	16507	-71.2	391.1	3	0.0	0.0	390.2	390.1	21.5	-1.9
11	70	18596	-72.6	430.2	3	0.0	0.0	429.1	428.9	9.2	-2.0
12	50	20599	/////	/////	///	////	////	/////	/////	/////	/////

15 JST MAY 03

NO	P(MB)	A(GPM)	T(C)	C(K)	U(%)	S	X	CS(K)	CX(K)	U(M/S)	V(M/S)
1	1000	125	29.1	302.3	84	21.3	21.8	370.6	358.5	-4.2	0.4
2	850	1536	16.4	303.4	55	7.5	7.6	340.8	323.3	3.8	0.5
3	700	3166	7.9	311.4	56	5.3	5.3	338.4	326.1	8.3	2.2
4	500	5864	-6.5	325.4	1	0.0	0.0	339.7	325.2	6.7	3.1
5	400	7562	-19.8	329.6	4	0.1	0.1	335.8	329.5	10.4	-1.5
6	300	9632	-34.2	337.6	3	0.0	0.0	339.6	337.2	18.9	-1.7
7	250	10878	-45.2	339.4	8	0.0	0.0	339.8	338.9	20.6	0.7
8	200	12327	-57.1	342.9	12	0.0	0.0	342.6	342.3	17.0	3.3
9	150	14099	-64.9	359.0	14	0.0	0.0	358.4	358.2	29.6	-1.0
10	100	16519	-72.8	388.0	4	0.0	0.0	387.1	387.0	17.2	-2.7
11	70	18605	-71.8	431.9	4	0.0	0.0	430.8	430.6	10.1	-3.7
12	50	20610	-64.9	492.0	2	0.0	0.0	491.1	490.4	0.6	-3.2

21 JST MAY 03

NO	P(MB)	A(GPM)	T(C)	C(K)	U(%)	S	X	CS(K)	CX(K)	U(M/S)	V(M/S)
1	1000	126	22.6	295.8	92	15.8	16.1	340.9	337.0	-3.8	4.7
2	850	1531	16.6	303.6	64	8.9	9.0	341.5	327.2	2.9	2.1
3	700	3162	7.3	310.7	65	5.9	6.0	336.6	327.2	10.9	0.4
4	500	5850	-7.8	323.8	5	0.2	0.2	336.7	324.2	12.0	0.0
5	400	7549	-19.2	330.3	4	0.1	0.1	336.9	330.3	8.7	5.7
6	300	9619	-34.6	337.0	22	0.1	0.1	339.0	337.1	17.6	2.2
7	250	10869	-43.8	341.4	54	0.2	0.2	342.1	341.5	30.3	2.6
8	200	12325	-56.4	344.0	30	0.0	0.0	343.7	343.5	28.8	-2.5
9	150	14100	-64.8	359.1	21	0.0	0.0	358.5	358.4	27.4	0.5
10	100	16525	-72.5	388.6	8	0.0	0.0	387.6	387.5	17.6	-3.7
11	70	18612	/////	/////	///	////	////	/////	/////	/////	/////

15 JST MAY 04

NO	P(MB)	A(GPM)	T(C)	C(K)	U(%)	S	X	CS(K)	CX(K)	U(M/S)	V(M/S)
1	1000	88	21.1	294.3	99	15.5	15.8	335.2	334.7	5.4	5.9
2	850	1493	16.6	303.6	76	10.6	10.7	341.5	331.9	6.0	6.6
3	700	3123	8.1	311.6	38	3.7	3.7	339.0	321.6	12.1	3.5
4	500	5810	-8.1	323.4	8	0.3	0.3	336.0	324.2	9.8	2.6
5	400	7502	-19.6	329.8	16	0.3	0.3	336.2	330.5	13.3	1.2
6	300	9578	-33.9	338.0	11	0.1	0.1	340.1	337.8	19.2	-7.4
7	250	10832	-43.6	341.7	10	0.0	0.0	342.4	341.3	3.7	-11.4
8	200	12287	-56.8	343.4	21	0.0	0.0	343.1	342.8	9.4	-23.2
9	150	14078	-66.3	356.6	12	0.0	0.0	355.9	355.8	23.2	-8.4
10	100	16505	-72.5	388.6	4	0.0	0.0	387.6	387.5	14.7	-9.5
11	70	18590	-71.1	433.4	3	0.0	0.0	432.3	432.1	4.5	-7.5
12	50	20589	-65.8	489.9	2	0.0	0.0	488.9	488.3	3.2	-3.0
13	30	23789	/////	/////	///	////	////	/////	/////	/////	/////

21 JST MAY 04

NO	P(MB)	A(GPM)	T(C)	C(K)	U(%)	S	X	CS(K)	CX(K)	U(M/S)	V(M/S)
1	1000	86	22.9	296.1	99	17.4	17.7	342.0	341.5	6.8	9.7
2	850	1496	16.6	303.6	91	12.7	12.8	341.5	337.9	12.7	9.6
3	700	3128	7.6	311.0	70	6.5	6.6	337.5	329.2	16.3	5.0
4	500	5813	-7.5	324.1	10	0.4	0.4	337.4	325.2	14.3	6.4
5	400	7509	-18.0	331.9	26	0.6	0.6	339.2	333.5	20.3	1.1
6	300	9603	-32.5	340.0	15	0.1	0.1	342.5	340.0	16.7	3.8

03 JST MAY 04

NO	P(MB)	A(GPM)	T(C)	C(K)	U(%)	S	X	CS(K)	CX(K)	U(M/S)	V(M/S)
1	1000	105	23.3	296.5	96	17.2	17.5	343.6	341.6	3.1	6.7
2	850	1513	16.8	303.8	69	9.7	9.8	342.2	329.7	6.7	0.7
3	700	3142	7.5	310.9	24	2.2	2.2	337.2	316.9	9.4	-1.3
4	500	5824	-9.0	322.3	4	0.2	0.2	334.0	322.5	6.6	-2.4
5	400	7515	-20.1	329.2	4	0.1	0.1	335.2	329.1	11.5	3.7
6	300	9584	-34.5	337.2	42	0.3	0.3	339.1	337.7	24.1	-3.4
7	250	10830	-45.0	339.6	54	0.1	0.1	340.1	339.7	28.4	-0.5
8	200	12279	-57.5	342.3	41	0.0	0.0	342.0	341.8	29.1	-2.5
9	150	14068	-62.2	363.6	18	0.0	0.0	363.1	362.9	26.3	-2.3
10	100	16506	-72.2	389.1	8	0.0	0.0	388.2	388.1	16.3	-5.3
11	70	18592	-73.4	428.5	7	0.0	0.0	427.3	427.2	10.6	-5.2

03 JST MAY 05

NO	P(MB)	A(GPM)	T(C)	C(K)	U(%)	S	X	CS(K)	CX(K)	U(M/S)	V(M/S)
1	1000	58	22.0	295.2	100	16.6	16.9	338.5	338.5	13.7	11.9
2	850	1465	15.9	302.9	100	13.3	13.5	339.0	339.0	20.2	9.9
3	700	3092	7.6	311.0	86	8.0	8.1	337.5	333.6	18.8	11.8
4	500	5778	-10.3	320.7	100	3.5	3.5	331.3	331.3	23.9	1.7
5	400	7479	-18.5	331.3	54	1.2	1.2	338.2	334.9	23.7	-3.8
6	300	9571	-32.1	340.6	78	0.7	0.7	343.2	342.5	17.2	-5.3
7	250	10831	-42.2	343.8	69	0.2	0.3	344.7	344.2	25.9	-5.0
8	200	12299	-54.9	346.4	35	0.0	0.0	346.2	345.9	24.9	-10.5
9	150	14077	-66.2	356.7	29	0.0	0.0	356.1	356.0	30.6	-3.8
10	100	16513	-68.1	397.1	15	0.0	0.0	396.2	396.1	18.1	-1.9
11	70	18604	-73.7	427.9	9	0.0	0.0	426.7	426.6	8.5	-5.8
12	50	20599	/////	/////	///	////	////	/////	/////	/////	/////

09 JST MAY 04

NO	P(MB)	A(GPM)	T(C)	C(K)	U(%)	S	X	CS(K)	CX(K)	U(M/S)	V(M/S)
1	1000	111	21.8	295.0	98	16.1	16.3	337.8	336.9	2.5	3.6
2	850	1517	16.4	303.4	61	8.4	8.4	340.8	325.6	4.2	2.3
3	700	3143	7.8	311.2	34	3.2	3.2	338.1	320.0	3.8	3.1
4	500	5826	-8.4	323.0	4	0.2	0.2	335.4	323.3	9.0	0.9
5	400	7514	-20.9	328.1	12	0.2	0.2	333.8	328.5	12.6	-1.8
6	300	9568	-37.4	333.1	12	0.1	0.1	334.4	332.8	11.2	0.2
7	250	10809	-44.8	339.9	17	0.0	0.0	340.5	339.6	11.4	-5.3
8	200	12265	-55.9	344.8	19	0.0	0.0	344.6	344.3	14.6	-6.8
9	150	14059	-61.0	365.7	6	0.0	0.0	365.2	364.9	23.8	-12.1
10	100	16507	-72.5	388.6	2	0.0	0.0	387.6	387.5	13.9	-10.8
11	70	18576	-75.6	423.8	2	0.0	0.0	422.6	422.5	7.1	-6.4
12	50	20584	-64.8	492.3	2	0.0	0.0	491.3	490.6	2.2	1.5

09 JST MAY 05

NO	P(MB)	A(GPM)	T(C)	C(K)	U(%)	S	X	CS(K)	CX(K)	U(M/S)	V(M/S)
1	1000	60	22.3	295.5	96	16.2	16.5	339.7	337.8	8.4	9.0
2	850	1464	15.7	302.7	90	11.8	12.0	338.3	334.6	17.4	6.7
3	700	3088	6.9	310.2	93	8.3	8.3	335.4	333.6	16.2	4.7
4	500	5787	-7.0	324.7	33	1.5	1.5	338.5	329.0	19.0	2.3
5	400	7488	-18.8	330.9	21	0.5	0.5	337.7	332.0	18.4	2.6
6	300	9579	-32.2	340.4	41	0.3	0.3	343.0	341.2	26.5	0.9
7	250	10839	-42.6	343.2	54	0.2	0.2	344.0	343.4	29.2	1.0
8	200	12308	-54.7	346.7	40	0.0	0.0	346.5	346.3	30.4	-1.6
9	150	14086	-65.3	358.3	26	0.0	0.0	357.7	357.6	29.1	-1.0
10	100	16517	-72.2	389.1	8	0.0	0.0	388.2	388.1	24.0	-5.1
11	70	18606	-71.0	433.7	6	0.0	0.0	432.5	432.4	6.1	-1.9
12	50	20627	-62.0	498.9	4	0.0	0.0	498.2	497.2	5.0	0.4

15 JST MAY 05

NO	P(MB)	A(GPM)	T(C)	C(K)	U(%)	S	X	CS(K)	CX(K)	U(M/S)	V(M/S)
1	1000	.58	22.0	295.2	97	16.1	16.3	338.5	337.1	13.9	1.9
2	850	1460	15.2	302.1	100	12.7	12.9	336.6	336.6	17.5	6.4
3	700	3084	6.7	310.0	100	8.8	8.8	334.8	334.8	19.0	4.4
4	500	5785	-6.8	325.0	100	4.6	4.6	339.0	339.0	21.9	3.1
5	400	7493	-17.5	332.6	89	2.1	2.1	340.2	339.3	21.3	5.3
6	300	9584	-32.5	340.0	71	0.6	0.6	342.5	341.6	27.1	2.8
7	250	10843	-41.9	344.3	58	0.2	0.2	345.2	344.6	34.4	8.6
8	200	12312	-54.6	346.9	41	0.0	0.0	346.7	346.4	38.7	3.4
9	150	14098	-65.4	358.1	24	0.0	0.0	357.5	357.4	30.5	1.6
10	100	16526	-72.5	388.6	16	0.0	0.0	387.6	387.6	27.3	-8.9
11	70	18621	-70.9	433.9	17	0.0	0.0	432.8	432.6	8.9	5.8
12	50	20651	/////	/////	///	////	////	/////	/////	/////	/////

21 JST MAY 05

NO	P(MB)	A(GPM)	T(C)	C(K)	U(%)	S	X	CS(K)	CX(K)	U(M/S)	V(M/S)
1	1000	75	20.8	294.0	97	14.9	15.2	334.1	332.8	5.1	1.0
2	850	1473	15.6	302.5	83	10.8	10.9	338.0	331.6	8.4	-1.2
3	700	3101	8.3	311.8	39	3.8	3.8	339.6	322.2	12.8	-1.3
4	500	5801	-7.6	324.0	58	2.5	2.5	337.2	331.5	21.1	-4.5
5	400	7508	-17.5	332.6	8	0.2	0.2	340.2	332.8	23.1	-4.1
6	300	9597	-32.1	340.6	75	0.6	0.6	343.2	342.4	26.8	7.7
7	250	10855	-42.8	342.9	66	0.2	0.2	343.7	343.2	31.7	2.8
8	200	12320	-54.9	346.4	46	0.0	0.0	346.2	346.0	34.4	1.2
9	150	14094	-67.0	355.4	39	0.0	0.0	354.7	354.6	39.4	2.1
10	100	16528	-71.2	391.1	22	0.0	0.0	390.2	390.1	28.0	-6.5
11	70	18648	-71.2	433.2	19	0.0	0.0	432.1	432.0	14.0	0.2
12	50	20654	-64.1	493.9	18	0.0	0.0	493.0	492.4	4.7	3.7
13	30	23858	/////	/////	///	////	////	/////	/////	/////	/////

03 JST MAY 06

NO	P(MB)	A(GPM)	T(C)	C(K)	U(%)	S	X	CS(K)	CX(K)	U(M/S)	V(M/S)
1	1000	91	20.2	293.4	96	14.2	14.4	332.0	330.3	0.5	-6.5
2	850	1483	15.3	302.2	31	3.9	4.0	337.0	312.5	4.0	-3.2
3	700	3109	8.1	311.6	11	1.1	1.1	339.0	314.4	8.4	-5.0
4	500	5812	-6.4	325.5	1	0.0	0.0	339.9	325.4	13.1	-8.2
5	400	7515	-16.6	333.7	4	0.1	0.1	342.0	333.7	21.8	-12.1
6	300	9604	-33.7	338.3	11	0.1	0.1	340.5	338.1	29.0	-10.0
7	250	10852	-44.8	339.9	12	0.0	0.0	340.5	339.5	33.1	-13.4
8	200	12306	-56.1	344.5	38	0.0	0.0	344.2	344.0	38.8	-4.1
9	150	14088	-64.2	360.2	23	0.0	0.0	359.6	359.4	36.7	-1.3
10	100	16526	-67.4	398.4	10	0.0	0.0	397.6	397.4	17.6	-10.1
11	70	18620	-74.0	427.2	6	0.0	0.0	426.1	425.9	13.2	-5.9
12	50	20632	-61.7	499.6	6	0.0	0.0	499.0	498.0	7.0	-1.1
13	30	23852	/////	/////	///	////	////	/////	/////	/////	/////

09 JST MAY 06

NO	P(MB)	A(GPM)	T(C)	C(K)	U(%)	S	X	CS(K)	CX(K)	U(M/S)	V(M/S)
1	1000	121	20.5	293.7	65	9.8	9.9	333.0	318.6	-4.9	-5.8
2	850	1506	17.3	304.3	5	0.7	0.7	344.0	306.1	3.2	-0.8
3	700	3134	9.9	313.6	2	0.2	0.2	344.7	314.0	4.4	-3.4
4	500	5839	-7.3	324.4	1	0.0	0.0	337.8	324.3	9.2	-4.1
5	400	7542	-18.1	331.8	7	0.2	0.2	339.0	332.0	17.2	-5.6
6	300	9624	-33.8	338.2	7	0.1	0.1	340.3	337.9	10.0	-8.4
7	250	10875	-44.2	340.8	5	0.0	0.0	341.4	340.4	14.0	-13.5
8	200	12329	-56.9	343.2	13	0.0	0.0	342.9	342.6	18.6	-4.6
9	150	14093	-64.6	359.5	19	0.0	0.0	358.9	358.7	23.8	-8.7
10	100	16540	-71.6	390.3	4	0.0	0.0	389.4	389.3	19.2	-9.4
11	70	18624	-73.8	427.7	3	0.0	0.0	426.5	426.4	10.9	-6.3
12	50	20620	-63.3	495.8	2	0.0	0.0	495.0	494.1	0.6	-2.4
13	30	23835	/////	/////	///	////	////	/////	/////	/////	/////

15 JST MAY 06

NO	P(MB)	A(GPM)	T(C)	C(K)	U(%)	S	X	CS(K)	CX(K)	U(M/S)	V(M/S)
1	1000	120	23.4	296.6	73	13.2	13.3	344.0	330.4	-7.3	0.3
2	850	1513	17.2	304.2	7	1.0	1.0	343.7	306.8	2.3	-1.9
3	700	3141	9.1	312.7	6	0.6	0.6	342.1	314.2	2.2	-2.0
4	500	5849	-6.5	325.4	2	0.1	0.1	339.7	325.4	10.5	2.8
5	400	7557	-17.3	332.8	15	0.4	0.4	340.6	333.7	13.8	0.0
6	300	9649	-32.7	339.7	5	0.0	0.0	342.2	339.4	14.2	3.5
7	250	10902	-44.1	341.0	16	0.0	0.0	341.6	340.6	17.0	-3.0
8	200	12358	-56.4	344.0	20	0.0	0.0	343.7	343.5	15.1	-1.6
9	150	14130	-63.4	361.6	21	0.0	0.0	361.0	360.8	19.7	-9.2
10	100	16569	-72.2	389.1	5	0.0	0.0	388.2	388.1	19.8	-16.0
11	70	18649	-74.4	426.4	4	0.0	0.0	425.2	425.1	11.2	-6.0
12	50	20662	-64.5	493.0	3	0.0	0.0	492.0	491.3	-1.6	2.7
13	30	23883	-53.9	599.8	1	0.0	0.0	603.1	597.5	-2.9	0.7

21 JST MAY 06

NO	P(MB)	A(GPM)	T(C)	C(K)	U(%)	S	X	CS(K)	CX(K)	U(M/S)	V(M/S)
1	1000	123	20.2	293.4	78	11.6	11.7	332.0	323.0	-3.2	3.6
2	850	1512	16.6	303.6	11	1.5	1.5	341.5	307.5	1.7	3.5
3	700	3140	9.2	312.8	4	0.4	0.4	342.4	313.8	3.5	5.0
4	500	5849	-5.9	326.1	31	1.5	1.5	341.1	330.5	12.6	1.5
5	400	7560	-17.6	332.4	32	0.8	0.8	340.0	334.6	13.2	5.3
6	300	9649	-33.0	339.3	19	0.1	0.1	341.6	339.4	14.3	2.8
7	250	10904	-42.9	342.8	39	0.1	0.1	343.5	342.7	13.9	0.2
8	200	12364	-55.8	345.0	37	0.0	0.0	344.7	344.5	16.5	-1.2
9	150	14142	-62.5	363.1	26	0.0	0.0	362.6	362.4	15.8	-7.0
10	100	16585	/////	/////	///	////	////	/////	/////	/////	/////

03 JST MAY 07

NO	P(MB)	A(GPM)	T(C)	C(K)	U(%)	S	X	CS(K)	CX(K)	U(M/S)	V(M/S)
1	1000	115	19.7	292.9	86	12.4	12.5	330.2	324.7	-1.3	8.0
2	850	1498	15.7	302.7	8	1.0	1.0	338.3	305.3	1.0	7.2
3	700	3122	8.4	311.9	25	2.4	2.5	339.9	318.6	9.9	1.4
4	500	5823	-7.6	324.0	59	2.5	2.5	337.2	331.6	11.3	2.8
5	400	7526	-18.5	331.3	56	1.2	1.2	338.2	335.0	9.1	3.9
6	300	9615	-32.3	340.2	13	0.1	0.1	342.8	340.2	13.9	-0.2
7	250	10871	-42.9	342.8	26	0.1	0.1	343.5	342.6	15.6	-3.3
8	200	12336	-54.9	346.4	20	0.0	0.0	346.2	345.9	15.6	-12.2
9	150	14125	-62.3	363.5	19	0.0	0.0	362.9	362.7	13.2	-16.3
10	100	16567	-72.1	389.3	5	0.0	0.0	388.4	388.3	17.1	-13.8
11	70	18649	-72.6	430.2	4	0.0	0.0	429.1	428.9	9.3	-8.7
12	50	20649	/////	/////	///	////	////	/////	/////	/////	/////

09 JST MAY 07

NO	P(MB)	A(GPM)	T(C)	C(K)	U(%)	S	X	CS(K)	CX(K)	U(M/S)	V(M/S)
1	1000	98	20.3	293.5	98	14.6	14.8	332.3	331.5	0.7	8.6
2	850	1491	15.1	302.0	100	12.6	12.8	336.3	336.3	9.8	7.9
3	700	3120	7.5	310.9	100	9.3	9.3	337.2	337.2	14.0	1.2
4	500	5817	-6.8	325.0	67	3.1	3.1	339.0	334.2	14.2	0.0
5	400	7531	-16.3	334.1	48	1.3	1.3	342.6	338.0	13.2	-2.8
6	300	9627	-30.9	342.3	36	0.3	0.3	345.2	343.0	15.0	-7.3
7	250	10897	-40.9	345.8	21	0.1	0.1	346.8	345.5	16.1	-8.2
8	200	12371	-54.2	347.5	32	0.0	0.0	347.3	347.0	15.0	-17.9
9	150	14163	-61.6	364.7	21	0.0	0.0	364.1	363.9	11.3	-28.0
10	100	16593	-73.3	387.0	5	0.0	0.0	386.1	386.0	11.6	-21.8
11	70	18670	-73.8	427.7	5	0.0	0.0	426.5	426.4	6.8	-8.4
12	50	20671	-64.2	493.7	4	0.0	0.0	492.8	492.0	-5.3	-9.6

15 JST MAY 07

NO	P(MB)	A(GPM)	T(C)	C(K)	U(%)	S	X	CS(K)	CX(K)	U(M/S)	V(M/S)
1	1000	54	21.9	295.1	97	16.0	16.2	338.2	336.8	14.0	13.0
2	850	1462	16.6	303.6	86	12.0	12.1	341.5	335.9	20.8	8.8
3	700	3098	8.4	311.9	71	7.0	7.0	339.9	331.5	19.9	5.0
4	500	5806	-5.2	326.9	58	3.0	3.0	342.8	335.9	20.7	3.6
5	400	7525	-16.1	334.4	50	1.4	1.4	343.0	338.5	19.0	1.7
6	300	9628	-29.5	344.2	65	0.7	0.7	347.7	346.3	18.0	-5.2
7	250	10902	-39.8	347.4	31	0.1	0.1	348.6	347.4	18.1	-2.9
8	200	12383	-53.1	349.3	37	0.0	0.0	349.2	348.8	19.5	-10.4
9	150	14186	-64.4	359.8	8	0.0	0.0	359.2	359.1	21.2	-25.3
10	100	16606	-76.1	381.6	3	0.0	0.0	380.6	380.6	17.4	-13.1
11	70	18658	-76.6	421.6	4	0.0	0.0	420.5	420.4	4.0	-7.8
12	50	20643	-68.4	483.8	3	0.0	0.0	482.6	482.1	-4.6	4.7

18 JST MAY 07

NO	P(MB)	A(GPM)	T(C)	C(K)	U(%)	S	X	CS(K)	CX(K)	U(M/S)	V(M/S)
1	1000	45	22.5	295.7	96	16.4	16.7	340.5	338.5	16.9	13.7
2	850	1456	18.3	305.4	72	11.1	11.3	347.8	335.3	25.1	7.2
3	700	3094	9.1	312.7	52	5.4	5.4	342.1	327.5	26.9	9.3
4	500	5802	-5.0	327.2	38	2.0	2.0	343.3	333.1	22.7	3.6
5	400	7518	-16.4	334.0	87	2.3	2.3	342.4	341.3	24.8	0.9
6	300	9629	-29.4	344.4	62	0.7	0.7	347.9	346.4	23.6	-3.7
7	250	10902	-40.2	346.8	54	0.2	0.2	348.0	347.2	22.4	-4.4
8	200	12381	-52.4	350.4	31	0.0	0.0	350.3	349.9	26.2	-11.7
9	150	14181	-65.5	357.9	14	0.0	0.0	357.3	357.2	25.1	-23.4
10	100	16597	-75.8	382.2	7	0.0	0.0	381.2	381.2	15.9	-12.4
11	70	18660	-76.7	421.4	7	0.0	0.0	420.2	420.2	7.8	-9.3
12	50	20657	/////	/////	///	////	////	/////	/////	/////	/////

21 JST MAY 07

NO	P(MB)	A(GPM)	T(C)	C(K)	U(%)	S	X	CS(K)	CX(K)	U(M/S)	V(M/S)
1	1000	43	22.7	295.9	89	15.4	15.6	341.3	335.9	18.8	13.6
2	850	1454	17.4	304.4	81	11.8	12.0	344.4	336.4	27.1	5.3
3	700	3092	10.7	314.5	36	4.1	4.1	347.3	325.8	28.5	7.1
4	500	5808	-5.5	326.6	99	5.0	5.0	342.1	341.9	27.3	1.9
5	400	7526	-15.1	335.7	75	2.2	2.2	345.1	342.6	24.9	-0.4
6	300	9639	-30.2	343.2	77	0.8	0.8	346.5	345.6	22.6	-3.2
7	250	10916	-39.0	348.6	66	0.3	0.3	350.0	349.3	27.6	-15.3
8	200	12405	-52.0	351.0	59	0.1	0.1	351.0	350.7	29.1	-15.5
9	150	14207	-64.5	359.7	38	0.0	0.0	359.1	359.0	25.6	-20.8
10	100	16621	-76.2	381.4	17	0.0	0.0	380.4	380.4	18.7	-9.1
11	70	18683	-76.9	421.0	13	0.0	0.0	419.8	419.7	6.4	-7.3
12	50	20711	/////	/////	///	////	////	/////	/////	/////	/////

24 JST MAY 07

NO	P(MB)	A(GPM)	T(C)	C(K)	U(%)	S	X	CS(K)	CX(K)	U(M/S)	V(M/S)
1	1000	32	22.6	295.8	96	16.5	16.8	340.9	338.9	19.9	11.9
2	850	1443	16.9	303.9	79	11.2	11.3	342.6	334.0	28.0	7.5
3	700	3079	9.2	312.8	100	10.4	10.5	342.4	342.4	29.7	3.1
4	500	5791	-5.8	326.2	100	4.9	5.0	341.4	341.4	29.0	-1.0
5	400	7513	-16.0	334.5	88	2.4	2.4	343.2	342.1	30.6	3.8
6	300	9623	-30.5	342.8	77	0.8	0.8	345.9	345.1	25.7	-5.9
7	250	10896	-39.3	348.1	73	0.4	0.4	349.5	349.0	36.5	-10.5
8	200	12380	-52.7	349.9	56	0.1	0.1	349.8	349.6	34.7	-8.7
9	150	14186	-63.8	360.9	35	0.0	0.0	360.3	360.2	25.9	-14.9
10	100	16601	-75.6	382.6	25	0.0	0.0	381.6	381.6	16.2	-10.5
11	70	18668	-72.7	430.0	27	0.0	0.0	428.9	428.8	7.4	-6.6

03 JST MAY 08

NO	P(MB)	A(GPM)	T(C)	C(K)	U(%)	S	X	CS(K)	CX(K)	U(M/S)	V(M/S)
1	1000	22	22.6	295.8	96	16.5	16.8	340.9	338.9	17.5	10.9
2	850	1438	22.9	310.2	100	20.7	21.1	367.7	367.7	27.0	2.8
3	700	3093	9.4	313.0	100	10.5	10.6	343.1	343.1	30.1	-3.2
4	500	5808	-6.3	325.6	99	4.7	4.7	340.2	340.0	25.4	-4.9
5	400	7530	-14.4	336.6	94	2.9	2.9	346.6	346.0	26.3	-0.5
6	300	9641	-31.1	342.0	71	0.7	0.7	344.9	343.9	30.1	-11.5
7	250	10910	-40.4	346.5	68	0.3	0.3	347.6	347.1	33.3	-4.7
8	200	12385	-54.0	347.8	54	0.1	0.1	347.7	347.5	34.5	-9.9
9	150	14199	-61.7	364.5	44	0.0	0.0	364.0	363.8	24.4	-14.7
10	100	16625	-73.2	387.2	33	0.0	0.0	386.3	386.2	10.7	-7.8
11	70	18698	-72.5	430.4	33	0.0	0.0	429.3	429.2	8.3	-10.6
12	50	20689	-65.8	489.9	38	0.0	0.0	488.9	488.5	6.1	-3.5

09 JST MAY 08

NO	P(MB)	A(GPM)	T(C)	C(K)	U(%)	S	X	CS(K)	CX(K)	U(M/S)	V(M/S)
1	1000	53	20.1	293.3	77	11.3	11.5	331.6	322.3	-6.3	-10.5
2	850	1437	13.7	300.6	99	11.4	11.6	331.7	331.4	14.6	-2.8
3	700	3064	9.1	312.7	72	7.4	7.5	342.1	333.5	20.2	-1.8
4	500	5775	-7.4	324.3	82	3.6	3.6	337.6	335.1	22.5	-2.8
5	400	7492	-15.5	335.2	30	0.9	0.9	344.3	337.6	29.9	1.6
6	300	9601	-31.6	341.3	59	0.5	0.5	344.0	342.7	31.0	-7.7
7	250	10862	-42.5	343.4	43	0.2	0.2	344.2	343.4	37.4	-9.3
8	200	12342	-49.7	354.7	3	0.0	0.0	354.8	354.0	34.6	-13.3
9	150	14172	-61.2	365.4	2	0.0	0.0	364.8	364.6	30.4	-14.8
10	100	16610	-72.5	388.6	1	0.0	0.0	387.6	387.5	19.3	-13.5
11	70	18678	-74.8	425.5	2	0.0	0.0	424.3	424.2	6.8	-5.1
12	50	20677	-63.7	494.9	2	0.0	0.0	494.0	493.2	-1.0	-6.5

15 JST MAY 08

NO	P(MB)	A(GPM)	T(C)	C(K)	U(%)	S	X	CS(K)	CX(K)	U(M/S)	V(M/S)
1	1000	70	20.5	293.7	74	11.2	11.3	333.0	322.2	-2.6	-12.2
2	850	1447	10.0	296.7	70	6.3	6.3	320.9	313.4	6.2	-7.6
3	700	3060	10.1	313.8	4	0.4	0.4	345.3	314.9	8.8	-4.9
4	500	5766	-7.1	324.6	10	0.4	0.4	338.3	325.7	13.1	-6.1
5	400	7469	-18.3	331.5	26	0.6	0.6	338.6	333.1	22.8	-4.8
6	300	9548	-34.8	336.7	62	0.4	0.4	338.6	337.7	29.5	-1.5
7	250	10794	-42.8	342.9	38	0.1	0.1	343.7	342.9	33.0	-15.4
8	200	12292	-46.0	360.5	1	0.0	0.0	361.1	359.9	35.5	-21.3
9	150	14144	-60.5	366.6	1	0.0	0.0	366.1	365.8	31.0	-10.7
10	100	16581	-72.6	388.4	1	0.0	0.0	387.4	387.3	18.0	-14.0
11	70	18661	-74.8	425.5	1	0.0	0.0	424.3	424.2	11.1	-6.4
12	50	20658	-66.2	489.0	2	0.0	0.0	487.9	487.3	-4.1	3.7
13	30	23874	-54.4	598.5	1	0.0	0.0	601.4	596.1	-1.4	1.3

NO	P(MB)	A(GPM)	T(C)	C(K)	U(%)	S	X	CS(K)	CX(K)	U(M/S)	V(M/S)